

**UNIVERSITY OF KWAZULU-NATAL**

**Optimal Sizing for a Grid-Connected Hybrid Renewable  
Energy System**

**by**

**Hudson Sibanda**

2021

## **PREFACE**

The research contained in this dissertation was completed by the candidate while based in the Discipline of Electrical Engineering, School of Engineering of the College of Agriculture, Engineering and Science, University of KwaZulu-Natal, Howard College, South Africa.

The contents of this work have not been submitted in any form to another university and, except where the work of others is acknowledged in the text, the results reported are due to investigations by the candidate.

Signed: Dr Farzad Ghayoor

Date: 1 March 2021

Signed: Dr Andrew Swanson

Date: 1 March 2021

## **DECLARATION 1: PLAGIARISM**

I, Hudson Sibanda, declare that:

(i) the research reported in this dissertation, except where otherwise indicated or acknowledged, is my original work;

(ii) this dissertation has not been submitted in full or in part for any degree or examination to any other university;

(iii) this dissertation does not contain other persons' data, pictures, graphs or other information, unless specifically acknowledged as being sourced from other persons;

(iv) this dissertation does not contain other persons' writing, unless specifically acknowledged as being sourced from other researchers. Where other written sources have been quoted, then:

a) their words have been re-written but the general information attributed to them has been referenced;

b) where their exact words have been used, their writing has been placed inside quotation marks, and referenced;

(v) where I have used material for which publications followed, I have indicated in detail my role in the work;

(vi) this dissertation is primarily a collection of material, prepared by myself, published as journal articles or presented as a poster and oral presentations at conferences. In some cases, additional material has been included;

(vii) this dissertation does not contain text, graphics or tables copied and pasted from the Internet, unless specifically acknowledged, and the source being detailed in the dissertation and in the References sections.

---

Signed: Hudson Sibanda

Date: 25 November 2020

## **ABSTRACT**

Hybrid renewable energy systems (HRESs) refer to power generating systems that integrate several sources of energy, including renewables, to provide electricity to consumers. HRESs can either work as standalone or grid-connected systems. Since wind and solar have complementary characteristics and are available in most areas, they are considered as suitable energy sources to be combined in an HRES. Moreover, the maturity of technologies needed for generating electricity from wind and solar has turned them into more economical options in many locations.

Many countries, including South Africa, have introduced policies and incentives to increase their renewable energy capacities in order to address environmental concerns and reduce pollutant emissions into the atmosphere. In addition, consumers in South Africa have faced the ever-increasing price of electricity and unreliability of the grid since 2007 due to the lack of sufficient electricity production. As a result, employing HRESs has gained popularity among consumers in different sectors.

This research is focused on grid-connected hybrid energy systems based on solar photovoltaic (PV) panels and wind turbines as a potential solution to reduce the dependency of residential sector consumers on the grid in Durban. The aim of the research is to identify the optimal sizing of such a HRES to be cost-effective for consumers over a certain period of time. Since the energy supplied by renewable sources are intermittent and dependent on the geographical location of the system, identifying optimal sizing becomes a challenging task in HRESs. In this research, Durban's meteorological data and eThekweni municipality tariff rates have been considered. Moreover, two artificial intelligence methods have been used to obtain the optimal sizing for different types of available PV panels, wind turbines and inverters in the market.

The results have shown that the combination of PV panels and battery storage (BS) can become a profitable option for Durban area. Moreover, the systems using higher rated power PV panels can start to become profitable in a shorter lifetime. Considering BS in a system can only become a cost-effective choice if we consider a long enough lifespan for the system.

## **ACKNOWLEDGMENTS**

I would like to express my gratitude to my supervisor Dr Farzad Ghayoor for his guidance and advice throughout the course of this project. The completion of this project is due to his unending encouragement and support.

I also want to extend my thanks to my family for keeping me motivated during the low moments. To my daughter, Thea, thank you for giving me a 'timeout' to work on this project.

# TABLE OF CONTENTS

	<u>Page</u>
PREFACE .....	i
DECLARATION 1: PLAGIARISM.....	ii
ABSTRACT .....	iii
ACKNOWLEDGMENTS.....	iv
TABLE OF CONTENTS .....	v
LIST OF TABLES .....	viii
LIST OF FIGURES.....	x
ABBREVIATIONS.....	xii
Chapter 1 : INTRODUCTION .....	1
1.1. Introduction .....	1
1.2. Motivation .....	2
1.3. Problem Statement .....	3
1.4. Aims and Objectives .....	3
1.5. Outline of Dissertation .....	4
Chapter 2 : LITERATURE REVIEW .....	5
2.1. Introduction .....	5
2.2. Hybrid Renewable Energy Systems Configurations.....	6
2.3. Evaluation Indicators.....	8
2.3.1. Economic Indicators .....	8
2.3.2. Reliability Indicators .....	10
2.3.3. Social and Environmental indicators .....	12
2.4. Optimal Sizing Methods.....	12
2.4.1. Classical Techniques .....	13
2.4.2. Modern Techniques .....	15
2.4.3. Hybrid Techniques.....	18
2.4.4. Computer Software Tools.....	19
2.4.5. The Comparison of Algorithms .....	21
2.5. Summary .....	22
Chapter 3 : MATHEMATICAL MODELLING .....	23

3.1. Introduction .....	23
3.2. Genetic Algorithm.....	23
3.2.1. Selection Operator .....	24
3.2.2. Crossover Implementation.....	26
3.2.3. Mutation Operator .....	27
3.3. Particle Swarm Optimization .....	29
3.4. Modelling of the Renewable Energy Sources .....	32
3.4.1. Wind Turbine Model .....	33
3.4.2. Solar Photovoltaic Model .....	34
3.5. Summary .....	34
Chapter 4 : METHODOLOGY .....	35
4.1. Introduction .....	35
4.2. Meteorological Data.....	36
4.3. Tariff Rates.....	38
4.4. Load Profile.....	40
4.5. PV Panels .....	42
4.6. Wind Turbine .....	44
4.7. Battery Storage.....	45
4.8. Inverter .....	46
4.9. Utility Grid .....	47
4.10. System Operation .....	48
4.11. Proposed Optimization Method .....	49
4.11.1. Cost Function.....	50
4.11.2. Constraints .....	52
4.11.3. Optimizers.....	52
4.11.3.1. GA .....	53
4.11.3.2. PSO.....	54
4.12. Summary .....	56
Chapter 5 : RESULTS AND DISCUSSION.....	58
5.1. Introduction .....	58
5.2. Optimal Sizing Results.....	58
5.3. Verification and Validation of the System Model .....	68
5.4. Operation of the System with Optimal Configuration .....	69

5.5. Summary .....	73
Chapter 6 : CONCLUSIONS .....	74
6.1. Summary and Contributions.....	74
6.2. Future Works and Recommendations .....	77
REFERENCES.....	78



## LIST OF TABLES

<b><u>Table</u></b>	<b><u>Page</u></b>
Table 4-1. THE METEOROLOGICAL STATION LOCATION .....	36
Table 4-2. GHI STATISTICS (W/m <sup>2</sup> ) .....	37
Table 4-3. TEMPERATURE STATISTICS (°C) .....	37
Table 4-4. WIND SPEED STATISTICS (m/s).....	38
Table 4-5. ETHEKWINI SINGLE PHASE RESIDENTIAL TARIFF .....	39
Table 4-6. ETHEKWINI SINGLE PHASE RESIDENTIAL PROJECTED TARIFF .....	40
Table 4-7. LOAD STATISTICS (kWh).....	41
Table 4-8. PV PANELS PARAMETERS.....	43
Table 4-9. WIND TURBINE PARAMETERS.....	44
Table 4-10. BATTERY PARAMETERS.....	46
Table 4-11. INVERTER PARAMETERS .....	46
Table 4-12. CONSIDERED ECONOMIC DATA FOR THE SYSTEM .....	51
Table 4-13. PARAMETERS USED IN THE GA OPTIMIZER .....	54
Table 4-14. PARAMETERS USED IN THE PSO OPTIMIZER.....	55
Table 5-1. A COMPARISON BETWEEN THE PERFORMANCE OF GA AND PSO OPTIMIZER IN OPTIMIZING THE SYSTEM WITH 10 YEARS LIFETIME.....	63
Table 5-2. THE OPTIMAL SIZE AND COST FUNCTION VALUE OF THE SYSTEM CONSIDERING DIFFERENT PV PANEL TYPES AND SYSTEM'S LIFETIME (OPTIMIZED BY GA) .....	67
Table 5-3. THE COST COMPONENTS OF THE SYSTEM CONSIDERING DIFFERENT PV PANEL TYPES AND SYSTEM'S LIFE TIME (OPTIMIZED BY GA).....	68

Table 5-4. THE AVERAGE VALUES OF THE BATTERY STORAGE AND LOAD DUMP FOR THE OPTIMAL SYSTEM..... 71

## LIST OF FIGURES

<b><u>Figure</u></b>	<b><u>Page</u></b>
Figure 3-1: Flowchart of GA.....	24
Figure 3-2: Roulette selection wheel.....	26
Figure 3-3: Binary encoding in GA.....	27
Figure 3-4: Mutation in GA .....	28
Figure 3-5: Flowchart of PSO .....	31
Figure 3-6: Wind turbine output curve.....	33
Figure 4-1: Block diagram of the grid-connected hybrid RES .....	35
Figure 4-2: Annual Global Horizontal Irradiance (GHI) data.....	36
Figure 4-3: Annual temperature data .....	37
Figure 4-4: Annual wind speed data .....	38
Figure 4-5: Single phase residential tariff in eThekweni municipality.....	39
Figure 4-6: Typical daily load profile .....	41
Figure 4-7: Annual load profile.....	41
Figure 4-8: Annual PV power output per panel: (a) Cinco 50W, (b) Cinco 100W, (c) Cinco 200W .....	42
Figure 4-9: Annual wind turbine output.....	44
Figure 4-10: System operation flowchart.....	48
Figure 5-1: The transition of cost function considering systems over 10 years of lifetime with (a) 200W PV panels optimized by GA, (b) 200W PV panels optimized by PSO .....	60
Figure 5-2: The transition of cost function considering systems over 10 years of lifetime with (a) 100W PV panels optimized by GA, (b) 100W PV panels optimized by PSO .....	61

Figure 5-3: The transition of cost function considering systems over 10 years of lifetime with (a) 50W PV panels optimized by GA, (b) 50W PV panels optimized by PSO .....	62
Figure 5-4: The transition of the cost function for a system with the 200W PV panels and optimized by GA for the system life span of (a) 10, (b) 9, (c) 8, (d) 7, (e) 6 years. ....	64
Figure 5-5: The transition of the cost function for a system with the 100W PV panels and optimized by GA for the system life span of (a) 10, (b) 9, (c) 8, (d) 7, (e) 6 years. ....	65
Figure 5-6: The transition of the cost function for a system with the 50W PV panels and optimized by GA for the system life span of (a) 10, (b) 9, (c) 8, (d) 7 years.....	66
Figure 5-7: Average annual consumption from the Grid and RES for an optimally sized system comprising of (a) 200W, (b) 100W, (c) 50W PV Panels.....	70
Figure 5-8: Averaged annual BS and Load Dump for the optimal size system with 10 years life time using (a) 200W, (b) 100W (c) 50W PV Panels .....	72

## ABBREVIATIONS

ABC	Artificial bee colony
ACS	Annualised cost of system
ACO	Ant colony optimization
AGA	Adaptive genetic algorithm
AI	Artificial intelligence
ANN	Artificial neural network
BBO	Biogeography-based optimization
BS	Battery storage
CCP	Chance constrained programming
CF-PSO	Constriction factor particle swarm optimization
COE	Cost of energy
CRF	Capital recovery factor
CS	Cuckoo search
DCHSSA	Discrete chaotic harmony search-based simulated annealing algorithm
DHS	Discrete harmony search
DPSP	Deficiency of power supply probability
ES	Energy storage
FPA	Flower pollination algorithm
GA	Genetic algorithm
HBB-BC	Hybrid big bang-big crunch algorithm
HOMER	Hybrid optimization model for electric renewables
HRES	Hybrid renewable system
HS	Harmony search
HSBCS	Harmony search-based chaotic search
ICA	Imperial competitive algorithm
IFOA	Improved fruit-fly optimization algorithm
iHOGA	Improved hybrid optimization by genetic algorithm
IPF	Iterative pareto fuzzy
LCA	Line-up competition algorithm
LCC	Life cycle cost
LCOE	Levelised cost of energy

LOEE	Loss of energy expected
LOLE	Loss of load expected
LOLP	Loss of load probability
LP	Linear programming
LPSP	Loss of power supply probability
MCS	Monte Carlo simulation
MILP	Mixed-integer linear programming
MOEA	Multi-objective evolutionary algorithm
MOO	Multi-objective optimization
MOPSO	Multi-objective particle swarm optimization
MPPT	Maximum power point tracking
MPSO	Modified Particle swarm optimization
NPC	Net present cost
NPV	Net present value
NSGA-II	Non-dominated sorting genetic algorithm
NSPSO	Natural selection particle swarm optimization
PHS	Pumped hydro storage
PICEA	Preference-inspired coevolutionary algorithm
PSO	Particle swarm optimization
PV	Photovoltaic
RES	Renewable energy sources
RO	Reverse osmosis
SA	Simulated annealing
SAPSO	Simulated annealing particle swarm optimization
SOO	Single objective optimization
STRONG	Stochastic trust-region response surface
TAC	Total annual cost
TAEP	Total annual energy production
TLBO	Teaching-learning-based optimization algorithm
TS	Tabu search

# Chapter 1 : INTRODUCTION

## 1.1. Introduction

The failure of utilities to provide consistent power supply coupled with the rising cost of electricity, lack of fossil fuels and global warming concerns encourage a shift towards alternative and greener sources of energy for generating electricity. Many countries, including South Africa, have introduced policies and incentives to increase their renewable energy capacities for addressing environmental concerns and reducing pollutant emissions into the atmosphere. In addition, with ongoing load-shedding, exploring alternative sources for generating reliable electricity is of great importance for the country. Due to the technology improvement needed for harvesting energy from alternative sources, using renewable energy sources (RES) for generating electricity has become more cost-effective than ever before. This is observable from many buildings across the country that have installed photovoltaic (PV) panels on their rooftops or wind turbines for generating electricity. Wind and solar have complementary characteristics, which make them ideal sources of energy for reducing power fluctuations and supplementing the system in the case of insufficient power delivery by a grid. In fact, the most commonly used renewable sources in small scale power generating systems are wind and solar energy.

Hybrid energy systems refer to power generating systems that benefit from integrating several sources of energy, such as RES, diesel generators and even storage units and can either work as standalone or grid-connected systems. Optimization plays a pivotal role in designing hybrid energy systems. Through optimization, a hybrid energy system can make the most effective usage of the available energy resources to obtain certain objectives. Objectives can be in the form of reducing costs, improving power reliability, lessening greenhouse gas emissions or other social and economic factors. In some cases, there might be multiple objectives that have to be satisfied, and sometimes there would be trade-offs between two or more conflicting objectives. For instance, although an oversized hybrid system can satisfy the load demand, it is costly. On the other hand, an undersized hybrid system can be cost-effective, but fails to meet the required load demand. During an optimization process, there are also some constraints, which impose on the system and limit the possible solutions.

Many hybrid energy systems consist of renewable sources of energy, including various combinations of wind and solar. However, optimizing hybrid energy systems consisting of renewable energy sources is more challenging, as the energy supplied by such sources are intermittent. In

addition, the availability of renewable sources is dependent on the geographical location of a system, and so, optimum solutions should be identified according to meteorological data. As a result, the optimal design of a hybrid system could be different for various geographical locations.

## **1.2. Motivation**

This research is motivated by the ever-increasing price of electricity in South Africa and the challenges that consumers face as a result of the unreliability of the grid. The availability of wind and solar in most areas and the maturity of technologies needed for generating electricity from such sources make them popular choices to be used in hybrid renewable energy systems. Solar energy is a daytime energy source that is variable and random. On a clear day, the solar irradiation increases from dawn till around midday and then decreases again till dusk. Solar energy also varies by the season, [with irradiation being](#) stronger in autumn and summer and weaker in winter and spring. Wind energy, on the other hand, is available throughout day and night. In most locations higher wind speeds are experienced at night compared to daytime, and also, wind speeds are higher in winter and spring compared to autumn and summer. Therefore, wind and solar have complementary characteristics and are suitable sources to be combined in a hybrid energy system.

In this research, we focus on hybrid energy systems, which use solar PV and wind turbines. We also consider using energy storage systems for the considered hybrid system. The combination of solar and wind with energy storage systems is an effective solution for tackling the randomness and unpredictability nature of wind and solar sources. Including energy storage units can also help to overcome the electricity fluctuation thereby increasing electricity quality.

Hybrid energy systems that combine wind, solar, energy storage and the grid can be a potential solution to reduce South African consumers' dependency on the grid and may lessen the overall cost of their consumed electricity over an extended period. Although it is common that a grid-connected hybrid system injects its excessive generated power back to the grid, the focus of this research is to obtain the least dependency on the grid, and so we try to find the best solution for storing the excessive energy within the system rather than injecting it back to the grid. Despite much research that has been done on optimizing different hybrid energy systems, identifying the specifications, objectives and constraints involved in optimization of a hybrid energy system capable of satisfying South African consumers' needs requires more investigation.



### **1.3. Problem Statement**

The increasing cost of electricity and reduced reliability of electricity in South Africa have raised concerns in many sectors of the economy and public. Many companies and individuals have lost productivity and revenue due to power cuts and have had reduced profits due to the increasing electricity costs. Consequently, consumers have supplemented the grid supply with other sources of energy such as solar PV systems, wind turbines or backup generators. In the majority of the cases, these alternative sources have not been optimized, and therefore, can become very expensive.

This research seeks to identify the optimal size of a grid-connected solar PV-wind turbine-battery storage hybrid system that is cost-effective compared to a purely grid-connected system. Cost-effectiveness is the sense that the consumer pays less for electricity compared to purchasing purely from the grid over a certain period of time. In other words, we try to identify the optimal size of each HRES's components so that a consumer can recover their investments over a certain period of time by saving from purchasing less electricity from the grid's service provider. Solar and wind energy are location-based and as such, the study has been done based on the meteorological data of Durban.

### **1.4. Aims and Objectives**

The aim of this research is to determine the optimal sizing of a grid-connected HRES to be cost-effective for consumers over a certain period of time. It will identify the type and number of PV panels, wind turbines and battery storage, and the cost that will result in an optimal hybrid generating system. Artificial intelligence methods will be employed to optimally size the HRES for different types of available PV panels, wind turbines and inverters in the market.

There are four primary objectives for this project that have direct significance to its application:

1. To model the load and HRES based on the residential consumer needs and available product in the market.
2. To define the optimization problem based on a cost evaluation indicator and identify constraints.
3. To determine the optimum combination of RES that will result in a hybrid generating system that has the lowest cost by employing two artificial intelligence methods.

4. To assess the cost of setting up a hybrid generating system for typical residential consumers willing to use green energy and reduce or eliminate effects of power cuts from the utility grid based on their power consumption needs.

## **1.5. Outline of Dissertation**

The rest of this dissertation is organized as follows:

- Chapter 2 discusses the literature review on the previous research applicable to this project, which are mainly research associated with combination of wind and solar hybrid systems.
- Chapter 3 focuses on mathematical modelling of HRES's components. Also, it covers the genetic algorithm and particle swarm optimization methods that are used to identify the optimal size of the HRES.
- Chapter 4 is devoted to define and solve the optimization problem for identifying the optimal size of the HRES.
- In Chapter 5 the results and discussion are provided. We evaluate the chosen models to determine if the objectives of this project have been satisfied.
- The final chapter, Chapter 6, fuses the work and gives conclusions and documentation of the contributions of this research. We also summarize the discoveries of the research, describe the limitations of the optimization methods, and offer further research paths.

## Chapter 2 : LITERATURE REVIEW

### 2.1. Introduction

The availability of wind and solar in most areas and the maturity of the technology needed for generating electricity from such sources make them popular choices in hybrid renewable energy systems. Wind and solar energy, both, have intermittent nature and are highly dependent on environmental conditions. As a result, using only wind or solar as the sole energy resource often leads to an oversized and expensive system. Nevertheless, wind and solar have complementary characteristics and so are suitable sources to be combined in a hybrid energy system.

Hybrid energy systems, which combine multiple energy sources to generate electricity, can be designed to work as stand-alone or grid-connected systems. They can also benefit from energy storage units. These energy storage units are essential in improving the output power quality. Different studies have shown that even though the load demand by a hybrid wind and solar system can be satisfied, the fluctuating characteristics of wind and solar combinations make the energy supply system uncontrollable, resulting in a reduced electricity quality [1-4].

Energy storage (ES) systems, such as batteries and fuel cells, are effective solutions to reduce quality deficiency in wind-solar hybrid energy systems. In such systems, charging and discharging mechanisms are implemented to adjust a system's output. ES systems can exist in other forms than batteries and fuel cells. For example, in a large-scale system, where using batteries due to their high cost is not feasible, pumped hydro storage (PHS) acts as an energy storage system. PHS proves to be superior to traditional batteries in large-scale systems when considering reliability, economic costs, capacity and flexibility [5-8]. Countries such as China, the United States and Brazil have feasible conditions for exploration of PHS. For a hybrid renewable system at a scale, which we are interested in this work, the battery storage (BS) is a suitable energy storage option.

Regardless of the number and type of energy sources combined to form a hybrid energy system, optimization is an important stage in designing such a system. Through optimization, the best design with regard to certain criteria and constraints can be obtained. The design objectives used in optimizing a hybrid energy system can be technical, financial, environmental, social, or a combination of them. Minimizing costs (initial purchase costs, maintenance costs, and operational costs) and maximizing power supply reliability are examples of the most commonly used objectives. Constraints,

on the other hand, limit the possible solutions and can be caused by the weather conditions, number of PV panels, or a wind turbine output power in a hybrid wind-solar system.

In this chapter, we first provide an overview of different configurations for hybrid energy systems, which use wind and solar as RES. We then look at different evaluation indicators that have been considered in the optimization of such systems. Finally, we review the optimization techniques that can be employed for optimizing HRESs.

## **2.2. Hybrid Renewable Energy Systems Configurations**

In this section, we provide a review of different hybrid renewable energy systems configurations, which use wind and solar as RES. As solar energy is random and intermittent, an ES system is required for lessening its intermittent characteristic. In Solar-ES systems, the exceeded energy generated by PVs during day time can be stored to meet the load demand at night. Alternatively, the stored energy can be sold to the grid [9-13].

A wind turbine can also be combined with an ES unit in a wind-ES configuration. In such a configuration, the ES, which is in the form of a BS, is used to stabilize fluctuation associated with wind power. Xu et al. [14] employed BS to smoothen fluctuations of generated power and cater for loss of power production from wind in a stand-alone wind-BS system. Moreover, the excessive generated power at night can be used during day time or can be sold to the grid [15].

Solar-BS configuration appears to be superior to the wind-BS system according to [16], as a result of the sudden drop in wind speed. However, [17] presented contrasting results in another area. Likewise, [18] and [19] obtained opposing conclusions in different regions based on the economy of the system. Therefore, it can be seen that design approaches will vary from one region to another because of meteorological and load characteristics, and so, it is important to reasonably select the energy resources for a specific area for which the hybrid system would be used.

Another possible configuration is wind-solar-BS [20-23] so that the deficit power can be obtained from the BS system. The complementary nature of wind and solar in this configuration reduces the storage requirements and improves system availability. For instance, a cost-effective and reliable off-grid hybrid system was developed by [24]. The site for this design has mild winters and dry and hot summers. The optimum results show that the wind-solar-BS and the solar-BS have the same capacity. However, the wind-solar-BS system is realized at a lower cost. In another research, the hybrid system was modelled to minimize the cost by considering seasonal load fluctuations [25]. The results of this

research showed that the combination of wind and solar greatly reduces the required battery storage capacity compared to solar-BS and wind-BS. These results have been also confirmed for ES in the form of fuel cell [26], where the wind-solar-fuel cell combination offers a lower system cost than the solar-fuel cell and the wind-fuel cell.

In addition to an ES system, a wind and solar hybrid system can be combined with other non-renewable sources of energy. For example, in a stand-alone HRES using wind and solar, a backup generator can be used for replacing the energy storage system [27]. In the event that the hybrid system does not meet the load power requirements, the deficit power is obtained from the backup generator. Compared to a sole backup generator system, the wind-solar-backup generator system offers a reduction in pollutant emissions and may also reduce the cost of generating power [28]. Diesel generators improve system economy and guarantee the reliability of the system in the event that the wind-solar system cannot satisfy load, such as in extreme weather conditions.

To further reduce pollutant emissions, an ES system is added to the wind-solar-backup generator system to ensure that the load is satisfied during the time of insufficient power generated by the RES [29, 30]. Nevertheless, batteries have a short lifespan and have to be replaced more often, which increases the maintenance cost of the system. Due to the pollutant emissions from the combustion of diesel, diesel fuel is only used when wind, solar and ES generated power is insufficient [31]. As a result, backup generators guarantee system reliability in the event that the wind-solar-BS system produces insufficient power, for example when there are extreme weather conditions. Other researchers have studied the combination of solar and wind with different sources of energy than diesel, such as solar-gas turbine [32] and wind-hydrogen [15] systems. Although, in isolated areas, the wind-solar-diesel-BS combination is a viable configuration regardless of the pollution caused by diesel generators, using a diesel generator is not considered in this research, as we consider a grid-connected system.

Wind-solar-grid combinations have been considered in [33, 34]. In this setup, the main source of power for the load is from the renewable sources. In the event that the renewable sources cannot meet the load demand, the grid provides the deficit power. It is also common to integrate an ES into the wind-solar-grid configuration [35-38].

In the wind-solar-ES-grid configuration, if the load is not satisfied by the wind-solar system, the deficit power is obtained from the ES. If the power from the ES is still insufficient, the required power will then be obtained from the grid. This combination utilizes the complementary nature of solar and wind and the charge and discharge cycles of the BS to improve the system's reliability. The power

from the grid would reduce energy storage requirements and improve system reliability. Senjyu et al. [35] presented optimum configurations for hybrid systems for a residential building based on a year's actual data for each hour. The model was developed using the average electrical energy consumption of a single house in Okinawa in Japan. The aim was to minimize the total cost of the system, which comprises of the sum of initial, operational, and maintenance costs per year. Xu et al. [36] presented an improved optimization method for a wind-solar-BS HRES in which total system cost was minimized. They developed models for, both, stand-alone and grid-connected systems. Power supply reliability and the total system cost are taken as system preferences. They showed that the grid-connected system could generate smoother power, with higher reliability and lower total system cost.

## **2.3. Evaluation Indicators**

Optimal sizing is essential in a hybrid renewable energy system so that the system can achieve a desired level of reliability with the least possible costs [39]. For optimizing a system, once the usable energy sources have been selected, the mathematical models should be developed. This is followed by identifying objectives, constraints and decision variables. Objective functions are then defined according to the identified objectives. Constraints are due to the limitations that are imposed on the system and limit the possible solutions. Decision variables are the variables that a decision-maker can adjust to achieve the system's optimum performance according to the objectives. An optimization algorithm helps to find the best answer among possible solutions. The effectiveness of an optimization algorithm for finding the best solution, in many cases, depends on the selected objective functions.

Objective functions for optimizing HRES are developed according to different evaluation indicators, which can be categorized as economic, reliability, social, and environmental indicators. The economic indicators are mostly used by researchers in single-objective optimization problems, while economic and system reliability indicators are considered for multi-objective problems. Social and environmental indicators have also been considered together with reliability and economic indicators.

### **2.3.1. Economic Indicators**

Economic indicators evaluate the costs involved in a hybrid energy system and the possible incomes as a result of using the system. The costs include initial costs, operational costs and maintenance costs, and the possible incomes are obtained from selling the excessive generated electricity and the residual value of the components of the HRES at the end of its lifespan. The most

commonly used indicators are net present value (NPV), life cycle cost (LCC), total annual cost (TAC), annualised cost of system (ACS), cost of energy (COE) and levelised cost of energy (LCOE).

NPV which is also referred to as net present cost (NPC) is obtained by subtracting the present discount values of the costs from the incomes. For instance, in grid-connected systems, NPV is calculated as

$$NPV = \sum NPV_{income} + \sum NPV_{end} - \sum NPV_{OM} - \sum NPV_r - C_{investment} \quad (2.1)$$

$NPV_{income}$ : The present discount value of income from selling the excessive generated power to the grid.

$NPV_{end}$  : The present discount value of the residual system's components values at the end of the system's lifetime.

$NPV_{OM}$  : The present discount value for subsequent operation and maintenance costs for the duration of the system's lifetime.

$NPV_r$  : The present discount value for future replacement costs during the system's lifetime.

$C_{investment}$  : The value of initial investment.

LCC is another economic indicator, which is calculated based on present discount value as

$$LCC = C_{investment} + \sum NPV_{OM} + \sum NPV_r - \sum NPV_{end} \quad (2.2)$$

The other economic indicator is TAC, which is equal to

$$TAC = C_{acap} + C_{amain} \quad (2.3)$$

$C_{acap}$  : The system's annual capital costs

$C_{amain}$  : The system's annual maintenance costs.

The capital recovery factor (CRF) formula helps to calculate the annual capital costs from the initial capital costs as

$$C_{acap} = (1 + CRF) \times C_{investment}$$

$$= \left(1 + \frac{i(1+i)^n}{(1+i)^n - 1}\right) \times C_{investment} \quad (2.4)$$

$i$  : The interest rate.

$n$  : The number of years considered for the payback on the initial capital costs.

By adding the annual replacement costs to TAC, another economic indicator is obtained, which is known as ACS and is calculated as

$$ACS = C_{acap} + C_{amain} + C_{arep} \quad (2.5)$$

$C_{arep}$  : The annual system replacement costs.

By taking ratio of summation of ACS to the summation of total annual energy production (TAEP) for the lifetime of the system, another indicator is acquired, called COE. By considering  $E_g(i)$  as the total daily energy production in the day  $i$  of the year  $n$ ,

$$TAEP_n = \sum_{i=1}^{365} E_g(i) \quad (2.6)$$

and

$$COE = \frac{\sum_n ACS_n}{\sum_n TAEP_n} \quad (2.7)$$

and finally, LCOE is defined as the ratio of TAC to  $E_{tot}$ .  $E_{tot}$  is the total annual energy that the HRES produces.

$$LCOE = \frac{TAC}{E_{tot}} \quad (2.8)$$

### 2.3.2. Reliability Indicators

Energy sources employed in hybrid systems are highly unpredictable, and so there is a need for indicators to demonstrate the reliability of a system. Reliability indicators are used to measure the HRES' ability to meet load requirements. The mostly used indicators are the loss of power supply probability (LPSP), loss of load probability (LOLP), deficiency of power supply probability (DPSP), loss of load expected (LOLE) and loss of energy expected (LOEE).



LPSP demonstrates the percentage that a power supply fails to meet the load demand and has been widely used as a reliability index in hybrid systems. LPSP is defined as

$$LPSP = \frac{\sum_{t=1}^T DE(t)}{\sum_{t=1}^T P_{load}(t)\Delta t} \quad (2.9)$$

$DE(t)$  : The deficit energy at time  $t$  (kWh).

$P_{load}(t)$  : The power required by the load at time  $t$  (kW).

$T$  : The total time periods.

$\Delta t$  : The time interval (h).

In some literature LPSP concept is used with a different name as LOLP [40-42]. LOLP is a ratio of all energy shortage to all energy required by the load over a certain time interval. LOLP over one year and with one-hour time intervals is calculated as:

$$LOLP = \frac{\sum_{t=1}^{8760} ES(t)}{\sum_{t=1}^{8760} LD(t)} \quad (2.10)$$

$ES(t)$  : Energy shortage at time  $t$  (kWh).

$LD(t)$  : The load demand at time  $t$  (kWh).

The other similar reliability indicator is DPSP, which is the ratio of all power supply deficiency to all load demand for a certain period and is calculated by

$$DPSP = \frac{\sum_{t=1}^T [LD(t) - E_{sist}(t)]}{\sum_{t=1}^T LD(t)} \quad (2.11)$$

$E_{sist}(t)$  : The energy supplied by the HRES at time  $t$  (kWh).

Deficiency of power supply occurs if the HRES generates insufficient power.

Besides the above reliability indicators, which represent the percentage that a HRES fails to satisfy load energy requirements, other reliability indicators are given as the total yearly hours, which the system fails to support the load demand. For instance, LOLE gives the expected number of hours during the year in which the load requirements are not met. LOLE (h/year) [41, 43-46] is calculated as

$$LOLE = \sum_{h=1}^{8760} \sum_{i \in S} P_i \times T_i \quad (2.12)$$

$S$  : The set of all loss of load states.

$P_i$  : The probability of occurrence of the state  $i$

$T_i$  : The time duration of that the state  $i$  (h)

Using expected values for representing reliability of the system have also been used to calculate the expected loss of energy. LOEE (kWh/year) represents the expected energy value that has not been provided by the hybrid energy system and is equal to

$$LOEE = \sum_{h=1}^{8760} \sum_{i \in S} P_i \times LOE_i \quad (2.13)$$

$LOE_i$  : The amount of energy loss during the state  $i$  (kWh).

### 2.3.3. Social and Environmental indicators

The development of HRESs has both social and environmental impacts. Social indicators represent social impact associated with developing a hybrid energy system. They can be in the form of the job creation and human development index, or can be in the form of the social resistance against employing renewable energy sources as a result of visual impact, use of land, noise pollution or electromagnetic interferences caused by a HRES [47]. From the environmental perspective, the implementation of HRESs reduces pollutant emissions, resulting in more sustainable energy production. Environmental indicators include carbon footprint of energy, amount of carbon emission, life cycle assessment and embodied energy [48], which all indicate the amount of reduction in the greenhouse gas emission as a result of using renewable energy sources.

## 2.4. Optimal Sizing Methods

Optimal sizing methods can be as a single objective optimization (SOO) or multi objective optimization (MOO) problem. SOO problems can be utilized when determining best solutions based on only one objective function, for instance, optimizing a HRES to minimize costs or to maximize reliability. On the other hand, MOO problems integrate at least two separate objective functions and determine a compromised solution, such as optimizing a HRES to minimize its costs and maximize its

reliability, simultaneously. MOO problems can, therefore, improve the reliability and cost-effectiveness of a HRES in contrast to SOO problems, which only minimize costs [49, 50].

Optimizers can be used on an objective function to try to find the most suitable solution [51]. In a SOO problem, the optimizer returns the best solution with regard to one objective function. However, in a MOO problem, there would be a group of solutions called Pareto-optimal points, where one objective cannot be improved without worsening the other objectives. The rest is the designer decision to select a solution among Pareto-optimal points.

Optimizers that have been used in HRES sizing problems are generally classified as classical techniques, modern techniques and software tools. In classical techniques, objective functions are estimated by deterministic or probabilistic functions [52] and their optimum solutions are either found by differential calculus or through searching the whole design space with iterative methods [53]. Designing an HRES, however, involves uncertainties related to renewable energy sources and constraints and technical factors associated with the HRES location and components that made up the system. As the complexity of the problem increases, classical techniques become less efficient in optimally sizing HRESs. Consequently, a shift towards the use of modern techniques based on meta-heuristics algorithms [52, 54] has been seen over the last few years. Such algorithms, which are known as modern techniques, do not use differential calculus for finding descent directions. Instead, they use a large number of points throughout the design space looking for the optimal solution. Although modern algorithms are successful in skipping local minima and identifying the best design region, they may not perform well in local searches. Therefore, they can be combined with the classical techniques to achieve a better performance. This category of optimizers is known as hybrid methods [52, 55]. Hybrid methods have shown better accuracy and convergence in finding optimal solutions and can establish the global optimum solutions. In addition to mathematical methods, there are different software tools, which are available for optimizing HRES. Hybrid Optimization Model for Electric Renewables (HOMER) and Improved Hybrid Optimization by Genetic Algorithm (iHOGA) are the most widely used packages used for finding optimal sizing [55, 56].

#### **2.4.1. Classical Techniques**

Classical techniques are generally used in SOO problems. In [46], the average solar irradiation and wind speed was used to identify an objective function and the problem was optimized based on a classical technique. Although this method is easy to implement, it overlooks many details, which include number of PV panels, PV area and wind turbine heights, which may lead to a solution far away from the optimal point. Other researchers have tried to model objective functions by estimating

the stochastic nature of wind and solar using probabilistic functions [15]. Although it is also simple to obtain objective functions using such probabilistic functions, the model cannot demonstrate the dynamic performance of the system and so it is not suitable for finding the optimal solution. In both of these methods, differential calculus has been used for optimization.

In addition to differential calculus, optimizations based on classical techniques have been done using iterative algorithms. In fact, most of the studies carried out through the use of classical techniques make use of iterative algorithms [23, 36, 57-60]. The authors in [23] used an iterative algorithm to optimally size a standalone solar-wind-fuel cell-BS-hydrogen tank hybrid energy system. The main objective of their design was to minimize the system's total COE. The authors have also used LOEE and LOLE to evaluate the HRES's reliability. The authors in [61] presented an optimization method for a stand-alone solar-wind-fuel cell-hydrogen tank HRES based on an iterative technique. They assessed technical performance of the hybrid system by calculating the fuel cell and electrolyzer powers. Minimizing capital cost of the system was their main objective. The results show that utilizing the complementary characteristics of solar and wind resulted in a reduction in storage requirements, which led to reduced installation costs, while meeting the load demand. The authors in [62] presented an iterative algorithm based on enumeration to optimally size a solar-wind-BS-diesel generator HRES. The feasibility of the HRES was evaluated by minimizing LCC. The system's reliability was assessed by observing the effect of LPSP and renewable energy penetration on LCC. A more efficient iterative algorithm that can be used to find global optimum of various problems is by DIRECT algorithm. The authors in [63] used DIRECT algorithm to obtain the best system components by minimizing the total system cost while guaranteeing energy availability. The authors have used the battery state of charge as well as the balance between generated power and load demand to evaluate the HRES's reliability.

Linear programming (LP) is another classical method that has been used to optimally size a stand-alone solar-wind HRES [64, 65]. The authors in [64] presented a method that employs LP to optimize an off-grid solar-wind-BS HRES by minimizing the total system cost, while meeting load requirements. The authors in [66] used the mixed-integer linear programming (MILP) in optimally sizing a solar-wind-BS-diesel generator system by reducing LCOE over a 20-year system lifetime. The authors in [67] presented a method that uses MILP and exact solve procedure, considering the energy requirements and energy resource maps in determining the location and the optimal combination of components of a solar-wind HRES. The initial system cost was the objective function to be minimized. The results of the study identified the optimal location and the size of the system to minimize initial investment costs.

Analytical methods that make use of theoretical and mathematical analysis and calculations are also part of classical techniques. These techniques utilize computational models to optimize economic feasibility of a hybrid energy system [48]. Certain logical steps must be defined and implemented to obtain an accurate model. This is in contrast to numerical methods, which do not require sequentially specified procedures for obtaining estimated models [68, 69]. Consequently, the computational time required in analytical methods is more than that of numerical methods [44]. The use of these methods has declined in recent years [70, 71]. In [72], an analytical method was used to estimate an objective function based on meteorological data to optimally size a solar-wind-BS-diesel generator hybrid system, taking into account solar irradiation and maximum and minimum wind speed in a year. In this optimization problem, minimizing the use of the generator was the objective function. In addition, state of charge and power balance was utilized in evaluating the HRES's reliability, while the HRES's economy was assessed by the decision to turn on the diesel generator. The authors in [70] also used an analytical technique for minimizing the generation cost of an independent solar-wind system. By comparing the results to Monte Carlo simulation (MCS), the authors were able to validate their results. The amount of meteorological data required for the analytical technique is less than that of MCS. As a result, the analytical technique offers lower computational time in comparison with MCS.

#### **2.4.2. Modern Techniques**

Modern techniques can find a solution to SOO or MOO problems. As a result, modern techniques provide more accurate solutions and have more flexibility when dealing with complex optimization problems. Artificial intelligence (AI) methods are able to manipulate MOO problems and generate the best solutions in the design of hybrid energy systems. In this section, we discuss the most recent AI algorithms that have been used for optimizing hybrid energy systems consist of solar and wind renewable sources.

Genetic Algorithm (GA) is amongst the best AI optimization algorithms. GA has been used by many researchers to determine the optimal size of HRESs [73-78]. The authors in [74] implemented GA for optimally sizing an off-grid HRES. They considered five different load demand combinations and traded a single big diesel generator for a cluster of small diesel generators. The economy, reliability, and environmental aspects associated with the HRES were assessed using the LCC, net dump load, and the total CO<sub>2</sub> emissions, respectively. The results of the study indicate that solar-wind-split diesel-BS hybrid energy system is the most optimal configuration with regards to the lowest LCC, COE, net dump energy and CO<sub>2</sub> emissions. Another key finding from the study is that the use of a cluster of smaller generators instead of one large generator was more cost-effective. In [75], GA was used to optimally size a HRES employing a BS. The main aim was to find the optimal size of the

system by minimizing COE and total cost. Adaptive GA (AGA) is implemented by [79] to optimally size off-grid solar-wind-BS HRES. AGA has an enhanced adaptability and computational simplicity in solving non-linear problems. Meteorological data was used to estimate solar and wind turbine production powers. Minimizing the installation cost of the HRES was the objective function. LOLP was used to evaluate the HRES's reliability. The resulting optimal system satisfied the total system cost as well as reliability requirements. Non-dominated sorting genetic algorithm (NSGA-II) which is an enhanced type of GA was implemented by [80, 81] to solve a MOO problem and the results were encouraging. The authors in [80] used NSGA-II algorithm to optimally size an off-grid solar-wind-BS HRES. Minimizing total cost and DPSP were the economic and reliability evaluation indicators. The DPSP value was estimated by making use of NSGA-II as well as chance constrained programming (CCP) because of the uncertainties associated with renewable resources that affect DPSP value. The study generated more conservative solution sets in comparison to MCS. [81] also used NSGA-II in optimizing solar-wind-BS HRES in a micro-grid. The cost and reliability were evaluated by obtaining minimum total investment cost values; expected energy not supplied and line losses. The authors in [82] used a variation of NSGA-II called controlled elitist GA in optimally sizing an off-grid solar-wind-BS HRES. The authors in this study used a triple multi-objective function combining LPSP, LCC, and expected energy. The obtained optimal solution catered for the reliability, economic and environmental assessment parameters.

Mine blast algorithm was used by [83] to optimize a HRES based on minimizing available transfer capability. The balance of power between load demand and production was used to evaluate the reliability of the system. Real meteorological data was used by the author to optimally size the HRES. A solar-wind-fuel cell system was determined to be the most cost-effective combination.

Particle swarm optimization (PSO) is another widely used heuristic algorithm. PSO is taken as an effective approach for solving real life optimization problems that are non-convex and non-linear. PSO boasts high efficiency, less reliant on gradient information, fast convergence speeds and is quite easy to implement. However, PSO has a possibility of being trapped in local minima. The search ability of PSO over a number of iterations is lost because of the change in velocity drops of the particles, which leads to particles resemble one another. PSO was used by the authors in [84] to find the optimal combination of PV panels, wind turbines, diesel generators, and battery units based on reliability, social cost of carbon and LCOE evaluation parameters. Using large storage units results in less storage units being required and a reduction in replacement cost, while meeting the reliability parameters. Additionally, integrating diesel generators with RES lowers social cost of carbon. The authors in [85] implemented PSO to optimally size a stand-alone HRES using solar, wind, fuel cell and hydrogen tank. Minimizing total cost was the objective function of the problem, whereas reliability of the HRES

was evaluated using LPSP. The optimal solution was based on the lowest total cost over the system life cycle of 20 years. The authors in [86] utilized PSO together with its variants to minimize LCC, while ensuring reliability using LPSP for a combination of solar, wind turbine, and BS. From the results, it can be seen that the PSO with inertia weight presents superior balance between local and global exploration due to the removal of early convergence, generates the lowest LCC in comparison with the first PSO as well as the other forms of PSO. In an analogous study [87], the optimal renewable combination is obtained by minimizing TAC. The conclusion from the results was that the Constriction Factor-PSO (CF-PSO) generates more encouraging results in comparison to other AI algorithms, PSO and its different variants. A modified PSO (MPSO) is presented by [88] to optimally size a stand-alone and grid connected HRES using solar, wind and BS. Minimizing the total initial cost was the objective function being optimized. The algorithm presented in the study was able to generate optimum total initial cost for an off-grid mode. Multi-objective PSO (MOPSO) was implemented by the authors in [49] to optimally size the HRES' economy and reliability, which are made of PV, wind turbine, fuel cell and hydrogen tank over a 20 year period. The objective functions were to obtain minimum values of TAC, LOEE and LOLE of the HRES. The annual system cost is affected by the reliability of each component. Taking this into account, the authors were able to optimize the system based on reliability and cost. MOPSO was also implemented in [89] to optimize a HRES using solar, wind turbine, diesel generator and BS micro-grid. Minimizing COE and LPSP achieves the optimal combination. The authors in [90] implemented PSO to optimally size a stand-alone HRES using solar, wind, BS and fuel cell. They utilized fuzzy logic controller to control energy flow in the HRES. The results of the study indicate that a well optimized fuel cell reduces the variation in batteries' state of charge, which enhances their lifetime.

In addition to GA and PSO, many other heuristic methods have been used for optimizing HRES. A MOO problem was optimized by [91] by using line-up competition algorithm (LCA). Ant colony optimization (ACO) was used to determine the optimal combination of solar, wind turbine, BS and diesel generator based on minimizing TAC [92]. ACO has an inherent ability of parallel computing, which enables it to solve complex problems that behave dynamically. A variation of ACO which uses integer programming called  $ACO_R$ , for continuous domains, was used by [93] to optimize a HRES. Preference-inspired coevolutionary algorithm (PICEA) has also been used for optimizing MOO problems [94, 95]. Authors in [96] made use of an improved Fruit-fly optimization algorithm (IFOA) to optimally size a stand-alone HRES using solar, wind, backup generator and battery. A population inspired technique called biogeography-based optimization (BBO) was utilized by [97, 98] to optimally size HRES comprising of solar, wind turbine, and other sources and storage units. In [99], the authors implemented artificial bee colony (ABC) to find best combination of solar-wind-biomass-battery storage HRES to minimize cost and improve reliability. Imperial competitive algorithm (ICA)

was used in [100] to optimize an off-grid and grid-connected HRES. Cuckoo search (CS) is another metaheuristic algorithm, which addresses multi-objective and complex optimization problems. Discrete harmony search (DHS) was used by [18] to optimize solar, wind, BS and diesel generator for minimizing TAC and total gas emissions. Stochastic trust-region response-surface (STRONG) technique was used by [101] in minimizing total cost of a HRES using solar, wind, battery and backup generator.

### **2.4.3. Hybrid Techniques**

AI optimization algorithms give sufficiently accurate group of best solutions in a quick computing time and a relatively low convergence. Nevertheless, as the use of solar-wind hybrid energy systems is rapidly growing, especially for off-grid applications, even more advanced and accurate optimization strategies are required. Hybrid algorithms are a mixture of at least two single algorithms (classical or modern), which complement each other in solving complicated optimization cases. Each one of the algorithms may have different constraints.

The GA has been combined with multi-objective evolutionary algorithm (MOEA) in [102]. The authors have first used MOEA to size the components by minimizing NPC and some other social indicators and then applied GA to determine the best control strategy based on NPC. A hybrid artificial neural network (ANN) and Monte Carlo Simulation (MCS) based GA optimization algorithm presented in [103], where solar irradiation and wind speed time series were generated using MCS to be used by an ANN-based GA. Hong et al. [104] proposed a Markov-based GA to optimize a HRES employing solar, wind, and diesel generator based on minimizing total system costs as well as CO<sub>2</sub> emissions, and the reliability was evaluated using LOLP. In their work, solar panels, wind turbines and load demand were modelled by Markov processes, while the optimal size was found using GA. The iterative method and GA have been combined in [105] to optimally size an off-grid solar, wind turbine, and BS system. For this purpose, first, a set of possible combinations of components of the hybrid energy system were generated using iterative method and then GA was used to find the optimal sizing. The GA has been combined with an exhaustive-search technique and used by [106] to optimize a stand-alone solar, wind and BS HRES by minimizing total cost and LPSP.

PSO can be combined with mutation operator from GA to prevent being trapped in local optimum values, resulting in the hybrid big bang–big crunch (HBB-BC) algorithm. The authors in [107] used HBB-BC in optimizing an off-grid hybrid solar, wind and BS system by minimizing total present cost and energy not supplied. Moreover, natural selection particle swarm optimization (NSPSO) is the combination of the selection strategy of GA and PSO. NSPSO was used by [50] to enhance the



accuracy of optimum results. An improved simulated annealing particle swarm optimization (SAPSO) method was presented by [108] to optimally size a HRES. Integrating an improved simulated annealing (SA) with PSO improves accuracy and extent to which the process can search.

The SA algorithm has also been combined with Tabu search (TS) method [109]. The SA offers fast convergence in the area close to the best solutions. On the other hand, TS, offers good efficiency in determining the optimal solution for a specific locality. Combining SA and TS offers advantages of improved solutions when dealing with more complex optimization problems. A discrete chaotic harmony search-based simulated annealing algorithm (DCHSSA) was proposed by Askarzadeh [110]. DCHSSA combines chaotic search (CS), harmony search (HS), and simulated annealing (SA). In [111], the authors presented harmony search-based chaotic search (HSBCS) which was used to optimize a solar-wind-BS HRES using reverse osmosis (RO). The wind and solar forecasting have been done using ANN, while system components were optimally sized using HSBCS. A hybrid flower pollination algorithm (FPA) and SA algorithm were proposed by [112] to optimally size solar-wind and BS HRES with the most cumulative savings as well as increased reliability.

Hybrid teaching-learning-based optimization algorithm (TLBO) is another hybrid method, which comprises of the size of the population as well as the parameters for the number of iterations. Improved TLBO was used by [113] for optimizing a solar, wind turbine, diesel generator and BS HRES. The authors used the fuel cost and TAC to assess the economy and LPSP to evaluate the system's reliability. Iterative-Pareto-Fuzzy (IPF) method combines iterative, fuzzy, as well as Pareto optimality methods and used by [114] to find the best solution for a stand-alone HRES using solar, wind, and BS to minimize the total cost, while considering reliability of the system according to the net dump energy, energy index of reliability and expected energy not supplied. Total system cost and net dump energy were minimized, while system reliability was maximized using the proposed algorithm. Long-term wind speed data was combined with estimated solar irradiation in [115] to optimize a HRES.

#### **2.4.4. Computer Software Tools**

Various software tools have been employed to optimally size HRES [116]. Hybrid optimization model for electric renewables (HOMER), developed by the U.S. National Renewable Energy Laboratory, is the most used software tool for optimizing capacity of HRES based on economic indicators. HOMER has the ability to simulate and optimize conventional and renewable energy systems including ES systems in stand-alone and grid-connected modes. The meteorological data from the past is used according to the area of the site to optimally size the HRES. HOMER Pro is an

enhanced edition of HOMER, which has additional attributes including options for load profile, limits on monthly demand, advanced battery characteristics, multi-year module, and capability of linking with Matlab software. However, HOMER only allows SOO based on optimizing NPC with the user having to insert the input variables [117].

Improved hybrid optimization by genetic algorithms (iHOGA) is another commonly used software tool for optimally sizing HRES. iHOGA is an optimal sizing software tool that is written by the University of Zaragoza. Input details for component, economy and resource constraints can be used to carry out the optimal sizing process. Simulation of the system is conducted over an hour interval during which all variables of the system are kept the same. GA is used in the software to optimize single or multi- objective functions as well as optimizing control procedures offering a lower computing time in comparison with GA alone. Additionally, iHOGA uses Monte Carlo Simulation for conducting probabilistic evaluation [46, 103]. An analysis for buying and selling electrical energy in grid-connected mode with various cases of net metering [48, 118] can also be performed in the software. The software also allows selling of the surplus hydrogen that the electrolyzer produces. A maximum power point tracking (MPPT) option in the solar panel charge controller and an estimation of the lifespan of the batteries [119], according to the model proposed by [120], can be considered. Furthermore, the inverter efficiency is considered as a function of the output power. The wind turbine height, air density and atmospheric pressure are also considered in the optimization process. Social indicators can be included in its version 2.0 PRO plus. The optimal size of HRES can be obtained by minimizing NPC and other variables.

Renewable Energy Research Laboratory of the University of Massachusetts created another software tool called HYBRID2. HYBRID2 supports simulation steps between 10 minutes to 1 hour, which is more accurate than HOMER and iHOGA. Therefore, it can be used in collaboration with HOMER or iHOGA to improve the accuracy of the optimization solution.

The aforementioned software tools are utilized in determining the optimal design of HRES for various locations across the world. In addition to them, MATLAB, HYBRIDS, RETSCREEN have also been widely used. HOMER has been used by [121] to determine the optimal HRES components combination and then the results have been used in Matlab to conduct energy management for the resulting HRES. HOMER Pro was used by [117] to find the optimal size of a solar-wind turbine-battery storage system. The system was able to achieve a minimum NPC. The authors in [122] employed iHOGA to optimally size a HRES to minimize the CO<sub>2</sub> emissions, COE and NPC. Also, iHOGA have been used to optimize a system based on MOEA algorithm and GA hybrid technique [123].

## 2.4.5. The Comparison of Algorithms

PSO is a widely used algorithm in optimization of HRESs because of its simplicity, flexibility and good performance. Nevertheless, the performance of PSO in optimizing a system with four or more decision variables is low and as a result, the optimization solutions become inadequate. Additionally, PSO may have a tendency of being stuck in local optima [124]. SAPSO was proposed by [108] to overcome the limitations of PSO. SAPSO has the ability to circumvent sticking at local optima, improves the diversity of PSO such that non-coordinate system can be solved, and reduces the computational time which improves the global searching. Improvements on computational time and convergence can be made on PSO. MPSO was proposed by [88] in determining the optimal combination of RES with the lowest investment cost. MPSO gave shorter computational time and faster convergence in comparison to PSO.

SA is a suitable choice for problems involving global optimization. SA has low accuracy solutions when compared to PSO, GA and other algorithms [87, 112, 124]. As a result, SA is not widely used in optimizing HRES. Combining SA with a search algorithm can be done to take advantage of SA's ability to avoid being trapped in local optima. A combination of SA with CS and HS gives DCHSSA. DCHSSA generates more accurate solutions in sizing HRES in comparison with DHSSA and DSA [110]. TS has the ability of avoiding being trapped in the local optima. Nevertheless, TS requires big number of simulations and has to begin from a feasible solution. The authors in [109] determined that combining TS and SA overcomes these limitations. SA can be used to determine the initial feasible result which is then supplied to TS.

GA can also avoid being trapped in local optima, but a large number of iterations are required, which increases the computational time [124]. Combining an exhaustive search algorithm with GA can overcome this limitation. The resulting hybrid algorithm can utilize GA's good convergence as well as its ability to avoid being stuck in local optima and advantage of lower computational time and effectiveness of an exhaustive search algorithm in finding optimal results [106]. The long computational time of GA can also be overcome by using a stochastic model for example Markov or chronology to forecast future state assumed from its current state. The high performance of GA can be combined with PSO to improve the accuracy of the solutions and global optimization ability [50]. A comparison of ACO with ABC and GA revealed that while optimal cost solutions are identical, ACO generated optimal solutions with fewer iterations and lower computational time [93].

Renewable energy sources are random in nature. As a result, the starting input data for the optimization methods are diverged and unbounded. Consequently, the results of the optimization

process may not be near the minimum global solutions. Sanchez et al. [85] assessed the PSO technique in optimally sizing HRES. For random initial conditions, PSO has provided optimal values near the global optimal solutions. Therefore, it is highly recommended to use PSO to optimize HRES with unbounded random initial conditions. Using a combination of algorithms can compensate for decay in population diversity and avoid being trapped in local optima.

## **2.5. Summary**

In this chapter, we first provided a literature review on the research that has been done on different configurations of HRES based on wind and solar RES. This followed by covering different evaluation indicators such as economic, reliability, social and environmental that are used for defining objective functions for optimally sizing HRESs. Finally, different solvers that have been used for obtaining optimum solutions in SOO and MOO problems were discussed and compared. This includes classical techniques, modern techniques, hybrid techniques and software tools.

## Chapter 3 : MATHEMATICAL MODELLING

### 3.1. Introduction

Classical techniques, especially those that are fundamentally based on searching the whole design space with iterative methods, can be utilized to find the solution of most optimization problems. However, the optimization of HRESs consisting of solar PVs and wind turbines is more complicated, and classical methods show some inadequacies in finding optimum solutions. Contemporary algorithms based on learning strategies provide more reliable optimal solutions. The majority of these algorithms are nature-inspired algorithms. In cases that meteorological data are not available, hybrid algorithms are better options for estimating such data and optimizing the problem. However, in this research, we have access to the required meteorological data and so we only use solvers to find the optimum solutions.

GA and PSO are widely used to optimally size HRESs. GA can avoid being trapped in local optima, but a large number of iterations are required, which increases its computational time. PSO, on the other hand, has less computational complexity and, at the same time, shows a good performance in three-dimensional coordinate problems, such as the one we have in hand in this research. Therefore, in this study, GA and PSO are employed to optimally size the HRES. In this chapter, we first provide an overview of GA and PSO, followed by providing mathematical models for different renewable energy sources of the PV-wind turbine-BS HRES.

### 3.2. Genetic Algorithm

GA is an optimization technique that is used to optimize constrained and unconstrained problems on the basis of the process of natural selection. GA does not use gradient information and as such, non-differentiable functions and functions with many local optima can be solved using GA. In GA, each individual in the population represents a possible solution to the optimization problem. A fitness value is assigned to every individual representing its goodness as a solution. Individuals who are extremely fit are given a chance to reproduce with other members of the population by cross breeding. The resulting offspring has features of each parent. The individuals with the lowest fitness are unlikely to get a chance to reproduce and therefore will die out.

If the finest individuals of the present population are mated, a new generation having a higher proportion of traits from the finest individuals of the preceding generation is produced. Subsequently,

over many generations, desired traits are spread throughout the population. Mating the superior individuals allows for the exploration of the best regions in the search space. By carefully designing the GA, the population will converge to the best solution of the problem.

Initially, a representation of the optimization problem is defined. A random process is then used to generate the starting population of strings. Thereafter, a set of operators are employed to generate consecutive populations that improve them over time. These operators are known as the selection operator, crossover operator and mutation operator. Figure 3-1 shows the flowchart of GA.

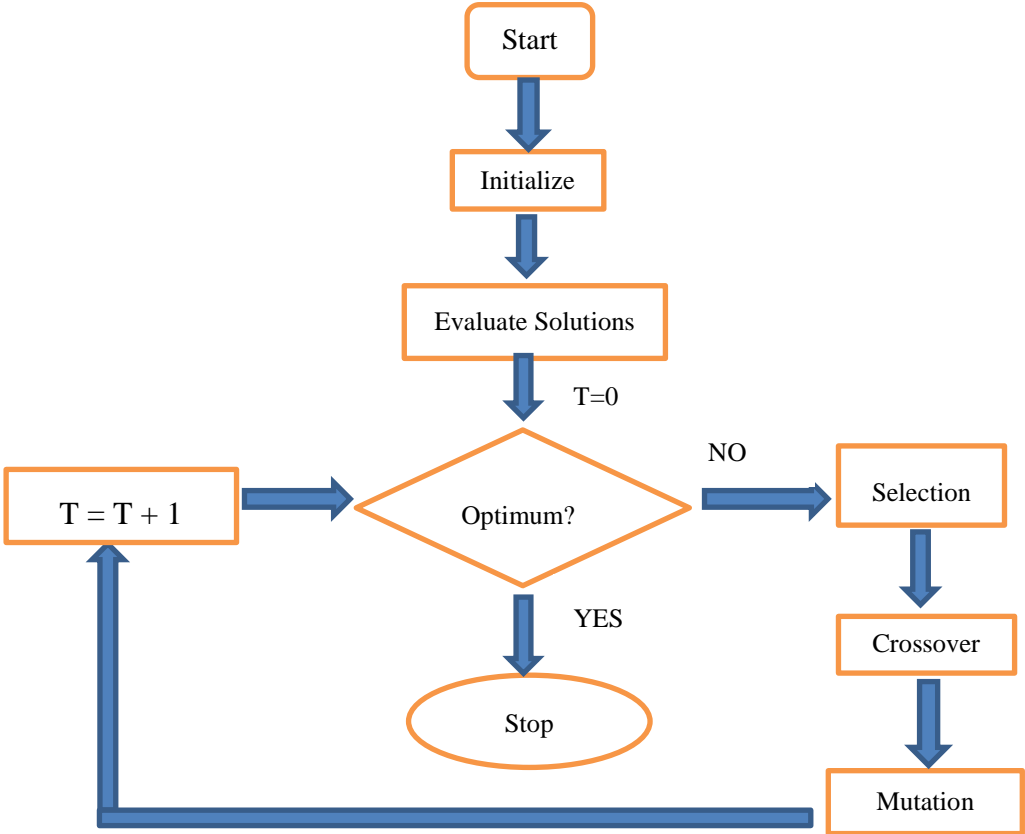


**Figure 3-1: Flowchart of GA**

**3.2.1. Selection Operator**

The selection process selects the optimal candidates and discards all the other solutions. The objective function value is used to make the selection. The solutions to be kept are determined and allowed to be reproduced. Also, the unfit strings are eliminated to keep the size of the population constant. Functions of the selection operator are as follows:

- Identify the optimal candidates in a population
- Replicate optimal candidates
- Eliminate bad candidates and replace them with the optimal candidates

The objective function is used to assign a measure of performance, known as the fitness score, to each individual according to a specific set of parameters. The fitness function converts that measure of performance into an assignment of reproductive chances. The assessment of one string expressing a set of parameters is independent of the assessment of any other string. However, the fitness of that string is always defined relative to other individuals in the current population.

In GA, fitness score is determined as  $f_i/f_A$  where  $f_i$  is the assessment related to string  $i$  and  $f_A$  is the average assessment of the entire string population. Selection in GA can be implemented using different algorithms including tournament selection, roulette wheel selection, rank selection, and steady state selection.

In tournament selection, a few individuals play many tournaments and then individuals are selected at random. The best solution of the first round is chosen for the next generation. Changing the tournament size can adjust the selection pressure. If the tournament consists of many individuals, the likelihood of selecting weaker individuals is low. Hence, the worst solution will not have copies, while the best solution will have two copies.

In roulette wheel selection, a fitness score is used to select parents. The worse chromosomes (bad solutions) have less chance of being selected, while the better chromosomes (best solutions) have a higher chance of being selected. The bad solutions are represented by the smaller sectors in the roulette wheel and the better solutions by the larger sectors as is shown in Figure 3-2. The arrow in the diagram represents the selection point. The larger sectors (best solutions), therefore, have a higher chance of being selected.

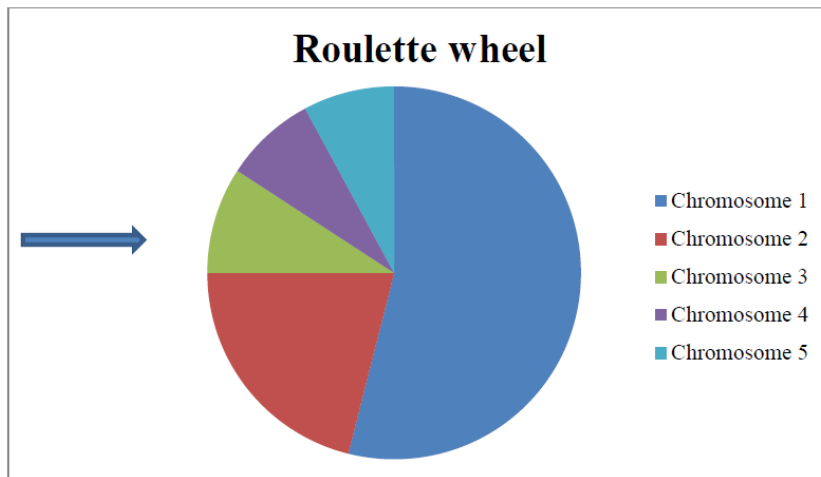


**Figure 3-2: Roulette selection wheel**

In the rank selection, the population is first sorted and ranked according to the fitness value. Each chromosome is assigned a selection probability based on its rank. Rank selection prevents premature convergence and overcomes scaling problems such as stagnation. Rank selection is more robust than other methods. The sum of ranks is first computed after which the selection probability of each individual is computed.

In steady state selection, some of the chromosomes, which possess superior traits, are used for generating new offspring in every successive generation. A few of the chromosomes having fewer desirable traits are discarded and replaced with the new offspring. The rest of the population is passed onto the next generation without going through the selection process.

### **3.2.2. Crossover Implementation**

Initially, the selection operator is used to generate optimal strings from the current population. The crossover operator is then applied to generate new solutions from the optimal strings of the previous population. A pair of offspring is produced by mixing elements of two parents resulting in an exchange of gene information. The information of the elements is encoded into a series of strings to represent a particular solution.

The most commonly used method for encoding is binary encoding. The string of 0s and 1s represent a chromosome and each location on the chromosome corresponds to a specific trait of the optimization problem. An example of binary encoding for two variables is given in Figure 3-3.



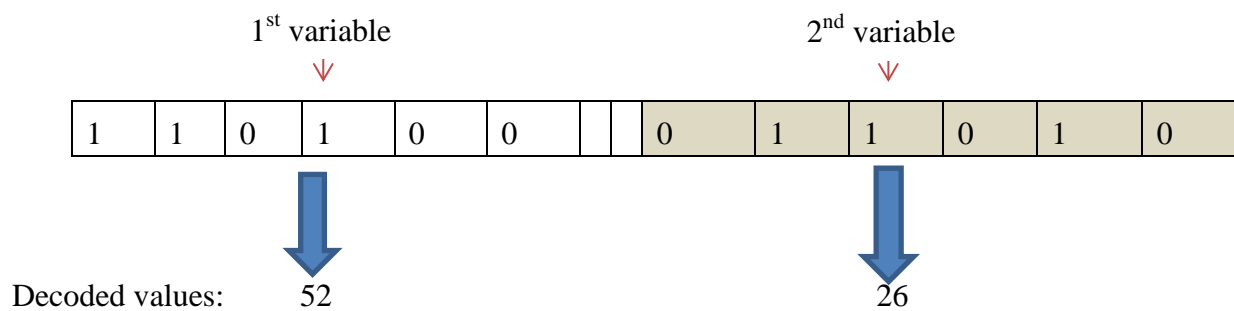


**Figure 3-3: Binary encoding in GA**

Thereafter, two solution strings from the mating pool are randomly selected. Parts of these strings are swapped between the two strings. The point of selection is taken at random. In order for a solution to go for crossover, a probability of crossover is introduced so as to give freedom to an individual solution.

The best individuals will most likely be selected many times in a generation; bad individuals may not be selected at all. After two parents have been selected, their chromosomes are integrated, generally by making use of crossover and mutation. Crossover is not normally applied to every pair of individuals chosen for mating. Not all chromosome pairs selected for mating experience crossover, the chance of crossover being applied is 0.6 to 1.0. Offspring are duplicated from the parents if crossover is not applied. This allows each individual an opportunity of passing on its genes without the interference of crossover.

### 3.2.3. Mutation Operator

Mutation is the random alteration of string values into the solution string of the population. Mutation has the effect of maintaining population diversity. While crossover is primarily used to search for the optimal solution, mutation can also help to achieve this purpose. Figure 3-4 illustrates how mutation occurs on the fourth gene of the chromosome. In binary mutation, the operator changes a 0 to a 1 or vice versa. Steady convergence is achieved by making the probability of mutation closer to zero.

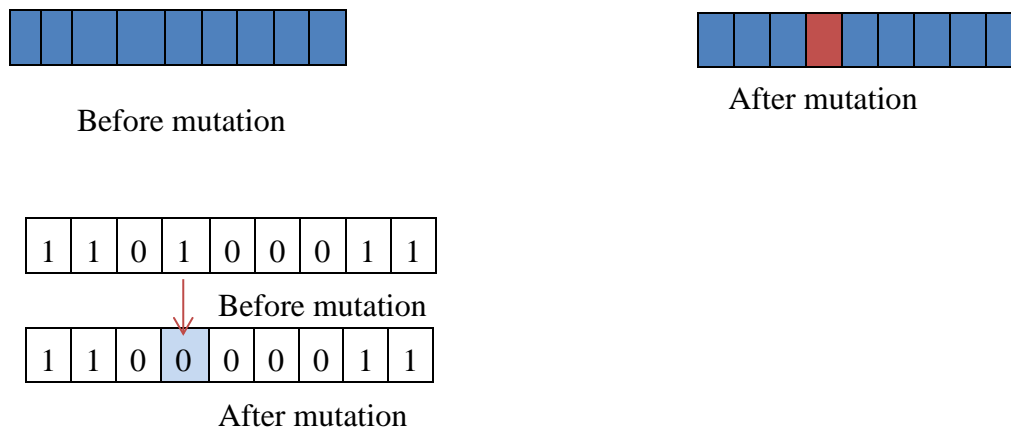


**Figure 3-4: Mutation in GA**

When crossover is complete, the mutation operator can then be utilized separately on individual offspring. Each gene is randomly altered with a low probability. The conventional view is that crossover is more significant than mutation for the fast exploration of the search region. Mutation guarantees that every point in the search region gets an opportunity to be explored.

In every iteration, the fitness of the above average individuals in each generation increases towards the optimal value. If 95% of individuals in a population share a gene, the gene is said to have converged. The population converges when all of the genes have converged. The fitness approaches the optimal individual when the population converges.

GA will always be prone to stochastic errors. Genetic drift is one of such problems. Even if there is no selection pressure (i.e. a constant fitness function), the individuals will still converge to some point in the search region. This occurs as a result of the accumulation of stochastic errors. A predominant gene in the population is likely to become more predominant in the next generation. Sustaining such dominance over many successive generations, in a finite population will result in the gene spreading to all members of the population. When a gene has converged in this manner, it is fixed. This means no new genes can be introduced by crossover. Similarly, as generations proceed, each gene eventually becomes fixed. The rate of genetic drift consequently gives a lower bound on the rate at which a GA can converge towards the optimal solution. In a case where GA has to utilize gradient information in the fitness function, the fitness function should supply a slope adequately large to prevent any genetic drift. Increasing the mutation rate can reduce the rate of genetic drift. Nevertheless, the search becomes effectively random should the mutation rate become too high, therefore the gradient information in the fitness function is not utilized. Elitism is also a method to preserve the population

pool. Elitism protects the best solutions from being destroyed by crossover and mutation and is defined in percentage or in number. The typical GA procedure is as follows:

1. Select starting population
2. Set a fitness basis
3. Carry out elitism
4. Carry out selection
5. Carry out crossover
6. Carry out mutation

### **3.3. Particle Swarm Optimization**

PSO is a stochastic optimization algorithm based on the behaviour of a population of some creatures like a flock of birds or school of fish. The swarm is made up of particles that have random velocities, and each particle represents a possible solution to the optimization problem. PSO is intuitive, simple, easy to implement, and has wide adaptability to various kinds of functions.

PSO determines the optimal solution by moving the particles through the solution space. The application of PSO is quite simple and straightforward, requiring just a few lines of programming code. The mathematical operators in PSO are simple, and as such, PSO is computationally economical with regard to both speed and memory requirements. PSO possesses features of both evolutionary strategies and GA. As a matter of fact, PSO does not require the differentiation of the objective function, and it offers fast computing time and simplicity and ease of being programmed. Combining PSO with other algorithms can eliminate being stuck in local optima and improve its performance.

PSO has experienced many enhancements since being presented in 1995. Newer modifications of PSO include chaotic and fuzzy PSO. PSO can be hybridized with other algorithms, such as with GA, simulated annealing, ant colony algorithm, Tabu search, harmonic search and artificial bee colony. In PSO, the particles are observed to follow a common approach in searching for food. Individual particles use their experiences and those of other particles to alter their search path.

The position and velocity of particles in PSO are updated based on the changes in environment to meet the stipulation of quality as well as closeness. The position of the particles is updated every iteration. The iteration index in PSO is denoted as  $t'$  where  $t' = 1, 2, \dots, t'_{max}$  and  $t'_{max}$  is the maximum number of iterations, which is adjusted by the user. The particles progress towards better positions in the search space. Initially, a particle population is generated randomly in the search space. Each particle is then able to use memory to navigate through

the search space in search of a better position than the present one. The particles are able to memorise their best experience,  $pbest$ , and best experience of the entire population,  $gbest$ . During each iteration,  $t'$ , the position of each particle is updated as follows:

$$v_j(t' + 1) = w(t')v_j(t') + c_1r_1[pbest_j(t') - x_j(t')] + c_2r_2[gbest(t') - x_j(t')] \quad (3.1)$$

$$x_j(t' + 1) = v_j(t' + 1) + x_j(t') \quad (3.2)$$

$x_j$  : Particle's position

$t' = 1, 2, \dots, t'_{max}$  : Iteration index

$j = 1, 2, \dots, N_p$  : Particle's index

$v_j$  : Particle's velocity

$r_1$  and  $r_2$  : Random numbers with uniform distribution form [0 1]

$c_1$  and  $c_2$  : Individual and social learning factors respectively

$w$  : Inertia weight

Inertia weight is adaptive and offers a good balance between local and global searches. A small inertia weight results in a local search while a large one results in a global search. In many cases the  $w$  value is updated as the iterations proceed as follows:

$$w(t') = w_{max} - \frac{w_{max} - w_{min}}{t'_{max}} \times t' \quad (3.3)$$

$w_{max}$  : Final inertia weight

$w_{min}$  : Initial inertia weight

Additionally, there are no restrictions of particle movement. Particles are free to search for the best solution in the search region. Figure 3-5 illustrates PSO flowchart.

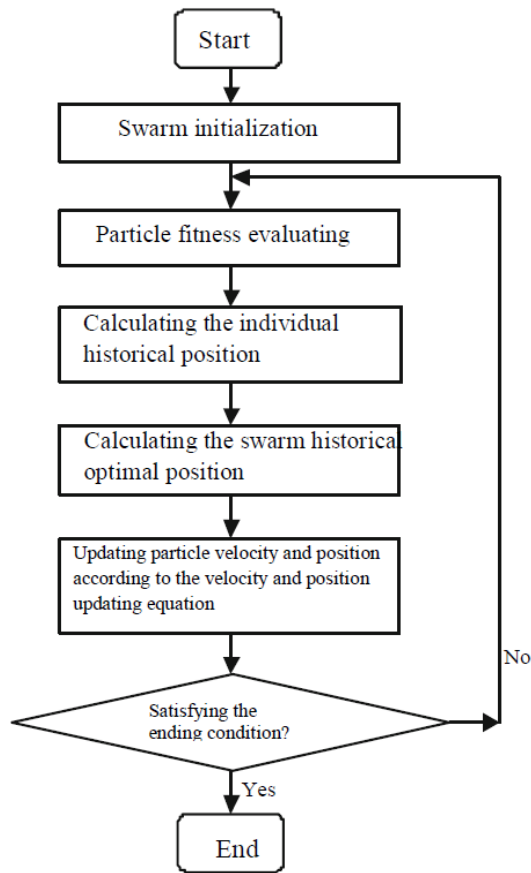


**Figure 3-5: Flowchart of PSO**

In summary: PSO has particles, which are possible solutions to an optimization problem. Each particle has the capability of memorizing its best position together with best position of the other members of the population. In addition, each particle has its own velocity. The particles are able to change their velocity and position based on the changes in the search region until the best solution is attained. Objective functions are used to connect various dimensions of the search space.

There are two types of PSO; local and global types. In local type, individual particles only track their best position referred to as *pbest* while in the global type, particles track *pbest* and the global best referred to as *gbest*. In many PSO methods, particles search for solutions largely due to chaoticity. These variations of PSO provide a thorough exploration of the search region compared to typical PSO. For instance, Foragers follow a Levy distribution and Richer and Blackwell in 2006 used this distribution to develop Levy PSO ( $PSO_{levy}$ ), which showed better performance compared to a standard

PSO. The Levy PSO overcomes the drawback of premature convergence and getting stuck in local optima. In PSO<sub>levy</sub>, (3.1) is replaced with the following equation:

$$v_j(t' + 1) = w(t')\mathbf{Levy}_j(t') + c_1r_1[pbest_j(t') - x_j(t')] + c_2r_2[gbest(t') - x_j(t')] \quad (3.4)$$

**Levy** : Vector with elements,  $lv$ , produced by the Levy distribution

The Levy distribution is generated by

$$lv = \frac{u}{|v|^{1/\beta}} \quad (3.5)$$

Where  $u$  and  $v$  are Gaussian random variables with the probability density functions of

$$u \sim N(0, \sigma_u^2) : \sigma_u = \left( \frac{\Gamma(1 + \beta)\sin(\beta\pi/2)}{\Gamma((1 + \beta)/2)\beta 2^{(\beta-1)/2}} \right)^{1/\beta} \quad (3.6)$$

$$v \sim N(0, 1) \quad (3.7)$$

$\Gamma$  : The standard gamma function

$\beta$  : An adjustable parameter (usually taken as 1.5)

As it is seen, in PSO<sub>levy</sub>, a Levy method replaces the velocity memory. By employing Levy flight, particles have a possibility of making lengthy jumps even in their final iterations, which enhances the original PSO global search capability.

For MOO problems, individual functions can be optimally sized, separately. However, it is likely that the objectives are in conflict, and therefore, it is highly unlikely that all objectives will be satisfied by the same solution. Consequently, Pareto optimal results can only be determined. In GA, there is bidirectional sharing of information between chromosomes during the crossover operation. However, in PSO algorithms, particles only receive information about  $gbest$  or  $pbest$ . As a result, selecting  $gbest$  and  $pbest$ , is the main problem of MOO. Selecting  $pbest$  follows an identical principle as standard PSO algorithm; however,  $gbest$  is found based on the Pareto dominance.

### 3.4. Modelling of the Renewable Energy Sources

This study considers a grid-connected HRES employing PV and wind turbine. In this section, we provide the mathematical models for the components of this HRES.

### 3.4.1. Wind Turbine Model

A wind turbine converts kinetic energy of the wind into electrical energy. The power output of a wind turbine,  $P_{WT}$ , can be calculated using wind speed,  $v$ , as [125]:

$$P_{WT}(v) = \begin{cases} 0 & v < v_{ci} \\ P_{rated} \times \frac{v - v_{ci}}{v_r - v_{ci}} & v_{ci} \leq v < v_r \\ P_{rated} & v_r \leq v < v_{co} \\ 0 & v \geq v_{co} \end{cases} \quad (3.8)$$

$v_{ci}$  : cut in speed

$v_r$  : rated speed

$v_{co}$  : cut-out speed

$P_{rated}$  : rated power of the wind turbine

According to (3.8), the power output of wind turbine is zero for wind speeds below  $v_{ci}$  and above  $v_{co}$ . We assume that as the wind speed increases from  $v_{ci}$ , the wind turbine output power increases linearly according to the wind speed,  $v$ , until reaches  $v_r$ . The wind turbine generates rated power for wind speeds between  $v_r$  and  $v_{co}$ . Figure 3-6 shows the wind turbine output curve.

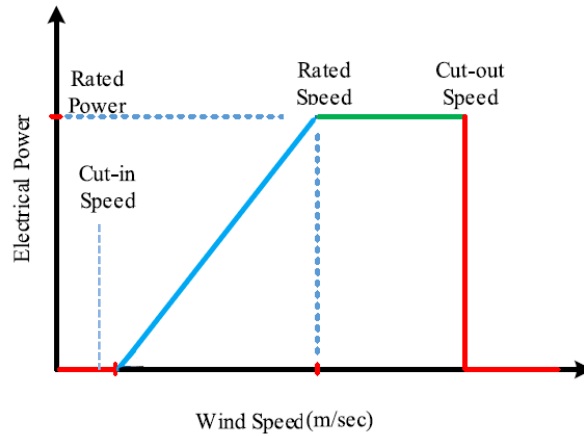


**Figure 3-6: Wind turbine output curve**

### 3.4.2. Solar Photovoltaic Model

A solar PV converts solar energy to electrical energy. Area, efficiency, solar irradiation and atmospheric temperature are factors that affect the output power of a PV generation system. The PV system is assumed to be equipped with a MPPT to maximize power generation of the PV system. The PV system's hourly output power can be calculated as

$$P_{PV}(t) = A_{PV}\eta_{PV}I(t)(1 - 0.005(T_0(t) - 25)) \quad (3.9)$$

$A_{PV}$  : The panel area in  $m^2$

$\eta_{PV}$  : The panel efficiency

$I$  : The solar irradiation in  $kW/m^2$

$T_0$  : The atmospheric temperature in  $^{\circ}C$

### 3.5. Summary

In this chapter, an overview of the GA and PSO was given. GA and PSO are selected as they are widely used to optimally size HRESs. GA can avoid being trapped in local optima, but a large number of iterations are required, which increases its computational time. PSO, on the other hand, has less computational complexity and, at the same time, shows a good performance in three-dimensional coordinate problems, such as the one we have in hand in this research. Thereafter, the renewable energy sources used in our considered HRES were modelled, which were the wind turbine and solar PV.



## Chapter 4 : METHODOLOGY

### 4.1. Introduction

This chapter covers the operation of the considered hybrid energy system and the definition of an optimization problem to identify the system's optimal sizing with respect to the size of the employed RES and BS. The hybrid energy system, which we consider in this study, is shown in Figure 4-1. It consists of PV arrays, wind turbines and battery storage systems. The selected wind turbines are considered to be equipped with internal rectifiers and battery storages. As a result, the output of the wind turbine is in the form of DC power. The output of PV arrays, wind turbines and BS are all integrated into a DC bus. Although it is common that a grid-connected hybrid system injects its excessive generated power back to the grid, the eThekweni municipality has not finalized its small-scale embedded generation (SSEG) systems' tariffs. Therefore, in this research, instead of injecting the excessive power generated by RES back to the grid, we try to find the best solution to store the energy within the system or dump it if necessary.

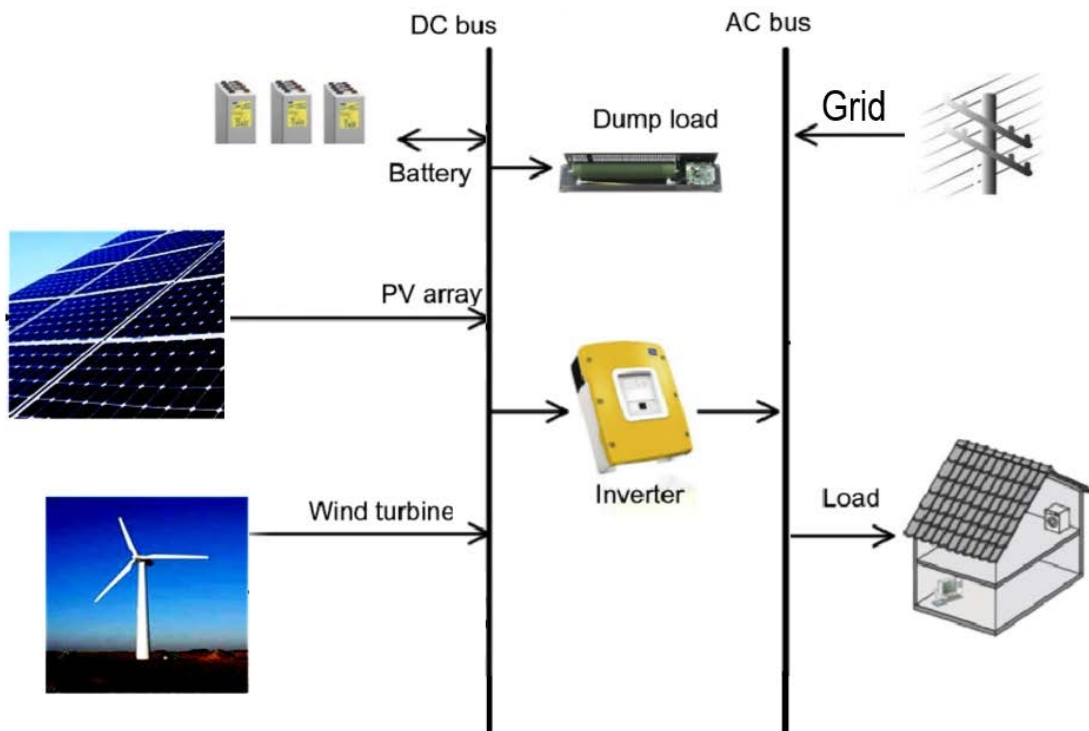


Figure 4-1: Block diagram of the grid-connected hybrid RES

## 4.2. Meteorological Data

The meteorological data used in this research, which includes global horizontal irradiance (GHI), temperature and wind speed, are obtained from the Southern African Universities Radiometric Network (SAURAN) database [126, 127]. The collected data are from the University of KwaZulu-Natal, Howard College Campus station, where its geographical location is given in Table 4.1. We used the average hourly data (8760 hours).

**Table 4-1. THE METEOROLOGICAL STATION LOCATION**

Location	Latitude	Longitude	Elevation	Topography
Durban, South Africa	-29.87097931	30.97694969	150 m	Roof of Desmond Clarence building

Figure 4-2 (a) shows the annual hourly GHI data of the given station. The sensor, which is used for the GHI measurements, was Kipp & Zonen CMP11 pyranometers. The histogram of the annual hourly GHI data and their corresponding statistics are given in Figure 4-2 (b) and Table 4-2, respectively. As is seen, the average hourly GHI for Durban is  $189 \text{ W/m}^2$  with the peak value of  $1116 \text{ W/m}^2$ . Considering there is no solar radiation during the night, the average hourly GHI during daytime can be estimated as  $323 \text{ W/m}^2$ .

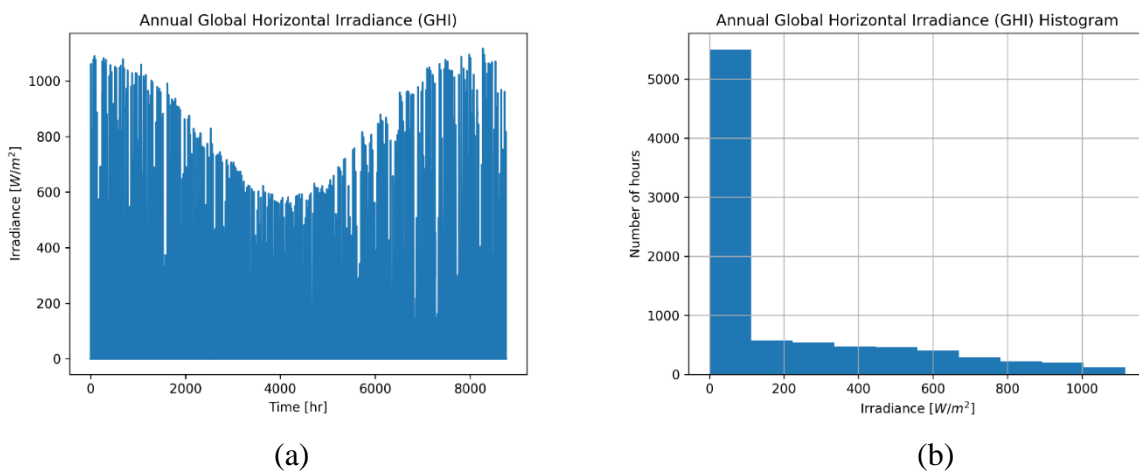


**Figure 4-2: Annual Global Horizontal Irradiance (GHI) data**

**Table 4-2. GHI STATISTICS (W/m<sup>2</sup>)**

mean	std	min	25%	50%	75%	max
189.02	281.62	0.0	0.0	4.51	323.73	1116.0

According to equation (3.9), in addition to the GHI data, the temperature data are also needed to estimate the PV panels' output power. Figure 4-3 (a) shows the annual temperature data of the given station, and Figure 4-3 (b) shows their histogram. The statistics for the annual temperature data are also given in Table 4-3, which shows the average hourly temperature of 20.65 °C, a maximum temperature of 34.99 °C and a minimum of 10.63 °C.

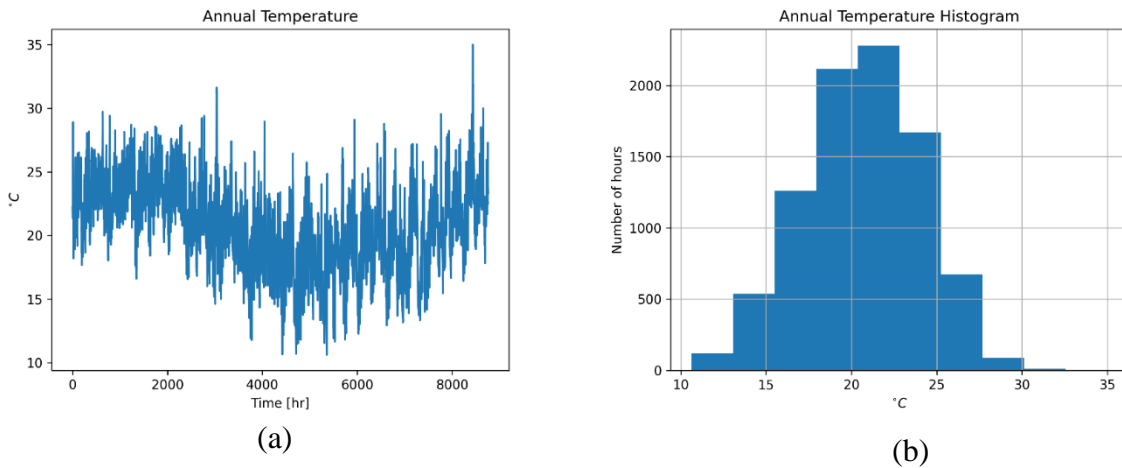


**Figure 4-3: Annual temperature data**

**Table 4-3. TEMPERATURE STATISTICS ( °C)**

mean	std	min	25%	50%	75%	max
20.65	3.43	10.63	18.33	20.75	23.10	34.99

Figure 4-4 (a) shows the annual wind speed data of the given station. According to equation (3.8), these data will be used to estimate the output power of the wind turbines. Moreover, the histogram of

the annual wind speed and their statistics are shown in Figure 4-4 (b), and Table 4-4, respectively. The average hourly wind speed for Durban is 2.16 m/s with the peak value of 10.95 m/s. These values are important in selecting a wind turbine with suitable cut-in and rated wind speeds specifications.

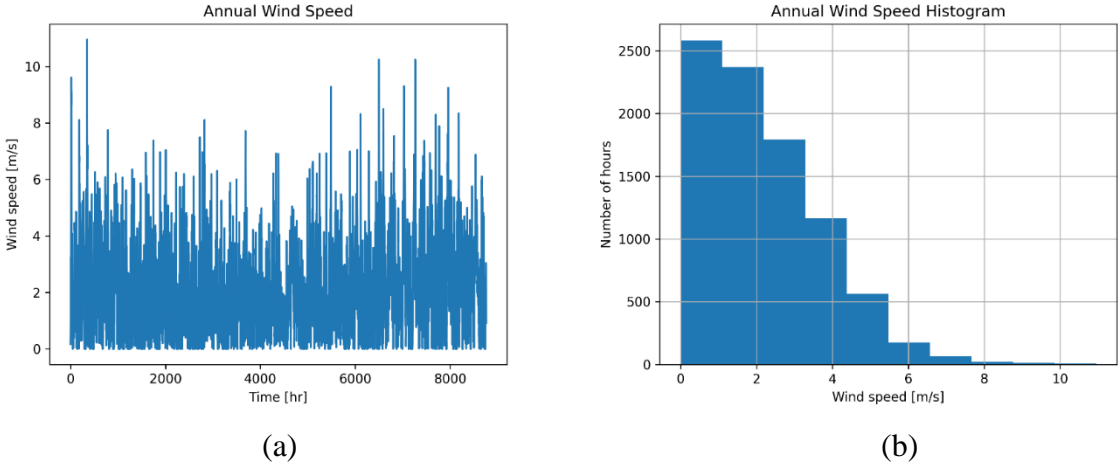


**Figure 4-4: Annual wind speed data**

**Table 4-4. WIND SPEED STATISTICS (m/s)**

mean	std	min	25%	50%	75%	max
2.16	1.60	0.00	0.90	1.94	3.15	10.95

**4.3. Tariff Rates**

Tariff rates that are used in this study were obtained from eThekwini website [128]. Table 4-5 shows the eThekwini tariffs structure from 2008 to 2020 for single-phase residential users. The rates are in c/kWh. It can be seen from this table that tariffs increase over the years with an average annual increase rate of 11.3%. Figure 4-5 shows the graphical representation of the tariff structure from 2008 to 2020 and the extrapolation for 2020 to 2030. Cubic (3rd order) polynomial trendline was used, as the best-fitted line, to fit the data from 2008 to 2020 and to predict tariff till 2030. The prediction gives an annual increase of 11.8%, which is in-line with the historical tariff increase. The predicted tariff rates are shown in Table 4-6.

**Table 4-5. ETHEKWINI SINGLE PHASE RESIDENTIAL TARIFF**

YEAR	Single-Phase Residential Tariff (c/kWh)
2008	58.0807
2009	73.2979
2010	90.16
2011	106.83
2012	117.29
2013	124.375
2014	131.46
2015	147.5
2016	158.78
2017	161.77
2018	174.35
2019	197.14
2020	209.4

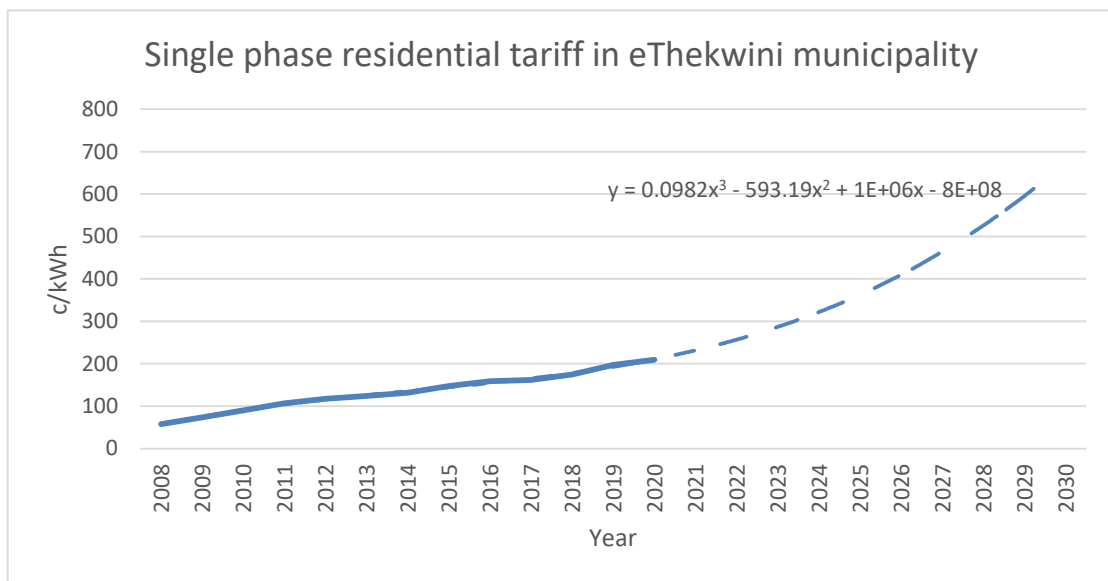


**Figure 4-5: Single phase residential tariff in eThekweni municipality**

**Table 4-6. ETHEKWINI SINGLE PHASE RESIDENTIAL PROJECTED TARIFF**

YEAR	Single-Phase Residential Tariff estimation (c/kWh)
2021	231.6743431
2022	256.8655806
2023	286.6790051
2024	321.7036421
2025	362.5285158
2026	409.7426529
2027	463.9350762
2028	525.6948128
2029	595.6108861
2030	674.2723217

#### 4.4. Load Profile

In this study, the size of the PV, wind turbine and battery storage components are determined, so that the HRES can meet the load requirements at the minimal cost. The data for the load profile has been obtained from the study that has been funded by the South African National Energy Development Initiative (SANEDI) and done by Stellenbosch University and the University of Cape Town on profiling Domestic Electrical Load [129]. We use the data that was collected from an 80m<sup>2</sup> residential building in Durban.

Figure 4-6 shows the typical daily load profile for a high-consumption and a low-consumption month. The load demand is higher in winter compared to summer as the days are shorter and more electricity is used to heat-up homes. Load demand is higher around 06:00 to 07:00 and more uniform during daytime hours. Again, it peaks up around 18:00 to 20:00, which are the highest load demand hours in both winter and summer months. This is due to more activities that are being done during these hours such as cooking, watching TV and having more lights on. The annual load profile of the given building is shown in Figure 4-7 and its corresponding statistics are recorded in Table 4-7. As it is seen, the average hourly load consumption is 0.68 kWh with the peak value of 2.55 kWh. These are important information for selecting the right sized inverter.

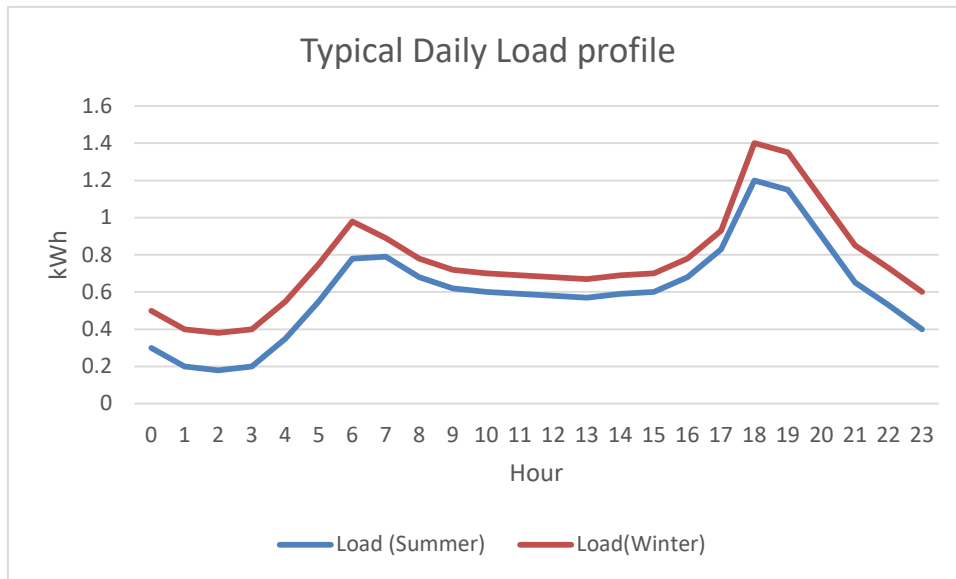


**Figure 4-6: Typical daily load profile**

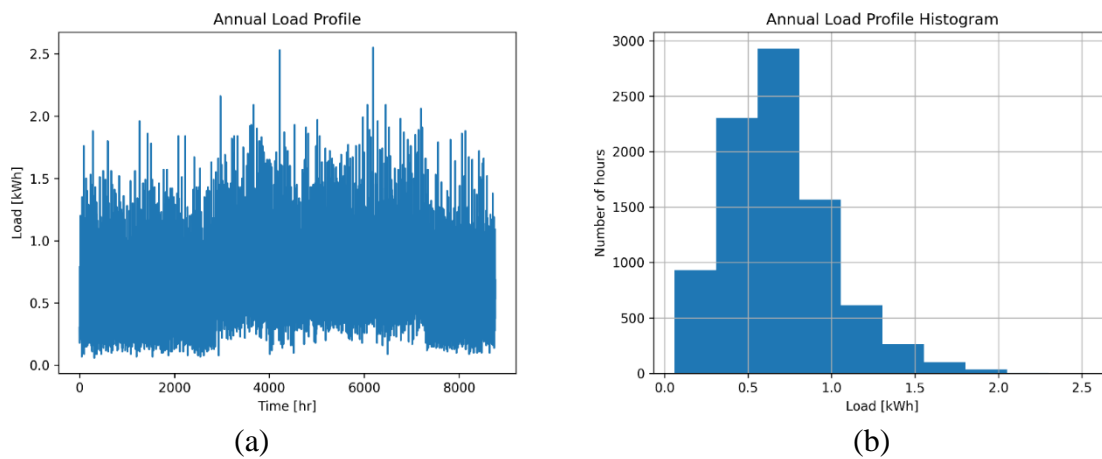


**Figure 4-7: Annual load profile**

**Table 4-7. LOAD STATISTICS (kWh)**

mean	std	min	25%	50%	75%	max
0.68	0.32	0.06	0.46	0.65	0.85	2.55

### 4.5. PV Panels

Based on equation (3-9), the solar irradiation and temperature data have been used to simulate the output power of three different PV panels: Cinco 50W, Cinco 100W, and Cinco 200W. The annual output power for each panel is shown in Figures 4-8. The specifications of these panels together with their current price on the market are given in Table 4.8 [130]. As it is seen, the output power increases by the increase in GHI and temperature until it reaches its maximum value for each panel.

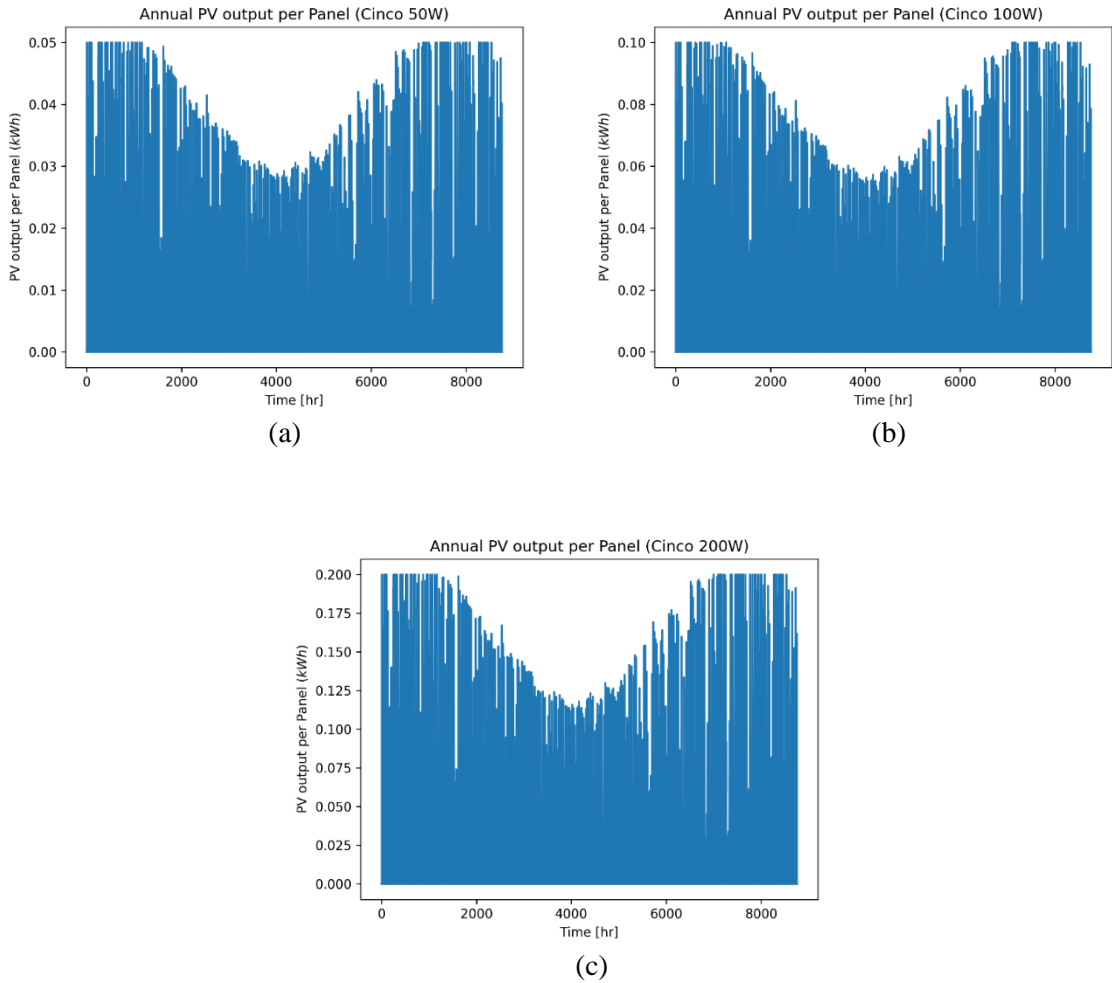


**Figure 4-8: Annual PV power output per panel: (a) Cinco 50W, (b) Cinco 100W, (c) Cinco 200W**



**Table 4-8. PV PANELS PARAMETERS**

<b>Maximum Power at STC (Pmax)</b>	<b>50W</b>	<b>100W</b>	<b>200W</b>
<b>Optimum Operating Voltage</b>	17.8V	36.6V	36.45V
<b>Optimum Operating Current</b>	2.81A	2.73A	5.488A
<b>Open-Circuit Voltage</b>	22.00V	45.38V	44.37V
<b>Short-Circuit Current</b>	3.01A	2.92A	6.01A
<b>Solar Module Efficiency (%)</b>	14.01	14.01	15.67
<b>Dimension (L × W × D)</b>	695 mm × 510 mm × 25mm	1020 mm × 680 mm × 30mm	1,580 mm × 808 mm × 35 mm
<b>Weight</b>	5kg	10kg	13.5kg
<b>Operating Temperature</b>	-40°C to 85°C	-40°C to 85°C	-40°C to 85°C
<b>Maximum System Voltage (DC)</b>	1000	1000	1000
<b>Maximum Series Fuse Rating</b>	10A	10A	15A
<b>Power Tolerance</b>	+/-3%	+/-3%	+/-3%
<b>Cell Type</b>	Poly	Poly	Mono
<b>Number of Cells</b>	36 Cell	72 Cell	72 Cell
<b>Warranty</b>	10 years power warranty (90% yield) 25 years power warranty (80% yield)	10 years limited product warranty, (90% yield) 25 years power warranty (80% yield)	10 years limited product warranty, (90% yield) 25 years power warranty (80% yield)
<b>Price:</b>	R 632.99	R999.01	R 1,890.00

According to the panel specifications, the generated power by these panels has a 90% yield in 10 years and 80% in 25 years. To reflect this in our simulation, we consider a linear decline in the performance of PV panels in their lifetime, and so we modify equation (3-9) to

$$P_{PV}(t) = (1 - 0.00067m)A_{PV}\eta_{PV}I(t)(1 - 0.005(T_0(t) - 25)) \quad (4.1)$$

where  $m$  is the number of months in the system's lifetime. This means after 120 months (10 years), the coefficient value is equal to  $1 - 0.00067 \times 120 = 0.9$  and after 300 months (25 years) is equal to 0.8.

## 4.6. Wind Turbine

We used the characteristics of a Kestrel e160i-600W wind turbine in our simulation. These characteristics are given in Table 4.9. The annual output power of this turbine based on the wind speed data given in Figure 4-4 is calculated by equation (3.8) and is shown in Figure 4.9. It can be seen that for the location of study, Durban, the amount of generated power by the wind turbine is lower in winter compared to summertime, and so we cannot benefit from wind and solar complementary characteristics in this sense.

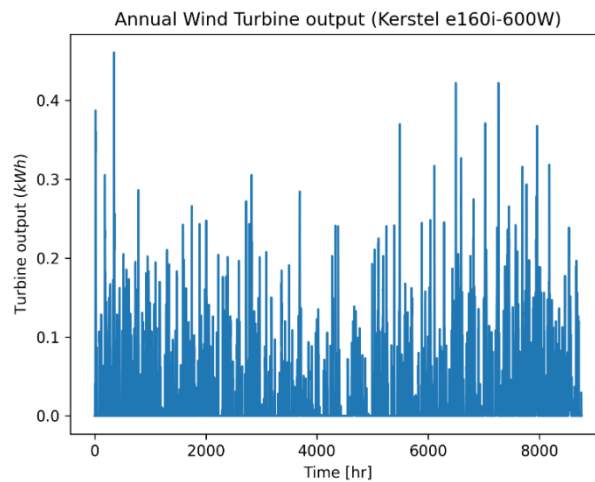


**Figure 4-9: Annual wind turbine output**

**Table 4-9. WIND TURBINE PARAMETERS**

<b>Small Wind Turbine Class:</b>	II
<b>Maximum Power:</b>	700W
<b>Rated Output:</b>	600W
<b>Rated Wind Speed:</b>	13.5m/s
<b>Cut-in Wind Speed:</b>	2.5m/s
<b>Generator Type:</b>	Permanent-magnet, Axial flux brushless
<b>Rotor Diameter:</b>	1.6m
<b>Number of Blades:</b>	5
<b>Blade Material:</b>	Fibreglass
<b>Tower Type:</b>	Monopole
<b>Over-speed Protection:</b>	Rotor Turbulence
<b>Controller Type:</b>	Charge or Dump
<b>Output Voltage:</b>	24, 48, 110 and 220 Vdc
<b>Application:</b>	Battery Charging, Grid Tie, Hybrid
<b>Price:</b>	R 21,968.00

## 4.7. Battery Storage

The output power from the PV panels and wind turbine is used to charge the battery storage system. The BS is used to store the excess power generated by RES when power production exceeds load demand. The BS provides power to the load during times when the HRES generates insufficient power. If the power from the RES and BS still does not meet load requirements, then power is purchased from the utility grid.

There are various BS technologies available, which include lithium ion, vanadium-redox, sodium-sulphur and lead-acid. Lithium ion batteries offer longer lifespan, more storage capacity (depth-of-discharge of 100%) and no maintenance. However, all these benefits come at a much larger cost. Vanadium-redox batteries have exceptionally large cycle life, average energy density with no self-discharge and moderate cost. Sodium-sulphur batteries offer high cycle life, high energy density and average cost. Lead-acid batteries are more mature and the least expensive of these technologies. Lead-acid batteries come in two types; flooded lead-acid and sealed lead-acid batteries. Flooded lead-acid batteries can be charged daily but release a gas as a by-product, so they require a well-ventilated space. These batteries require regular maintenance to replace the water lost in the form of the emitted gas. Sealed lead-acid batteries do not produce a gas as such they do not need to be refilled like flooded lead-acid batteries. Consequently, they require minimal maintenance and can be installed in a variety of locations. Additionally, sealed lead-acid batteries do not self-discharge as rapidly if unused over a long period of time. There are two types of sealed lead-acid batteries, namely, absorbent glass mat (AGM) and gel. The AGM battery offers some advantages which include; spill proof, can withstand extreme temperatures, lower self-discharge rate, requires less maintenance and are vibration and shock resistant. Despite the relatively poor performance of lead-acid batteries (depth-of-discharge of 50%) compared to the lithium-ions, their affordability and availability motivated for the use of this technology in this project. The battery type used in this study is a SonX 100Ah 12V AGM, which we use them in a bundle of four to be suitable for operating with the selected inverter. The battery parameters are shown in Table 4.10. We consider a maintenance costs to replace the batteries when their lifetime has been reached.

**Table 4-10. BATTERY PARAMETERS**

Battery	SonX 100Ah 12V AGM
Cells per Unit	6
Voltage per Unit	12V
Capacity	100Ah@10hr-rate to 1.80V per cell @ 25°C
Max. Discharge Current	1000A (5 sec)
Internal Resistance	5mΩ
Recommended Maximum Charging Current Limit	30A
Equalization and Cycle Service	14.6Vdc to 14.8 Vdc / unit Average at 25°C
Self-Discharge	VRLA batteries can be stored for more than 6 months at 25°C. Self-discharging ratio less than 3% per month at 25°C
Terminal	Terminal F5/F12
Operating Temperature Range	
Discharge	(-) 20°C to 60 °C
Charge	0°C to 50°C
Storage	(-) 20°C - 60°C
Normal Operating Temperature Range	25°C +/- 5°C
Float charging Voltage	13.6Vdc to 13.8 Vdc / unit Average at 25°C
Container Material	A.B.S. (UL94-HB), Flammability resistance of UL94-V1 can be available upon request
Dimensions (L × W × H)	32,8cm × 17,2cm × 22, 2 cm
Weight	30.0 Kg
Price	R 3,193.00

#### 4.8. Inverter

Based on the configuration of the proposed HRES and by considering the load profile, a 3kW hybrid inverter can provide sufficient power. The specification of the selected hybrid inverter is given in Table 4.11.

**Table 4-11. INVERTER PARAMETERS**

Model:	RCT-AXPERT 3K - 48V
Rated Power:	3000VA/3000W
Input Voltage:	230 VAC
Frequency Range:	50 Hz/60 Hz (Auto sensing)
<b>Output</b>	

AC Voltage Regulation:	230 Vac $\pm$ 5%
Surge Power:	6000VA for 5 sec
Efficiency (Peak):	93 % at Line Mode, 90% at Battery Mode
Transfer Time:	10 ms (For Personal Computers); 20 ms (For Home Appliances)
Waveform:	Pure sine wave.
<b>Battery</b>	
Battery Voltage:	48 Vdc
Floating Charge Voltage:	27 Vdc
Overcharge Protection:	31 Vdc
<b>Solar Charger &amp; AC Charger</b>	
Solar Charger Type:	MPPT
Maximum PV Array power	900 W
Maximum PV Array Open Circuit Voltage:	102 Vdc
Maximum Solar Charge Current:	18 A
Maximum AC Charge Current:	15 A
Maximum Charge Current:	33 A
<b>Physical</b>	
Dimension, D $\times$ W $\times$ H (mm):	100 $\times$ 272 $\times$ 355
Net Weight (kgs):	7.4
Price:	R 8,670

#### 4.9. Utility Grid

The utility grid will guarantee the load demand if the hybrid generating system cannot meet load demand. The utility grid power at any given time can be calculated as

$$P_{grid}(t) = P_L(t) - \sum [P_{WT}(t), P_{PV}(t), P_{BS}(t)] \quad (4.2)$$

$P_{grid}$  : The power that is supplied to or by the utility grid

$P_L$  : The load power demand

$P_{WT}$  : The power that the wind turbine supplies

$P_{PV}$  : The power that the PV arrays supplies

$P_{BS}$  : The power that the BS supplies

### 4.10. System Operation

Our considered HRES uses the energy produced by the PV and WT systems as well as the energy stored in BS to satisfy the load demand with the option of purchasing insufficient energy from the utility grid. At any given time, a comparison between the load demand and energy produced by RES is made. If the demand is less than the energy produced by RES, the excess energy will be used to charge the BS, and upon the BS reaches its full capacity, the excessive power will be dumped. On the condition that the load demand is greater than the energy produced by RES, the system uses the power stored in the BS to cover a part or all the power deficiency. If the BS does not contain sufficient energy then the deficit energy should be purchased from the utility grid.

Figure 4-10 shows the system operation flowchart.  $P_{PV}$  and  $P_{WT}$  is the power generated by PV panels and wind turbines at time  $t$ . The load demand and BS power at time  $t$  is represented by  $P_L$  and  $P_{BS}$ , respectively. The BS can be discharged until its power reaches a minimum value of  $P_{BS\_min}$ . The inverter efficiency is shown by  $\eta$ .

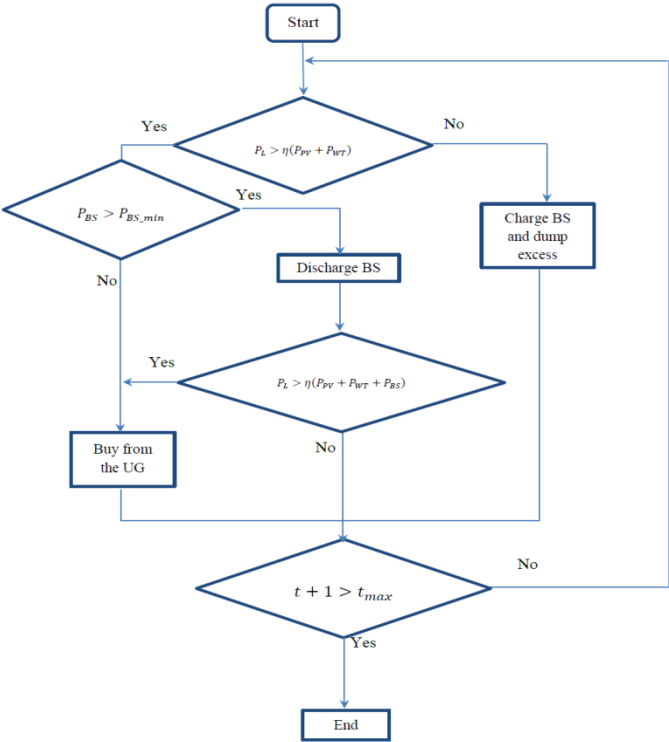


Figure 4-10: System operation flowchart

#### 4.11. Proposed Optimization Method

In this study, the optimization objective is to minimize the cost of the hybrid system such that the user would be able to pay back the cost of the system by the amount of money saved over a period of time as a result of using RES for generating electricity. There are various cost components involved in the system including the initial investment costs, installation costs and operation and maintenance costs.

The power produced by RES is a function of  $P_{PV}$ ,  $P_{WT}$  and  $P_{BS}$ . These values are affected by the number of PV panels, wind turbines and BS that have been used in the system. The power produced by the RES at time  $t$  can be determined as

$$P_{RES}(t) = N_{PV}P_{PV1}(t) + N_{WT}P_{WT1}(t) \quad (4.3)$$

subject to

$$0 \leq N_{PV} \leq N_{PV\_max} \quad (4.4)$$

$$0 \leq N_{WT} \leq N_{WT\_max} \quad (4.5)$$

$N_{PV}$  : The number of PV panels

$P_{PV1}(t)$  : The power produced by each PV panel

$N_{WT}$  : The number of wind turbines

$P_{WT1}(t)$  : The power produced by each wind turbine

$N_{PV\_max}$  : The maximum number of PV panels

$N_{WT\_max}$  : The maximum number of wind turbines

A BS can also be considered for the system to store the excess power generated by the RES. The excess power at time  $t$  is calculated by

$$P_{excess}(t) = \eta P_{RES}(t) - P_L(t) \quad (4.6)$$

where  $P_L(t)$  is the load demand, and  $\eta$  is the inverter efficiency. When the load demand exceeded the system's RES generated power, the BS power can be used to compensate for this deficiency. The amount of power stored in the BS is equal to

$$P_{BS}(t) = \max\{\eta P_{RES}(t) - P_L(t), P_{BS\_max}\} \quad (4.7)$$

The load obtains power primarily from the RES. If the power produced by RES is insufficient then the deficit power is obtained from the BS. If the power in the BS is greater than the minimum allowable power in the BS, the BS discharges to supply the load. Otherwise, the insufficient energy is purchased from the utility grid. The total power of the RES and BS can be modelled as

$$P_{RES-BS}(t) = \eta(N_{PV}P_{PV1}(t) + N_{WT}P_{WT1}(t) + N_{BS}P_{BS1}(t)) \quad (4.8)$$

$P_{RES-BS}$ : The total power produced by the RES and BS

$N_{BS}$  : The number of BS units

$P_{BS1}$  : The power provided by each BS unit

#### 4.11.1. Cost Function

We have used the NPV for calculating the cost function. The costs involved in the system is made up of the total initial investment cost including installation, total maintenance and operational costs, and the total income generated by using the RES for generating electricity. NPV is obtained by subtracting the present discount values of the costs from the incomes as

$$NPV = C_{investment} + \sum NPV_{OM} - \sum NPV_{income} \quad (4.9)$$

$C_{investment}$  : The value of initial investment including installation.

$NPV_{OM}$  : The net present value of operation and maintenance cost

$NPV_{income}$  : The net present value of the income generated by using the HRES

The investment cost is made up of the cost of purchasing PV panels as given in Table 4.8, the cost of purchasing wind turbines as given in Table 4.9, the cost of purchasing batteries as given in Table 4.10 and the cost of purchasing the inverter as given in Table 4.11. Additionally, the investment costs include an additional 20% of the component prices for installation. The nominal annual interest and



inflation rates used for NPV calculations are given in Table 4.12. The investment costs (inclusive of installation) can be calculated as

$$C_{investment} = (N_{PV}PV_{price} + N_{WT}WT_{price} + N_{BS}BS_{price} + INV_{price}) \times 1.2 \quad (4.10)$$

$PV_{price}$  : The price of a single PV panel

$WT_{price}$  : The price of a single wind turbine

$BS_{price}$  : The price of a single bundle of battery storage

$INV_{price}$  : The price of a single inverter

**Table 4-12. CONSIDERED ECONOMIC DATA FOR THE SYSTEM**

Yearly operation and maintenance costs	Installation Costs	Nominal interest rate (%)	Inflation rate (%)
2% of initial purchase costs	20% of initial purchase costs	3.7	4.6

In this study the yearly operation and maintenance costs are taken to be 2% of the initial costs of the components as given in Table 4.12. Therefore, the monthly operation and maintenance cost factor can be calculated by dividing the yearly percentage by 12 to obtain 0.0017. The net present value of operation and maintenance can be determined based by

$$Monthly_{OM} = 0.0017 \times (N_{PV}PV_{price} + N_{WT}WT_{price} + N_{BS}BS_{price} + INV_{price}) \quad (4.11)$$

The money saved as a result of using RES to generate electricity instead of purchasing that from the grid is considered as an income for the system. This income is used to recover the initial investments and operation and maintenance costs. The monthly power generated by the RES can be determined and the income is therefore equal to the product of the power generated by RES and the tariff at a given time. The tariff rates for eThekweni municipality from 2008 to 2020 are given in Table 4.5 and the projected tariffs up to the year 2030 are given in Table 4.6. The income at a given time  $t$  is equal to

$$I(t) = T(t) \times P_{RES-BS}(t) \quad (4.12)$$

$T(t)$  : The tariff at time  $t$

The objective of this study is to find the optimal combination of PV, WT, and BS to minimize the outcome of equation (4.9). This means that when the value of equation (4.9) is a negative number, the sum of the initial investment and the operation and maintenance costs of the system are less than the generated income, and hence, using the HRES becomes profitable.

#### 4.11.2. Constraints

There are three constraints in this optimization problem, which are on the number of PV panels, wind turbines and the BS units. These numbers should be positive integers. Also, the maximum number of PV panels should not exceed the available installation area of the proposed site. Therefore, these constraints can be listed as

$$0 \leq N_{PV} \leq N_{PV\_max} \quad (4.13)$$

$$0 \leq N_{WT} \leq \infty \quad (4.14)$$

$$0 \leq N_{BS} \leq \infty \quad (4.15)$$

where

$$N_{PV\_max} \times A_{PV} \leq A_{inst} \quad (4.16)$$

$A_{PV}$  : The surface of a PV panel ( $m^2$ )

$A_{inst}$  : Installation area of the considered site ( $m^2$ )

The PV panel dimensions considered in this study are given in Table 4.8.

#### 4.11.3. Optimizers

GA and PSO have been used to find the optimal solution of equation (4.9) constrained by (4.13) - (4.15). GA has been chosen because of its ability to avoid being trapped in local optima. However, it requires a large number of iterations, which increases its computational time. PSO, on the other hand,

has less computational complexity and at the same time shows a good performance in the three-dimensional problems, such as the one we have in hand.

#### **4.11.3.1. GA**

The two main parameters in GA are the crossover and mutation probabilities. Crossover probability refers to the likelihood of a crossover being implemented. If crossover is not implemented then the resulting offspring are exactly the same as parents, and if 100% chance of crossover is considered then all the offspring are due to crossover. The crossover is implemented to increase the good genes in the offspring. We consider a 50% crossover probability in our developed GA algorithm.

Mutation probability refers to the likelihood of mutation being implemented. If mutation is not implemented then offspring remain the same as after crossover. On the other hand, if 100% mutation is implemented then the entire offspring is changed after crossover. Mutation is implemented occasionally to avoid being stuck in local optima. The mutation probability considered in our GA optimizer is 10%.

Another parameter in GA is population size, which refers to the number of individuals in one generation. If there are many individuals then the computational time becomes longer, while too few individuals result in the search region not being effectively explored. We considered a population size of 100.

We consider no limitation on the maximum number of iterations, however, to increase the speed of algorithm, we limit the number of iterations without improvement to 10 iterations. Table 4.13 gives the parameters that are used for developing the GA optimizer.

**Table 4-13. PARAMETERS USED IN THE GA OPTIMIZER**

Parameters	Values
Maximum number of iterations	None
Maximum number of iterations without improvement	10
Population size	100
Mutation Probability	10%
Elite Ratio	10%
Cross over Probability	50%
Parents Portion	30%
Crossover Type	Uniform

**4.11.3.2. PSO**

The parameters of PSO algorithm includes the number of particles,  $n$ , constants for acceleration,  $c_1$  and  $c_2$ , and the inertia weight,  $w$ . The maximum number of iterations,  $t_{max}$ , and calculated accuracy,  $\epsilon$ , are also utilized in ending the iteration. The number of particles refers to the number of individuals in the population. Increasing the number of particles increases the computational time as well as reliability while reducing the number of particles affects the PSO performance. We consider 30 particles in our PSO optimizer. Table 4.14 gives the parameters that are used for developing the PSO optimizer.

Constants for acceleration refer to acceleration weight in the direction of  $pbest$  as well as  $gbest$ . If the acceleration constant is small then the particles are directed towards a specific area, while a large accelerate constant may cause the particles to move quickly and away from the specified area. In general, acceleration constants are used to motivate individuals to explore the entire search region. This prevents convergence at local optima and improves convergence in the direction of global optima

resulting in more efficient determination of the optimal solution. The values selected for  $c_1$  and  $c_2$  are 0.5 and 0.3, respectively.

Inertia weight refers to how the present velocity is affected by the preceding velocity. The zero value for  $w$  means the particle's velocity is based on the present  $pbest$  and  $gbest$ . A small value of  $w$  will result in local search due to a small velocity, while a large value results in global search due to a larger velocity. We selected  $w$  equal to 0.9.

Maximum velocity  $v_{max}$  gives an indication of the search capability of a particle. If  $v_{max}$  is too large the particle can overshoot good solutions while a small  $v_{max}$  results in localized search. Both of these situations may reduce PSO performance. We consider  $v_{max}=1$ .

**Table 4-14. PARAMETERS USED IN THE PSO OPTIMIZER**

Parameters	Values
Maximum number of iterations	100
Population size	30
$C_1$	0.5
$C_2$	0.3
$w$	0.9

In order to apply PSO for optimally sizing the hybrid system, a population of feasible solutions is produced and updated by making use of PSO till the optimal solution is determined. The PSO procedure is given as follows:

*Step 1:* Initially, a population of 30 solutions (feasible particles) is generated. In sizing the hybrid system, individual particle's position is given by a vector that is made up of three elements,  $x = [N_{PV} \ N_{WT} \ N_{BS}]$ .

*Step 2:* An initial velocity is generated for every particle. This velocity is a vector made of three elements which are randomly valued.

*Step 3:* The objective function value is calculated for each particle.

*Step 4:* At the beginning, the particle's initial position is taken as its *pbest* and the best particle of the population is selected as *gbest*. *gbest* is the position of the particle with the lowest cost function value.

*Step 5:* The velocity of each particle is then updated using (3.1) and the particle progresses to a new position in the search space by (3.2). New solution vectors are generated in this step.

*Step 6:* If the position is infeasible then the particle moves to its preceding position.

*Step 7:* The values of the objective function are calculated for each new position.

*Step 8:* Each particle compares its new position to the previously memorised position and updates its *pbest*, provided that the new position provides a better value. The best particle in the population is then taken as *gbest*.

*Step 9:* The termination basis is examined (getting to  $t'_{max}=100$ ). If  $t$  is not satisfied, steps 5-8 are repeated, or else PSO is ended and elements in *gbest* are taken as the optimal solution.

#### **4.12. Summary**

In this chapter, the methodology that we have used for setting up a grid-connected HRES was given. In our study, we used the meteorological data of Durban. First, we have gathered and analysed the meteorological data. We then studied the eThekweni municipality tariff rates from 2008 to 2020, and based on that, we estimated the tariff up to 2030. Moreover, the load profile for a residential building in Durban was collected and analysed. We used the collected meteorological data to identify the output of three different types of PV panels and a selected wind turbine. Moreover, the specifications and prices of different components of the proposed HRES, including PV panels, wind turbine, BS and inverter, were given. The system operation was then explained, and the proposed optimization method was developed. We used the NPV to define a cost function for the HRES. Minimizing the NPV is the objective of this study. Economic data associated with the cost function

was tabulated. We then defined the system constraints for this optimization problem. Finally, we discussed the GA and PSO as the optimizers used in this study.

## **Chapter 5 : RESULTS AND DISCUSSION**

### **5.1. Introduction**

This chapter covers the results of the optimal sizing of the considered HRES based on the two selected optimizers, namely GA and PSO. The objective of this study is to minimize the cost of the HRES. The aim of the optimization is that the users would be able to pay back the cost of the system by the amount of money saved over a period of time as a result of using RES instead of buying electricity from the grid. The cost function's value shows the amount of money spent on the HRES after a certain number of years. Therefore, a negative value shows a profitable system configuration. Cinco 50W, Cinco 100W and Cinco 200W are the three types of PV panels that have been considered in this study. In addition to the PV panels, we also considered using wind turbines and BS for the HRES. The specification of the selected wind turbine and BS are given in the previous chapter. We first provide a comparison between the two employed optimizers, showing GA outperforms PSO in finding the global minimum of the defined cost function. We then used the GA algorithm, as the outperformer optimiser, to find the optimal size of the system based on different types of selected PV panels and for various system lifetimes. Thereafter, the operation of the optimally sized HRES for a system with 10 years of lifetime has been studied.

### **5.2. Optimal Sizing Results**

We used Python3 on an Intel core 1.8GHz i5 processor to simulate the system and obtain optimal solutions. In this study, three different types of PV panels have been considered. These panels have different power output and price values. The two selected optimizers, GA and PSO, have been widely used in optimally sizing of HRESs. Generally, GA has the ability to avoid being trapped in local optima; however, it usually requires a large number of iterations, which increases its computational time. On the other hand, PSO has less computational complexity and showing a good performance in three-dimensional coordinate problems.

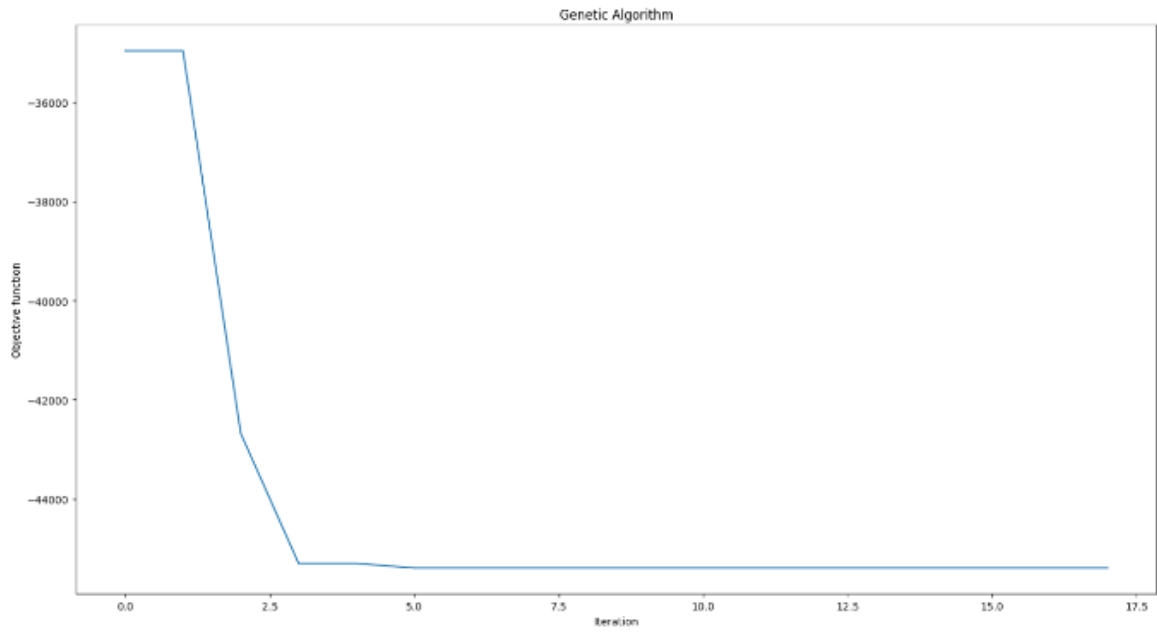
In this section, we provide a comparison between GA and PSO in identifying the optimal size of our considered HRESs over 10 years of lifetime. A separate comparison is made for systems using 50W, 100W and 200W PV panels. The number of PV panels is constrained by the surface area of the selected building rooftop. All systems were allowed to have wind turbines and BS.



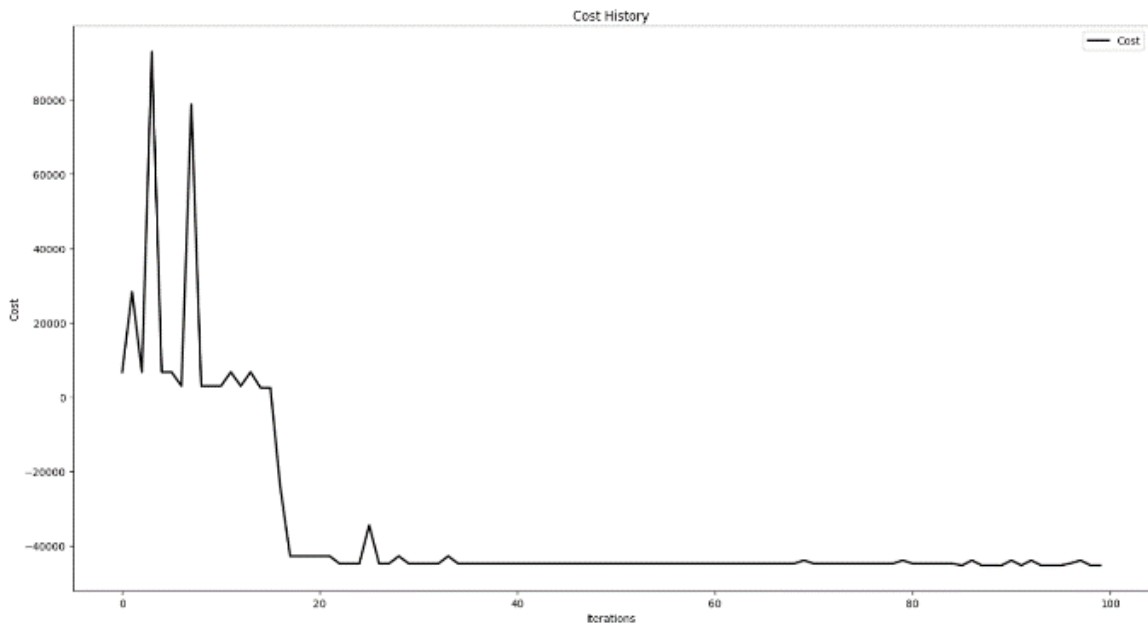
There is usually no restriction on the number of iterations for obtaining the optimal values in the GA algorithm. Instead, the algorithm will usually set to stop when 95% of the genes converged. However, this usually takes a long time. We first optimized the system based on the original GA. However, it was realized that in this particular problem, the optimization could be stopped after 10 iterations with no further improvement, without making a sacrifice on the optimiser performance. Therefore, we considered this stopping criterion in addition to the GA parameters given in Table 4.13.

PSO, on the other hand, is limited by the number of iterations. In PSO algorithms, the optimal solution is obtained by moving the particles through the search space until the algorithm reaches its maximum number of iterations. The parameters used for developing a PSO algorithm are given in Table 4.14. As is seen, the maximum number of iterations that we considered for the employed PSO algorithm is set to 100 iterations.

The transition of the cost function with respect to iterations is shown in Figures 5-1 to 5-3. Figure 5-1(a) and (b) shows the transition diagram for optimizing a hybrid system using 200W PV panels optimized by GA and PSO, respectively. For this system, GA requires 7 iterations to reach the optimal solution, and the algorithm stops after 17 iterations. However, the PSO algorithm could not obtain the optimal solutions and only stops due to reaching its iteration limit. The transition diagram for a HRES using 100W PV panels are shown next, where Figure 5-2(a) shows the transition diagram for the GA algorithm and Figure 5-2(b) is for the PSO. Again, the GA algorithm reaches the optimal solution after 7 iterations and stops after 10 more iterations, while PSO terminated without getting into the global minimum point. Finally, Figure 5-3(a) and (b) depict the transition diagram for optimizing a HRES based on 50W PV panels. As is seen, the GA algorithm gets into the optimal solution after only 11 iterations and stops at 21, while PSO again could not reach to the optimal solution.

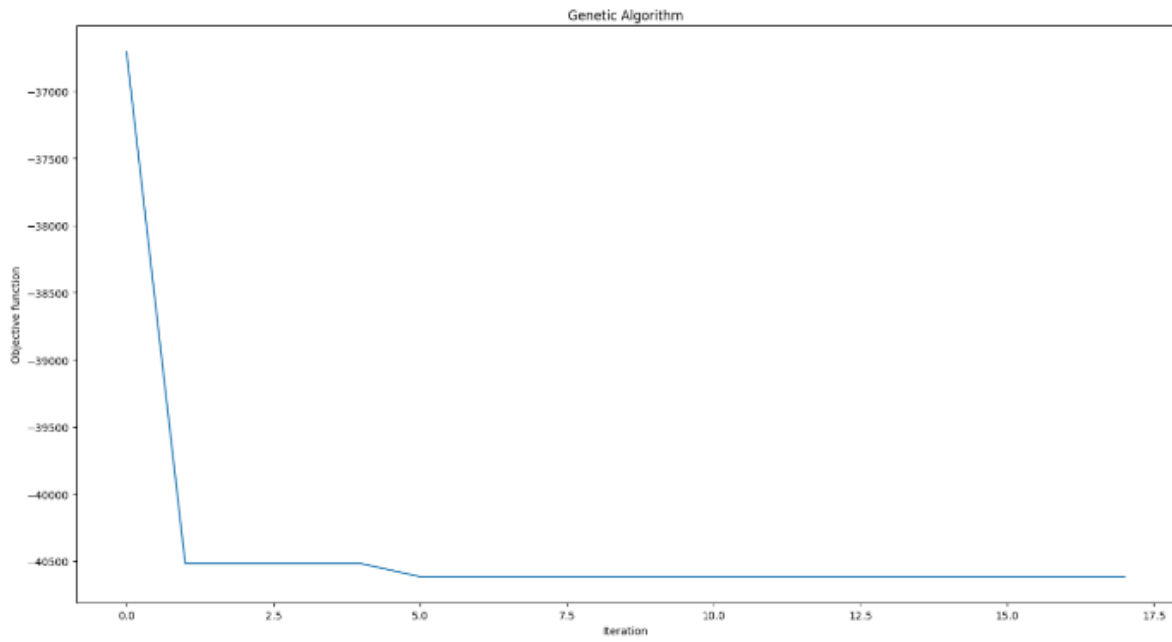


(a)

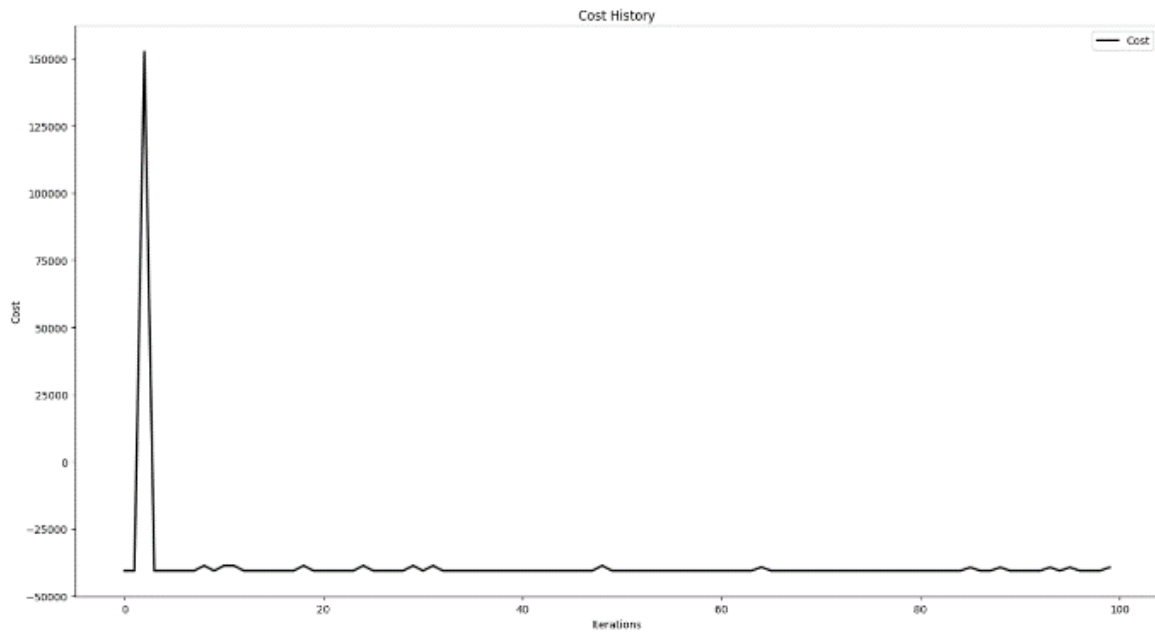


(b)

**Figure 5-1: The transition of cost function considering systems over 10 years of lifetime with (a) 200W PV panels optimized by GA, (b) 200W PV panels optimized by PSO**

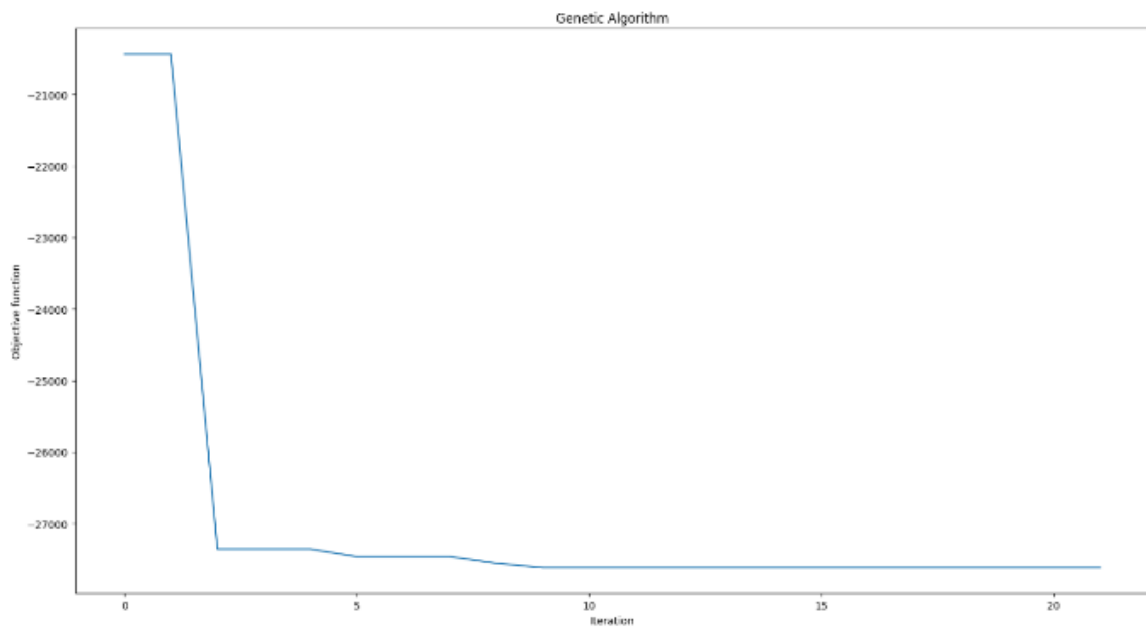


(a)

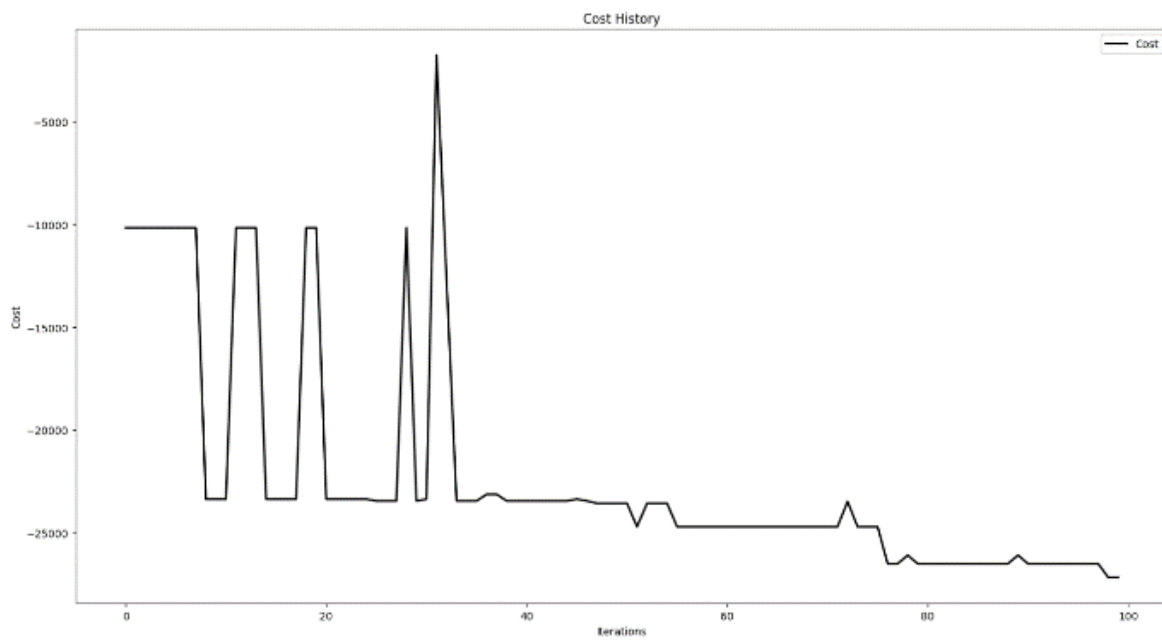


(b)

**Figure 5-2: The transition of cost function considering systems over 10 years of lifetime with (a) 100W PV panels optimized by GA, (b) 100W PV panels optimized by PSO**



(a)



(b)

**Figure 5-3: The transition of cost function considering systems over 10 years of lifetime with (a) 50W PV panels optimized by GA, (b) 50W PV panels optimized by PSO**

In Table 5.1, a comparison between the performance of GA and PSO optimizers in optimizing systems with 10 years of lifetime is given. For a system using a 200 W PV panel, GA provides the optimal sizing as a system with 21 PV panels, no wind turbines and 2 battery storage units. The value of the cost function for this system is –R45,395.70. PSO, on the other hand, was only able to minimize the cost function to the value of –R45,299.40. This is achieved by a system containing 22 PV panels, no wind turbines and 2 battery storage units. The other interesting observation is that the GA not only has a better performance over PSO but also can achieve this over a shorter period of time. The total simulation time using GA was 528.9 seconds, while the same for the PSO was 1066.4 seconds. This is due to the modification that we have made to the GA to stop it after 10 iterations without improvement. Similar performance can be observed for a HRES using 100W and 50W PV panels.

In all three systems, GA can achieve a sizing that provides a lower-valued cost function in a shorter amount of time compared to the PSO algorithm. Moreover, the required time for solving the optimization problem, in both methods, is directly proportional to the size of the search space. This can be seen by comparing the required time for optimizing the system components' size for different types of PV panels. The surface area of the 200W PV panels is larger than the others, and so the maximum number of the 200W PV panels that can be installed is less than the other two types. As a result, the search space for the 200W is the smallest among the three. This follows by the 100W and 50W panels, respectively.

**Table 5-1. A COMPARISON BETWEEN THE PERFORMANCE OF GA AND PSO OPTIMIZER IN OPTIMIZING THE SYSTEM WITH 10 YEARS LIFETIME**

Type of PV Panel	Optimizer	The Optimal Size			Cost Function value	Simulation Time (s)
		$N_{PV}$	$N_{WT}$	$N_{BS}$		
200 W	GA	21	0	2	-R45395.70	528.9
	PSO	22	0	2	-R45299.40	1066.4
100 W	GA	41	0	2	-R40616.40	513.3
	PSO	43	0	2	-R39332.00	1159.3
50 W	GA	74	0	2	-R27618.50	651.01
	PSO	80	0	2	-R27171.90	1160.1

Due to the GA algorithm's superiority, we decided to use that to find the optimal size of the HRES's components for different system's lifetimes. We consider three different scenarios based on the type of the employed PV panels. Figure 5-4, 5-5 and 5-6 show the transition of the cost function for a system using the 200W, 100W and 50W PV panels, respectively. Again, as is seen, the algorithm stops after 10 iterations without improvements.

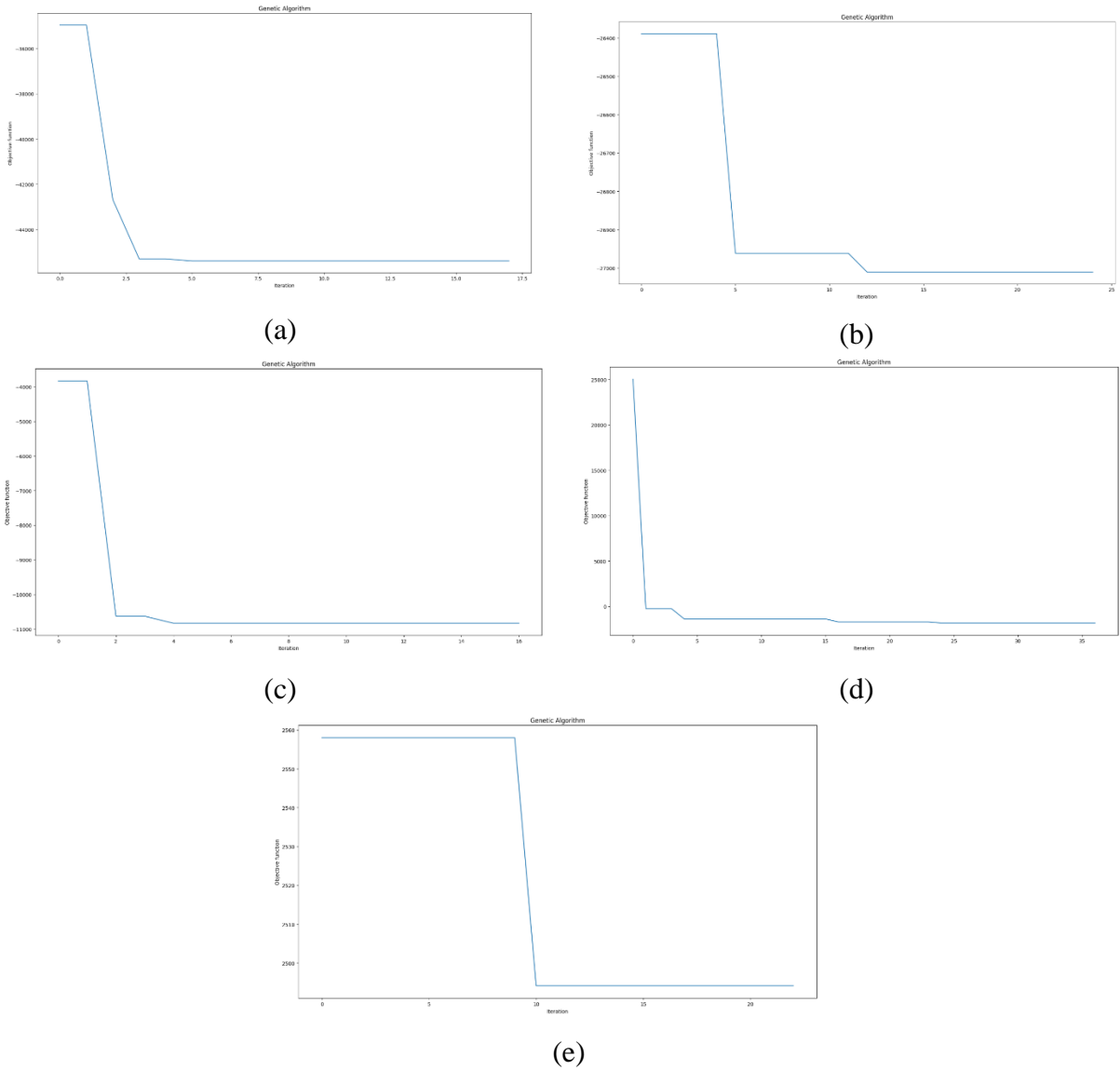
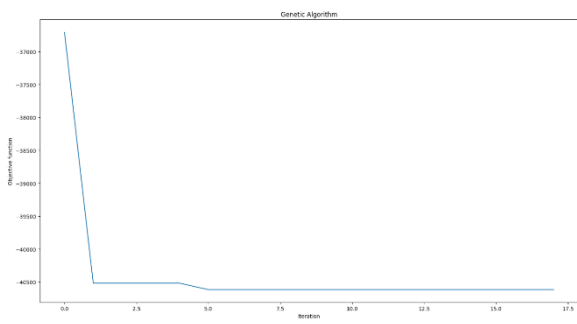
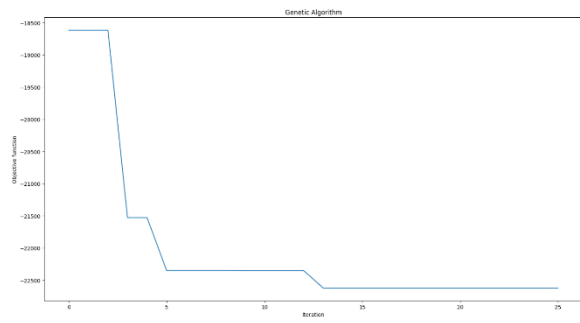


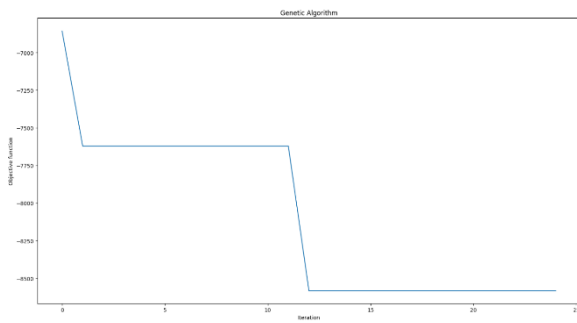
**Figure 5-4: The transition of the cost function for a system with the 200W PV panels and optimized by GA for the system life span of (a) 10, (b) 9, (c) 8, (d) 7, (e) 6 years.**



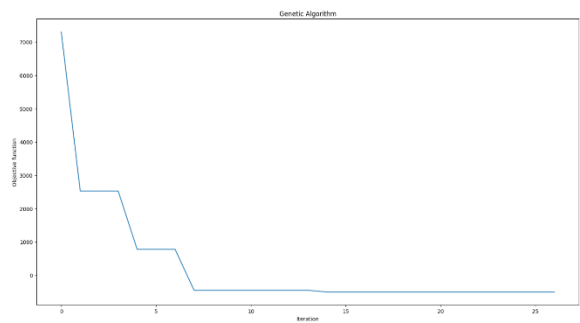
(a)



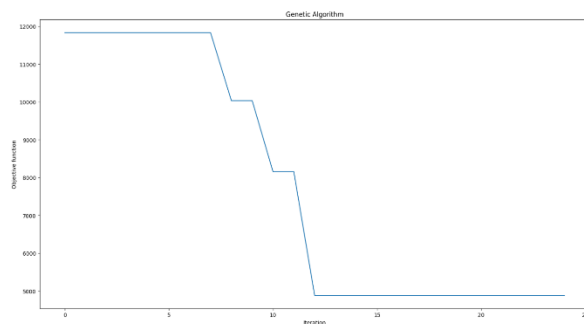
(b)



(c)



(d)



(e)

**Figure 5-5: The transition of the cost function for a system with the 100W PV panels and optimized by GA for the system life span of (a) 10, (b) 9, (c) 8, (d) 7, (e) 6 years.**

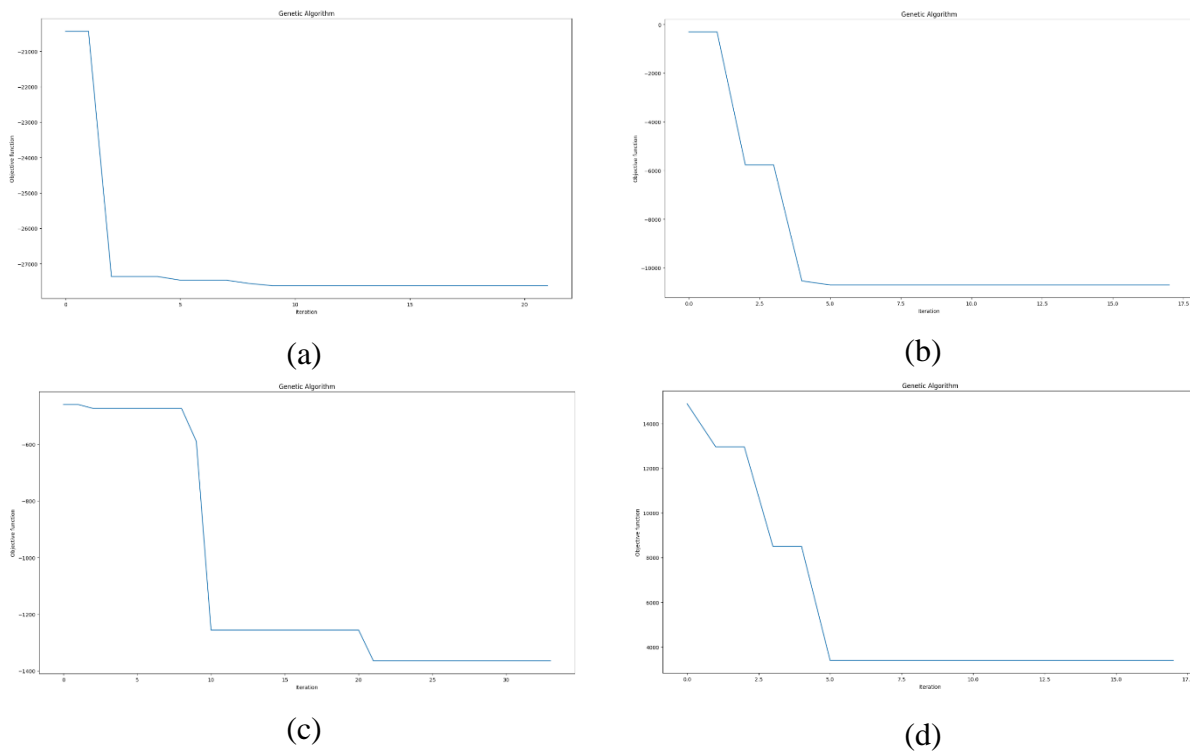


**Figure 5-6: The transition of the cost function for a system with the 50W PV panels and optimized by GA for the system life span of (a) 10, (b) 9, (c) 8, (d) 7 years.**

The optimal size and cost function value of systems using different types of PV panel and lifetime are shown in Table 5.2. All the values are obtained using the GA algorithm. It can be seen from the table that the system profitability increases by its lifetime. This means that the system can generate more income over a longer period of time as the income of the first few years would be used to cover the initial costs. Moreover, the profitability is increased by using PV panels with higher rated power. This is because the per Watt price of the PV panels decreases as the PV panel rated power increases. In other words, a 200W PV panel cost is less than the fourfold price of a 50W PV panel.

A HRES using the 100W and 200W can start becoming profitable after 6 years, while a user of a HRES based on the 50W panel should at least wait for 7 years. The other finding is that in the Durban area, employing wind turbines (based on the selected specification and price) would not be a cost-effective option. One reason can be because of the weather conditions in Durban, which unlike many other locations has a lesser wind speed during winter than in summer. So, the wind-solar combination cannot fully achieve their expected complementary characteristics. Moreover, employing BS can only



become an economic decision if we consider a long enough lifetime for a system. This means that storing energy is not always an economical choice, but sometimes dumping the excess power would become more cost-effective.

**Table 5-2. THE OPTIMAL SIZE AND COST FUNCTION VALUE OF THE SYSTEM CONSIDERING DIFFERENT PV PANEL TYPES AND SYSTEM'S LIFETIME (OPTIMIZED BY GA)**

Type of PV Panel	System's Life Time	The Optimal Size			Cost Function value
		$N_{PV}$	$N_{WT}$	$N_{BS}$	
<b>200 W</b>	10 Years	21	0	2	-R45395.70
	9 Years	20	0	2	-R27010.90
	8 Years	18	0	2	-R10835.30
	7 Years	6	0	0	-R1828.90
	6 Years	5	0	0	R2494.20
<b>100 W</b>	10 Years	41	0	2	-R40616.40
	9 Years	40	0	2	-R22622.80
	8 Years	26	0	1	-R8582.90
	7 Years	12	0	0	-R507.80
	6 Years	15	0	0	R4878.50
<b>50 W</b>	10 Years	74	0	2	-R27618.50
	9 Years	68	0	2	-R10701.60
	8 Years	23	0	0	-R1364.80
	7 Years	24	0	0	R3393.10

Table 5.3 gives the breakup of the cost function values given in Table 5.2 based on their different components. By studying this table, it can be seen how much of the income would be spent to recover the initial investment and how much it costs to maintain the system over a given lifetime. In all cases, the income value is greater than the summation of the initial investment and the operation and maintenance costs, making the total cost a negative value.

**Table 5-3. THE COST COMPONENTS OF THE SYSTEM CONSIDERING DIFFERENT PV PANEL TYPES AND SYSTEM'S LIFE TIME (OPTIMIZED BY GA)**

Type of PV Panel	System's Life Time	Costs		
		$C_{investment}$	$\sum NPV_{OM}$	$\sum NPV_{income}$
200 W	10 Years	R81842.00	R12661.90	R139899.70
	9 Years	R79574.00	R11296.00	R117881.00
	8 Years	R75038.00	R9679.10	R95552.30
	7 Years	R22278.00	R2527.00	R26634.00
100 W	10 Years	R83364.80	R12879.40	R136860.60
	9 Years	R82166.00	R11634.80	R116423.60
	8 Years	R52610.80	R6726.00	R67919.80
	7 Years	R23055.60	R2608.90	R26172.30
50 W	10 Years	R90424.40	R13887.30	R131930.20
	9 Years	R85866.80	R12118.6	R108686.90
	8 Years	R26140.80	R3295.1	R30800.60

### 5.3. Verification and Validation of the System Model

The meteorological data, tariff rates and the load profile used in this study have been collected from reliable sources, which are SAURAN, eThekwini website and Domestic Electrical Load databases. Also, the mathematical models that are used for the employed components, which are PV panels, wind turbines, batteries and inverters are based on the models that have been widely used in the literature. The parameters for each component have been set according to the datasheet of the used components, which are given in Chapter 4. Moreover, the installation and maintenance costs that have been used are in line with the percentages that the other researchers in the literature use.

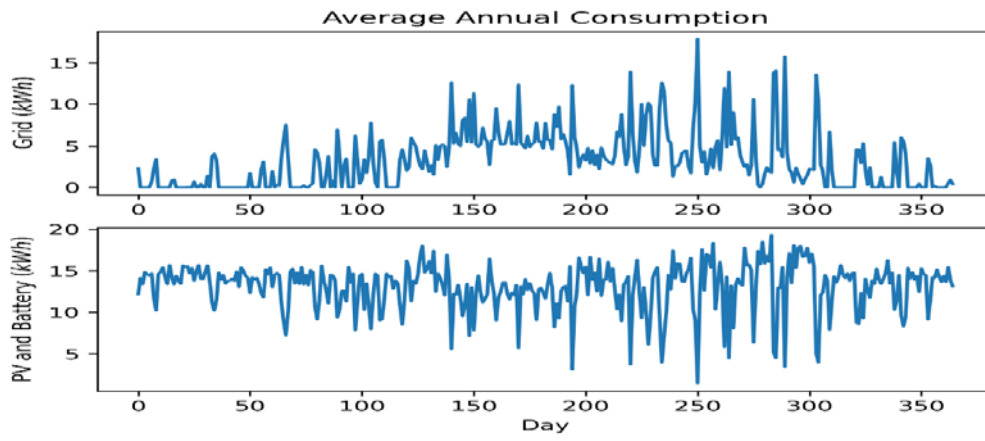
We, further, validate our model by studying the performance of the system using different wattage PV panels. Although using the 50W PV panels may be unrealistic in practical applications, this can help to validate the implemented model. As it is seen in Table 5-3, the installation and maintenance costs of a system based on 50W panels is greater than that when higher wattage panels are being used.

This would be true when considering the number of connections and so the failure points in a system built from 50W panels will be relatively higher than a system built with 100W and 200W PV panels.

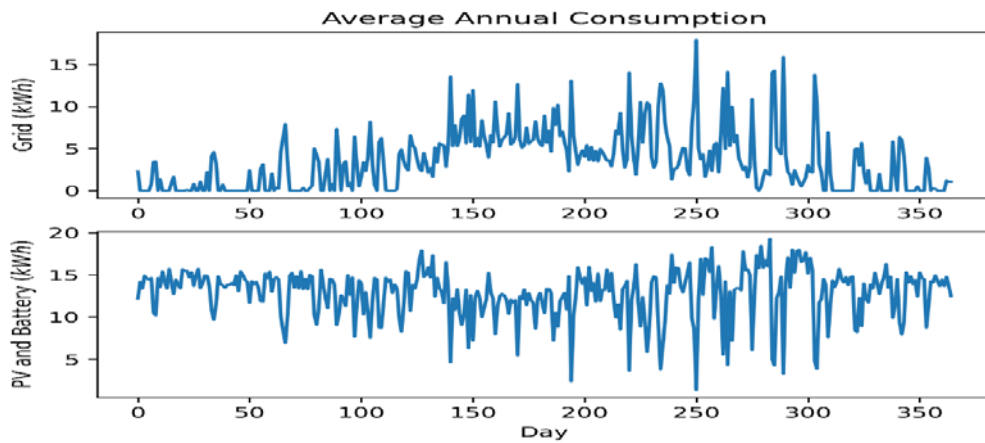
#### **5.4. Operation of the System with Optimal Configuration**

In this section, we study the operation of an optimally configured HRES. The system is optimally sized over 10 years of lifetime. Figure 5-7 shows the average annual consumption of the system from the grid as well as from the PV panels and BS for different PV panel types. The horizontal axis shows the days over a period of one year, starting from the first day of January, and the vertical axis shows the consumption (in kWh).

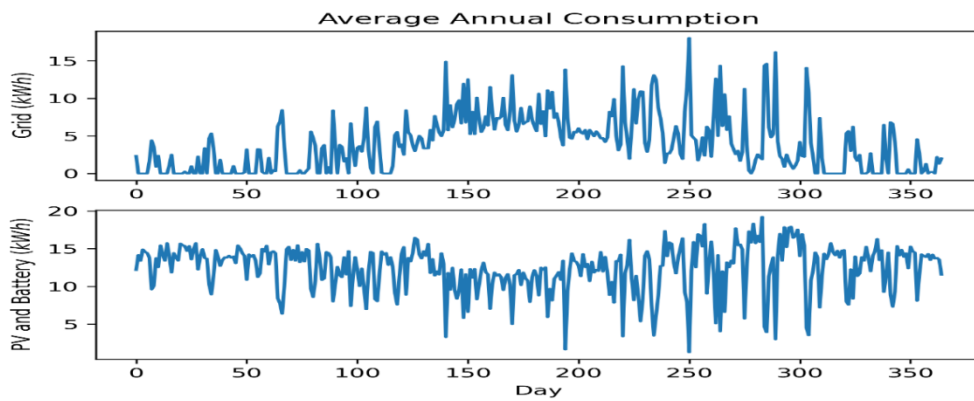
As is seen, there is more power consumption from the grid during wintertime, where the demand is high, and the solar irradiation is low. However, during summertime, where the solar irradiation is high, the PV panels generate more power. As a result of lower demand, the power generated by the PV panels on some summer days is sufficient to be the sole source of power for the system.



(a)



(b)



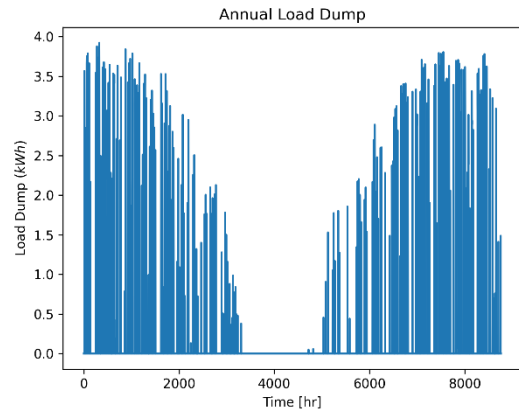
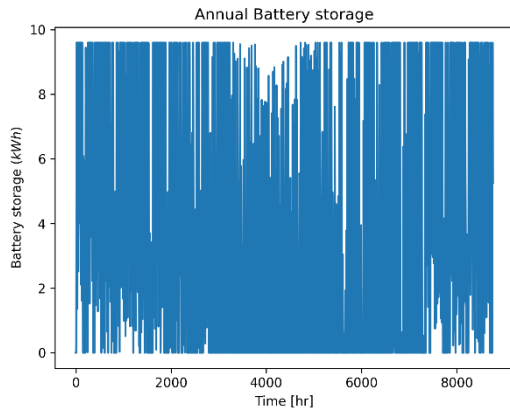
(c)

**Figure 5-7: Average annual consumption from the Grid and RES for an optimally sized system comprising of (a) 200W, (b) 100W, (c) 50W PV Panels**

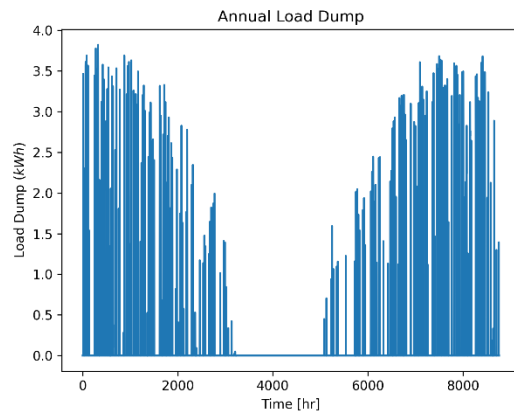
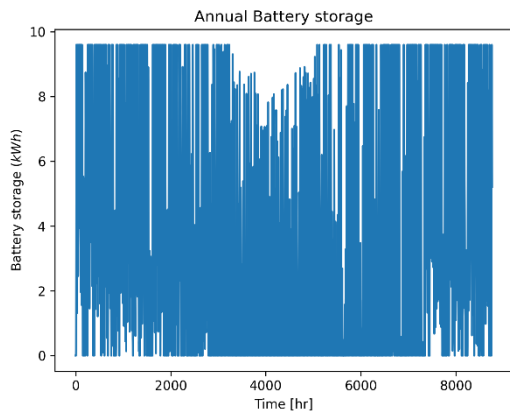
Figure 5-8 shows the average annual stored and dumped power for the optimally sized HRES using different types of PV panels. As is shown, the amount of stored power is increased by employing higher power PV panels. Moreover, as is was expected, we dumped more energy during summertime as there is more excessive generated power due to high solar irradiation and low consumption. However, during wintertime, where the load demand is high, all the generated energy by the PV panels is either stored or used by the load. The average values of data shown by graphs of Figure 5-8 are tabulated in Table 5.4. The averaged values, of both, stored energy and dumped load are increased by using higher power PV panels. However, the ratio of the dumped energy to the stored energy is less in the system that uses the 50W than the 100W and 200W.

**Table 5-4. THE AVERAGE VALUES OF THE BATTERY STORAGE AND LOAD DUMP FOR THE OPTIMAL SYSTEM**

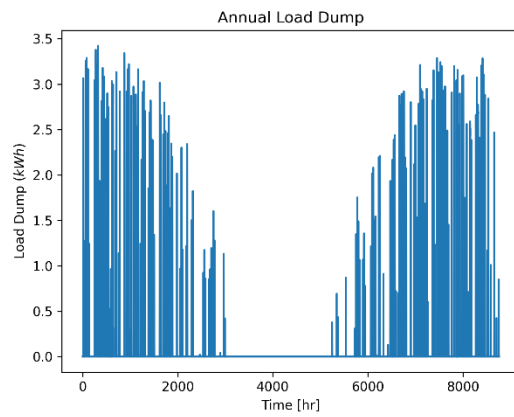
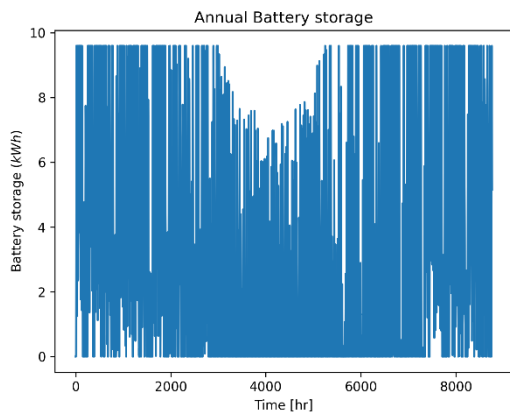
<b>200W PV Panel</b>		<b>100W PV Panel</b>		<b>50W PV Panel</b>	
<b>Average Battery Storage (kWh)</b>	<b>Average Load Dump (kWh)</b>	<b>Average Battery Storage (kWh)</b>	<b>Average Load Dump (kWh)</b>	<b>Average Battery Storage (kWh)</b>	<b>Average Load Dump (kWh)</b>
<b>3.602</b>	<b>0.188</b>	<b>3.424</b>	<b>0.160</b>	<b>3.149</b>	<b>0.121</b>



(a)



(b)



(c)

**Figure 5-8: Averaged annual BS and Load Dump for the optimal size system with 10 years life time using (a) 200W, (b) 100W (c) 50W PV Panels**

## **5.5. Summary**

In this chapter, the results obtained from simulating the system were discussed. We first discussed the performance of the deployed optimisers. It was shown that with a small modification to the GA, we could achieve the globally optimized sizing of the system in a relatively short amount of time. We then used this modified GA to optimize the HRES for different types of PV panels and over various lifetimes. The results have shown that the combination of PV panels and BS can become a profitable option for Durban area. Moreover, the systems using higher rated power PV panels can start to become profitable in a shorter lifetime. Considering BS in a system can only become a cost-effective choice if we consider a long enough lifetime for the system.

## Chapter 6 : CONCLUSIONS

### 6.1. Summary and Contributions

HRESs use different RES, energy storage systems such as BS and can even be connected to the utility grid for supplying energy to a load. The implementation of such systems seeks to supply load demand, while reducing pollutant emissions into the atmosphere to address environmental concerns at a reasonable system cost. RES are intermittent in nature; as such implementation of two or more RES allows the system to overcome the drawback of using a single energy source by capitalising on the complementary characteristics of the energy sources. As such, correctly choosing the RES based on the location of a site can result in a reliable energy generating system. BS can also be utilized in a hybrid energy system to store the excess energy produced by the RES and smooth the output power to overcome power fluctuations providing an improvement of power quality. The RES that were considered for the HRES in this research are solar and wind because of their complementary characteristics. In this study we considered a grid-connected hybrid generating system using PV, wind turbine and BS.

In South Africa, consumers have been faced with ever-increasing cost of electricity and an unreliable grid supply dating as far back as 2007 due to insufficient electricity production. The focus of this research is aimed at identifying the optimal sizing of a grid-connected HRES that is cost-effective for consumers over a period of time. By developing an optimal system, the consumers' dependency on the grid is reduced while the net cost of their electricity over a period of time is lowered. To achieve this, the system components and constraints were identified, and then a mathematical model of the system was developed and optimized.

Much research has been conducted in optimally sizing of various HRESs. Most of this research has been focussed in systems using wind and solar due to their availability. However, no similar research has been conducted for the Durban area. Similarly, solar and wind have been considered in this study as Durban promises good solar irradiation and wind speeds. As such, this research seeks to identify the specifications, objectives and constraints associated with optimization of a HRES to suit South African consumers' needs. Various evaluation indicators have been used by researchers to optimally size HRESs which include economic, reliability, social and environmental indicators. Some of the concerns that consumers have when it comes to setting up a HRES are the associated costs as well as the returns on such an investment. As a result, the NPV of the costs has been selected as the economic indicator for this study.



The HRES is optimally sized using a defined cost function. The cost function is obtained by summing the investment cost and net present values of operation and maintenance costs and subtracting the net present values of income generated by use of the HRES. A negative cost function value translates to a profitable system. This means that the income generated by the use of the HRES is greater than the sum of expenses i.e. investment costs, and operation and maintenance costs. To determine the investment cost, 20% of the total costs of system components have been added to account for the installation costs. The yearly operation and maintenance costs have been taken to be 2% of the total initial costs. A HRES was modelled based on residential consumer needs and available products in the market. After developing the NPV cost evaluation indicator, the HRES constraints were identified. The constraints were applied to the number of PV panels, number of wind turbines and number of battery storage units. The presented optimal sizing method was able to determine the optimal number of PV panels, wind turbines and BS units, which resulted in a reasonable HRES. This allows for the cost of setting up a hybrid generating system for typical residential consumers to be assessed.

To optimize the HRES, two optimizers were used, that is GA and PSO. GA and PSO have been widely used by researchers in optimally sizing HRESs. The reason for selecting GA is its ability to avoid being trapped in the local optima. The drawback of GA is that a large number of iterations are usually required which results in a longer computational time. On the contrary, PSO was selected as it offers good performance and lower computational requirements leading to a lower computational time. This study used a modified GA according to Table 4.13. This modified GA shows a lower computational time and better performance than PSO. PSO was unable to determine the optimal solution and was limited due to the pre-set limit on the number of iterations. As a result, the modified GA was used in finding the optimal size of the HRES.

To optimize the system size, the meteorological data of Durban and load information for a residential building in Durban were gathered and analysed. Meteorological data includes GHI, atmospheric temperature and wind speed. GHI and atmospheric temperature are required to determine the PV panel output power while the wind speed data is required to determine the wind turbine output power. Additionally, the tariff structure for eThekweni municipality from 2008 to 2020 was tabulated and used to calculate the income of the HRES. The tariff was estimated using cubic polynomial trendline up to 2030. Furthermore, the specifications and prices of various HRES components were used for calculating the different costs associated with the system.

Three different PV panels were considered in this study; Cinco 50W, Cinco 100W and Cinco 200W. Due to the limited rooftop area for installation of PV panels, the higher rated panel resulted in a

more profitable HRES. A minimum of 6 years is required for the HRES to be profitable to the user. The 100W and 200W PV panels produce HRESs that would become profitable in 6 years while the 50W PV panel system requires 7 years to become profitable. Although with an increase in PV panel rated power, there would be an increase in initial investment and operation and maintenance costs, the income generated by the HRES also increases with an increase in PV panel rated power. This study shows that in the Durban area, using wind turbines (according to the specification and price of the selected wind turbine) would not be a feasible option. This can be attributed to the weather conditions in Durban, which unlike many other locations has lower wind speed during winter compared to summer. Consequently, the solar and wind combination is unable to fully achieve their expected complementary characteristics. Moreover, using BS is only cost-effective after 8 years for the systems using the 200W and 100W PV panels while 9 years are required for the 50W PV panel system. This means that for shorter system lifespans, it is more cost-effective to dump any excess power that is produced instead of storing it.

In the first few years of the system's lifetime, the income is used to pay for the investment, operation and maintenance costs. The options of three different PV panels allow users to choose the optimal HRES that meets their initial affordability. The flexibility in the optimal sizing strategy of the HRES has potential to increase adoption of the installation of the HRES by many consumers as different price points are proposed. Additionally, the system design is flexible to allow for adjusting for different meteorological data, load requirements and system components such as availability of different PV panel types in the market and initial costs. Moreover, the system model is made more realistic by filtering in the installation area of the PV panels according to the available installation area on the proposed site.

While minimizing the cost of the HRES is the primary objective of this study, it is important to note that the system is reliable as deficit energy is purchased from the utility grid, as such the load is always satisfied. In the event of load shedding by the grid, the load can be supplied by the energy stored in the battery storage or generated by the RES. This allows consumers to remain operational and thus maintain their productivity and ensure their revenue. Moreover, the optimal HRES obtained from this study is able to address the issue of increasing cost of electricity as the system is able to be paid back by the income generated by the use of the RES. Once the investment cost, operation and maintenance costs have been paid, the income generated becomes profit for the user. The lack of grid reliability has resulted in an enhanced social acceptance, since HRESs are able to supplement the grid and over a certain period of time the system pays for itself.

## **6.2. Future Works and Recommendations**

It is customary that a grid-connected HRES sells its surplus generated power to the grid. However, eThekweni municipality has not concluded its small-scale embedded generation (SSEG) systems' tariffs. In winter there is less energy production by the HRES and a higher load demand, and so more energy is purchased from the grid in winter. On the other hand, more energy than the need is generated in summer when there is more solar irradiation and less load demand. It was shown that it is more economical to dump a portion of the excess generated energy. This dumped energy could have been sold to the grid increasing the income and making the HRES more profitable for the user. Therefore, further research can be undertaken once the tariff structure becomes available to maximise on the power that can be sold to the grid instead of dumping. Following this path of research will also require the HRES design to factor in the smoothening of the power sold to the grid as this will affect the grid power quality. Consequently, guaranteeing high power reliability could be the objective of such a study.

## REFERENCES

- [1] B. S. Borowy and Z. M. Salameh, "Optimum photovoltaic array size for a hybrid wind/PV system," *IEEE Transactions on Energy Conversion*, vol. 9, no. 3, pp. 482-488, 1994, doi: [10.1109/60.326466](https://doi.org/10.1109/60.326466).
- [2] S. Becker *et al.*, "Features of a fully renewable US electricity system: Optimized mixes of wind and solar PV and transmission grid extensions," *Energy*, vol. 72, pp. 443-458, 2014/08/01/ 2014, doi: <https://doi.org/10.1016/j.energy.2014.05.067>.
- [3] T. A. Deetjen, H. Martin, J. D. Rhodes, and M. E. Webber, "Modeling the optimal mix and location of wind and solar with transmission and carbon pricing considerations," *Renewable Energy*, vol. 120, pp. 35-50, 2018/05/01/ 2018, doi: <https://doi.org/10.1016/j.renene.2017.12.059>.
- [4] A. González, J.-R. Riba, A. Rius, and R. Puig, "Optimal sizing of a hybrid grid-connected photovoltaic and wind power system," *Applied Energy*, vol. 154, pp. 752-762, 2015/09/15/ 2015, doi: <https://doi.org/10.1016/j.apenergy.2015.04.105>.
- [5] Y. An, W. Fang, B. Ming, and Q. Huang, "Theories and methodology of complementary hydro/photovoltaic operation: Applications to short-term scheduling," *Journal of Renewable and Sustainable Energy*, vol. 7, no. 6, p. 063133, 2015, doi: [10.1063/1.4939056](https://doi.org/10.1063/1.4939056).
- [6] W. Fang, Q. Huang, S. Huang, J. Yang, E. Meng, and Y. Li, "Optimal sizing of utility-scale photovoltaic power generation complementarily operating with hydropower: A case study of the world's largest hydro-photovoltaic plant," *Energy Conversion and Management*, vol. 136, pp. 161-172, 2017/03/15/ 2017, doi: <https://doi.org/10.1016/j.enconman.2017.01.012>.
- [7] J. Jurasz and B. Ciapała, "Integrating photovoltaics into energy systems by using a run-off-river power plant with pondage to smooth energy exchange with the power grid," *Applied Energy*, vol. 198, pp. 21-35, 2017/07/15/ 2017, doi: <https://doi.org/10.1016/j.apenergy.2017.04.042>.
- [8] J. Mahmoudimehr and M. Shabani, "Optimal design of hybrid photovoltaic-hydroelectric standalone energy system for north and south of Iran," *Renewable Energy*, vol. 115, pp. 238-251, 2018/01/01/ 2018, doi: <https://doi.org/10.1016/j.renene.2017.08.054>.
- [9] O. Erdinc, N. G. Paterakis, I. N. Pappi, A. G. Bakirtzis, and J. P. S. Catalão, "A new perspective for sizing of distributed generation and energy storage for smart households under demand response," *Applied Energy*, vol. 143, pp. 26-37, 2015/04/01/ 2015, doi: <https://doi.org/10.1016/j.apenergy.2015.01.025>.
- [10] A. S. Jacob, R. Banerjee, and P. C. Ghosh, "Sizing of hybrid energy storage system for a PV based microgrid through design space approach," *Applied Energy*, vol. 212, pp. 640-653, 2018/02/15/ 2018, doi: <https://doi.org/10.1016/j.apenergy.2017.12.040>.
- [11] C. V. T. Cabral, D. O. Filho, A. S. A. C. Diniz, J. H. Martins, O. M. Toledo, and L. d. V. B. Machado Neto, "A stochastic method for stand-alone photovoltaic system sizing," *Solar Energy*, vol. 84, no. 9, pp. 1628-1636, 2010/09/01/ 2010, doi: <https://doi.org/10.1016/j.solener.2010.06.006>.
- [12] S.-G. Chen, "An efficient sizing method for a stand-alone PV system in terms of the observed block extremes," *Applied Energy*, vol. 91, no. 1, pp. 375-384, 2012/03/01/ 2012, doi: <https://doi.org/10.1016/j.apenergy.2011.09.043>.
- [13] Z. Hua, C. Ma, J. Lian, X. Pang, and W. Yang, "Optimal capacity allocation of multiple solar trackers and storage capacity for utility-scale photovoltaic plants considering output characteristics and complementary demand," *Applied Energy*, vol. 238, pp. 721-733, 2019/03/15/ 2019, doi: <https://doi.org/10.1016/j.apenergy.2019.01.099>.
- [14] F. Xu, J. Liu, S. Lin, Q. Dai, and C. Li, "A multi-objective optimization model of hybrid energy storage system for non-grid-connected wind power: A case study in

- China," *Energy*, vol. 163, pp. 585-603, 2018/11/15/ 2018, doi: <https://doi.org/10.1016/j.energy.2018.08.152>.
- [15] J. G. García Clúa, R. J. Mantz, and H. De Battista, "Optimal sizing of a grid-assisted wind-hydrogen system," *Energy Conversion and Management*, vol. 166, pp. 402-408, 2018/06/15/ 2018, doi: 10.1016/j.enconman.2018.04.047.
- [16] I. B. Askari and M. Ameri, "Techno-economic Feasibility Analysis of Stand-alone Renewable Energy Systems (PV/bat, Wind/bat and Hybrid PV/wind/bat) in Kerman, Iran," *Energy Sources, Part B: Economics, Planning, and Policy*, vol. 7, no. 1, pp. 45-60, 2012/01/01 2012, doi: 10.1080/15567240903330384.
- [17] A. Maleki, M. G. Khajeh, and M. Ameri, "Optimal sizing of a grid independent hybrid renewable energy system incorporating resource uncertainty, and load uncertainty," *International Journal of Electrical Power & Energy Systems*, vol. 83, pp. 514-524, 2016/12/01/ 2016, doi: <https://doi.org/10.1016/j.ijepes.2016.04.008>.
- [18] A. Maleki and A. Askarzadeh, "Optimal sizing of a PV/wind/diesel system with battery storage for electrification to an off-grid remote region: A case study of Rafsanjan, Iran," *Sustainable Energy Technologies and Assessments*, vol. 7, pp. 147-153, 2014/09/01/ 2014, doi: <https://doi.org/10.1016/j.seta.2014.04.005>.
- [19] V. Khare, S. Nema, and P. Baredar, "Optimisation of the hybrid renewable energy system by HOMER, PSO and CPSO for the study area," *International Journal of Sustainable Energy*, vol. 36, no. 4, pp. 326-343, 2017/04/21 2017, doi: 10.1080/14786451.2015.1017500.
- [20] R. Atia and N. Yamada, "Sizing and Analysis of Renewable Energy and Battery Systems in Residential Microgrids," *IEEE Transactions on Smart Grid*, vol. 7, no. 3, pp. 1204-1213, 2016, doi: 10.1109/TSG.2016.2519541.
- [21] A. Mahesh and K. S. Sandhu, "Optimal sizing of a PV/Wind hybrid system using pigeon inspired optimization," in *2016 IEEE 7th Power India International Conference (PIICON)*, 25-27 Nov. 2016 2016, pp. 1-6, doi: 10.1109/POWERI.2016.8077412.
- [22] A. Ahadi, S.-K. Kang, and J.-H. Lee, "A novel approach for optimal combinations of wind, PV, and energy storage system in diesel-free isolated communities," *Applied Energy*, vol. 170, pp. 101-115, 2016/05/15/ 2016, doi: <https://doi.org/10.1016/j.apenergy.2016.02.110>.
- [23] R. Hosseinalizadeh, H. Shakouri G, Mohsen S. Amalnick, and P. Taghipour, "Economic sizing of a hybrid (PV–WT–FC) renewable energy system (HRES) for stand-alone usages by an optimization-simulation model: Case study of Iran," *Renewable and Sustainable Energy Reviews*, vol. 54, pp. 139-150, 2016/02/01/ 2016, doi: <https://doi.org/10.1016/j.rser.2015.09.046>.
- [24] G. Panayiotou, S. Kalogirou, and S. Tassou, "Design and simulation of a PV and a PV–Wind standalone energy system to power a household application," *Renewable Energy*, vol. 37, no. 1, pp. 355-363, 2012/01/01/ 2012, doi: 10.1016/j.renene.2011.06.038.
- [25] S. Sanajaoba and E. Fernandez, "Maiden application of Cuckoo Search algorithm for optimal sizing of a remote hybrid renewable energy System," *Renewable Energy*, vol. 96, pp. 1-10, 2016/10/01/ 2016, doi: <https://doi.org/10.1016/j.renene.2016.04.069>.
- [26] A. Maleki and A. Askarzadeh, "Artificial bee swarm optimization for optimum sizing of a stand-alone PV/WT/FC hybrid system considering LPSP concept," *Solar Energy*, vol. 107, pp. 227-235, 2014/09/01/ 2014, doi: <https://doi.org/10.1016/j.solener.2014.05.016>.
- [27] A. Askarzadeh, "Solution for sizing a PV/diesel HPGS for isolated sites," *IET Renewable Power Generation*, vol. 11, no. 1, pp. 143-151, 2017, doi: 10.1049/iet-rpg.2016.0319.
- [28] L. Olatomiwa, S. Mekhilef, A. S. N. Huda, and K. Sanusi, "Techno-economic analysis of hybrid PV–diesel–battery and PV–wind–diesel–battery power systems for mobile BTS: the way forward for rural development," *Energy Science & Engineering*, vol. 3, no. 4, pp. 271-285, 2015, doi: 10.1002/ese3.71.

- [29] W. D. Kellogg, M. H. Nehrir, G. Venkataramanan, and V. Gerez, "Generation unit sizing and cost analysis for stand-alone wind, photovoltaic, and hybrid wind/PV systems," *IEEE Transactions on Energy Conversion*, pp. Medium: X; Size: pp. 70-75, 1998.
- [30] U. Akram, M. Khalid, and S. Shafiq, "An improved optimal sizing methodology for future autonomous residential smart power systems," *IEEE Access*, vol. 6, pp. 5986-6000, 2018.
- [31] S. Mandal, B. K. Das, and N. Hoque, "Optimum sizing of a stand-alone hybrid energy system for rural electrification in Bangladesh," *Journal of Cleaner Production*, vol. 200, pp. 12-27, 2018/11/01/ 2018, doi: <https://doi.org/10.1016/j.jclepro.2018.07.257>.
- [32] L. Luo *et al.*, "Optimal siting and sizing of distributed generation in distribution systems with PV solar farm utilized as STATCOM (PV-STATCOM)," *Applied Energy*, vol. 210, pp. 1092-1100, 2018/01/15/ 2018, doi: <https://doi.org/10.1016/j.apenergy.2017.08.165>.
- [33] M. Alsayed, M. Cacciato, G. Scarcella, and G. Scelba, "Multicriteria Optimal Sizing of Photovoltaic-Wind Turbine Grid Connected Systems," *IEEE Transactions on Energy Conversion*, vol. 28, no. 2, pp. 370-379, 2013, doi: 10.1109/TEC.2013.2245669.
- [34] S. Barakat, H. Ibrahim, and A. A. Elbaset, "Multi-objective optimization of grid-connected PV-wind hybrid system considering reliability, cost, and environmental aspects," *Sustainable Cities and Society*, vol. 60, p. 102178, 2020/09/01/ 2020, doi: <https://doi.org/10.1016/j.scs.2020.102178>.
- [35] T. Senjyu, D. Hayashi, N. Urasaki, and T. Funabashi, "Optimum configuration for renewable generating systems in residence using genetic algorithm," *IEEE Transactions on Energy Conversion*, vol. 21, no. 2, pp. 459-466, 2006, doi: 10.1109/TEC.2006.874250.
- [36] L. Xu, X. Ruan, C. Mao, B. Zhang, and Y. Luo, "An improved optimal sizing method for wind-solar-battery hybrid power system," *IEEE transactions on Sustainable Energy*, vol. 4, no. 3, pp. 774-785, 2013.
- [37] U. Akram, M. Khalid, and S. Shafiq, "An Innovative Hybrid Wind-Solar and Battery-Supercapacitor Microgrid System—Development and Optimization," *IEEE Access*, vol. 5, pp. 25897-25912, 2017, doi: 10.1109/ACCESS.2017.2767618.
- [38] U. Akram, M. Khalid, and S. Shafiq, "Optimal Sizing of a Wind/Solar/Battery Hybrid Grid-connected Microgrid System," *IET Renewable Power Generation*, vol. 12, 10/09 2017, doi: 10.1049/iet-rpg.2017.0010.
- [39] A. S. Al Busaidi, H. A. Kazem, and M. F. Khan, "A review of optimum sizing techniques for off-grid hybrid PV-wind renewable energy systems," *International journal of students research in technology & management*, vol. 2, no. 03, pp. 93-102, 2014.
- [40] T. Khatib, I. A. Ibrahim, and A. Mohamed, "A review on sizing methodologies of photovoltaic array and storage battery in a standalone photovoltaic system," *Energy Conversion and Management*, vol. 120, pp. 430-448, 2016/07/15/ 2016, doi: <https://doi.org/10.1016/j.enconman.2016.05.011>.
- [41] K. Anoune, M. Bouya, A. Astito, and A. B. Abdellah, "Sizing methods and optimization techniques for PV-wind based hybrid renewable energy system: A review," *Renewable and Sustainable Energy Reviews*, vol. 93, pp. 652-673, 2018/10/01/ 2018, doi: <https://doi.org/10.1016/j.rser.2018.05.032>.
- [42] T. Tezer, R. Yaman, and G. Yaman, "Evaluation of approaches used for optimization of stand-alone hybrid renewable energy systems," *Renewable and Sustainable Energy Reviews*, vol. 73, pp. 840-853, 2017/06/01/ 2017, doi: <https://doi.org/10.1016/j.rser.2017.01.118>.
- [43] H. Yang, Z. Wei, and L. Chengzhi, "Optimal design and techno-economic analysis of a hybrid solar-wind power generation system," *Applied Energy*, vol. 86, no. 2, pp. 163-169, 2009/02/01/ 2009, doi: <https://doi.org/10.1016/j.apenergy.2008.03.008>.
- [44] R. Luna-Rubio, M. Trejo-Perea, D. Vargas-Vázquez, and G. J. Ríos-Moreno, "Optimal sizing of renewable hybrids energy systems: A review of methodologies,"

- Solar Energy*, vol. 86, no. 4, pp. 1077-1088, 2012/04/01/ 2012, doi: <https://doi.org/10.1016/j.solener.2011.10.016>.
- [45] S. Diaf, G. Notton, M. Belhamel, M. Haddadi, and A. Louche, "Design and techno-economical optimization for hybrid PV/wind system under various meteorological conditions," *Applied Energy*, vol. 85, no. 10, pp. 968-987, 2008/10/01/ 2008, doi: <https://doi.org/10.1016/j.apenergy.2008.02.012>.
- [46] A. Chauhan and R. P. Saini, "A review on Integrated Renewable Energy System based power generation for stand-alone applications: Configurations, storage options, sizing methodologies and control," *Renewable and Sustainable Energy Reviews*, vol. 38, pp. 99-120, 2014/10/01/ 2014, doi: <https://doi.org/10.1016/j.rser.2014.05.079>.
- [47] E. Hau, *Wind turbines: fundamentals, technologies, application, economics*. Springer Science & Business Media, 2013.
- [48] S. Upadhyay and M. P. Sharma, "A review on configurations, control and sizing methodologies of hybrid energy systems," *Renewable and Sustainable Energy Reviews*, vol. 38, pp. 47-63, 2014/10/01/ 2014, doi: <https://doi.org/10.1016/j.rser.2014.05.057>.
- [49] H. R. Baghaee, M. Mirsalim, G. B. Gharehpetian, and H. A. Talebi, "Reliability/cost-based multi-objective Pareto optimal design of stand-alone wind/PV/FC generation microgrid system," *Energy*, vol. 115, pp. 1022-1041, 2016/11/15/ 2016, doi: <https://doi.org/10.1016/j.energy.2016.09.007>.
- [50] G. Ma, G. Xu, Y. Chen, and R. Ju, "Multi-objective optimal configuration method for a standalone wind-solar-battery hybrid power system," *IET Renewable Power Generation*, vol. 11, no. 1, pp. 194-202, 2016.
- [51] M. Fadaee and M. A. M. Radzi, "Multi-objective optimization of a stand-alone hybrid renewable energy system by using evolutionary algorithms: A review," *Renewable and Sustainable Energy Reviews*, vol. 16, no. 5, pp. 3364-3369, 2012/06/01/ 2012, doi: <https://doi.org/10.1016/j.rser.2012.02.071>.
- [52] S. Sinha and S. S. Chandel, "Review of recent trends in optimization techniques for solar photovoltaic-wind based hybrid energy systems," *Renewable and Sustainable Energy Reviews*, vol. 50, pp. 755-769, 2015/10/01/ 2015, doi: <https://doi.org/10.1016/j.rser.2015.05.040>.
- [53] R. Siddaiah and R. P. Saini, "A review on planning, configurations, modeling and optimization techniques of hybrid renewable energy systems for off grid applications," *Renewable and Sustainable Energy Reviews*, vol. 58, pp. 376-396, 2016/05/01/ 2016, doi: <https://doi.org/10.1016/j.rser.2015.12.281>.
- [54] M. Sharafi and T. Y. Elmekawy, "Multi-objective optimal design of hybrid renewable energy systems using PSO-simulation based approach," *Renewable Energy*, vol. 68, pp. 67-79, 2014/08/01/ 2014, doi: <https://doi.org/10.1016/j.renene.2014.01.011>.
- [55] A. Mahesh and K. S. Sandhu, "Hybrid wind/photovoltaic energy system developments: Critical review and findings," *Renewable and Sustainable Energy Reviews*, vol. 52, pp. 1135-1147, 2015/12/01/ 2015, doi: <https://doi.org/10.1016/j.rser.2015.08.008>.
- [56] S. Bahramara, M. P. Moghaddam, and M. R. Haghifam, "Optimal planning of hybrid renewable energy systems using HOMER: A review," *Renewable and Sustainable Energy Reviews*, vol. 62, pp. 609-620, 2016/09/01/ 2016, doi: <https://doi.org/10.1016/j.rser.2016.05.039>.
- [57] S. El Alimi, T. Maatallah, and S. Ben Nasrallah, "Break-even analysis and optimization of a stand-alone hybrid system with battery storage for residential load consumption—A case study," *Renewable and Sustainable Energy Reviews*, vol. 37, pp. 408-423, 2014/09/01/ 2014, doi: <https://doi.org/10.1016/j.rser.2014.04.059>.
- [58] H. Belmili, M. Haddadi, S. Bacha, M. F. Almi, and B. Bendib, "Sizing stand-alone photovoltaic-wind hybrid system: Techno-economic analysis and optimization," *Renewable and Sustainable Energy Reviews*, vol. 30, pp. 821-832, 2014/02/01/ 2014, doi: <https://doi.org/10.1016/j.rser.2013.11.011>.

- [59] A. Kaabeche and R. Ibtouen, "Techno-economic optimization of hybrid photovoltaic/wind/diesel/battery generation in a stand-alone power system," *Solar Energy*, vol. 103, pp. 171-182, 2014/05/01/ 2014, doi: <https://doi.org/10.1016/j.solener.2014.02.017>.
- [60] T. Khatib, A. Mohamed, K. Sopian, and M. Mahmoud, "Optimal Sizing of Hybrid PV/Wind Systems for Malaysia Using Loss of Load Probability," *Energy Sources, Part A: Recovery, Utilization, and Environmental Effects*, vol. 37, no. 7, pp. 687-695, 2015/04/03 2015, doi: 10.1080/15567036.2011.592920.
- [61] M. Smaoui, A. Abdelkafi, and L. Krichen, "Optimal sizing of stand-alone photovoltaic/wind/hydrogen hybrid system supplying a desalination unit," *Solar Energy*, vol. 120, pp. 263-276, 2015/10/01/ 2015, doi: <https://doi.org/10.1016/j.solener.2015.07.032>.
- [62] F. A. Bhuiyan, A. Yazdani, and S. L. Primak, "Optimal sizing approach for islanded microgrids," *IET Renewable Power Generation*, vol. 9, no. 2, pp. 166-175, 2014.
- [63] R. Belfkira, L. Zhang, and G. Barakat, "Optimal sizing study of hybrid wind/PV/diesel power generation unit," *Solar Energy*, vol. 85, no. 1, pp. 100-110, 2011/01/01/ 2011, doi: <https://doi.org/10.1016/j.solener.2010.10.018>.
- [64] C. E. C. Nogueira *et al.*, "Sizing and simulation of a photovoltaic-wind energy system using batteries, applied for a small rural property located in the south of Brazil," *Renewable and Sustainable Energy Reviews*, vol. 29, pp. 151-157, 2014/01/01/ 2014, doi: <https://doi.org/10.1016/j.rser.2013.08.071>.
- [65] F. Huneke, J. Henkel, J. A. B. González, and G. Erdmann, "Optimisation of hybrid off-grid energy systems by linear programming," *Energy, Sustainability and Society*, vol. 2, no. 1, p. 7, 2012.
- [66] A. Malheiro, P. M. Castro, R. M. Lima, and A. Estanqueiro, "Integrated sizing and scheduling of wind/PV/diesel/battery isolated systems," *Renewable Energy*, vol. 83, pp. 646-657, 2015/11/01/ 2015, doi: <https://doi.org/10.1016/j.renene.2015.04.066>.
- [67] L. Ferrer-Martí, B. Domenech, A. García-Villoria, and R. Pastor, "A MILP model to design hybrid wind-photovoltaic isolated rural electrification projects in developing countries," *European Journal of Operational Research*, vol. 226, no. 2, pp. 293-300, 2013/04/16/ 2013, doi: <https://doi.org/10.1016/j.ejor.2012.11.018>.
- [68] W.-S. Tan, M. Y. Hassan, M. S. Majid, and H. Abdul Rahman, "Optimal distributed renewable generation planning: A review of different approaches," *Renewable and Sustainable Energy Reviews*, vol. 18, pp. 626-645, 2013/02/01/ 2013, doi: <https://doi.org/10.1016/j.rser.2012.10.039>.
- [69] S. C. Lee, "Numerical estimation model of energy conversion for small hybrid solar-wind system," *Solar Energy*, vol. 86, no. 11, pp. 3125-3136, 2012/11/01/ 2012, doi: <https://doi.org/10.1016/j.solener.2012.08.001>.
- [70] D. K. Khatod, V. Pant, and J. Sharma, "Analytical Approach for Well-Being Assessment of Small Autonomous Power Systems With Solar and Wind Energy Sources," *IEEE Transactions on Energy Conversion*, vol. 25, no. 2, pp. 535-545, 2010, doi: 10.1109/TEC.2009.2033881.
- [71] A. B. Kanase-Patil, R. P. Saini, and M. P. Sharma, "Sizing of integrated renewable energy system based on load profiles and reliability index for the state of Uttarakhand in India," *Renewable Energy*, vol. 36, no. 11, pp. 2809-2821, 2011/11/01/ 2011, doi: <https://doi.org/10.1016/j.renene.2011.04.022>.
- [72] L. K. Gan, J. K. H. Shek, and M. A. Mueller, "Hybrid wind-photovoltaic-diesel-battery system sizing tool development using empirical approach, life-cycle cost and performance analysis: A case study in Scotland," *Energy Conversion and Management*, vol. 106, pp. 479-494, 2015/12/01/ 2015, doi: <https://doi.org/10.1016/j.enconman.2015.09.029>.
- [73] B. Zhao, X. Zhang, P. Li, K. Wang, M. Xue, and C. Wang, "Optimal sizing, operating strategy and operational experience of a stand-alone microgrid on Dongfushan Island," *Applied Energy*, vol. 113, pp. 1656-1666, 2014/01/01/ 2014, doi: <https://doi.org/10.1016/j.apenergy.2013.09.015>.



- [74] A. S. O. Ogunjuyigbe, T. R. Ayodele, and O. A. Akinola, "Optimal allocation and sizing of PV/Wind/Split-diesel/Battery hybrid energy system for minimizing life cycle cost, carbon emission and dump energy of remote residential building," *Applied Energy*, vol. 171, pp. 153-171, 2016/06/01/ 2016, doi: <https://doi.org/10.1016/j.apenergy.2016.03.051>.
- [75] S. Rajanna and R. P. Saini, "Development of optimal integrated renewable energy model with battery storage for a remote Indian area," *Energy*, vol. 111, pp. 803-817, 2016/09/15/ 2016, doi: <https://doi.org/10.1016/j.energy.2016.06.005>.
- [76] B. Elliston, I. MacGill, and M. Diesendorf, "Least cost 100% renewable electricity scenarios in the Australian National Electricity Market," *Energy Policy*, vol. 59, pp. 270-282, 2013/08/01/ 2013, doi: <https://doi.org/10.1016/j.enpol.2013.03.038>.
- [77] L. K. Gan, J. K. H. Shek, and M. A. Mueller, "Optimised operation of an off-grid hybrid wind-diesel-battery system using genetic algorithm," *Energy Conversion and Management*, vol. 126, pp. 446-462, 2016/10/15/ 2016, doi: <https://doi.org/10.1016/j.enconman.2016.07.062>.
- [78] G. Merei, C. Berger, and D. U. Sauer, "Optimization of an off-grid hybrid PV–Wind–Diesel system with different battery technologies using genetic algorithm," *Solar Energy*, vol. 97, pp. 460-473, 2013/11/01/ 2013, doi: <https://doi.org/10.1016/j.solener.2013.08.016>.
- [79] H.-C. Chen, "Optimum capacity determination of stand-alone hybrid generation system considering cost and reliability," *Applied Energy*, vol. 103, pp. 155-164, 2013/03/01/ 2013, doi: <https://doi.org/10.1016/j.apenergy.2012.09.022>.
- [80] A. Kamjoo, A. Maheri, A. M. Dizqah, and G. A. Putrus, "Multi-objective design under uncertainties of hybrid renewable energy system using NSGA-II and chance constrained programming," *International Journal of Electrical Power & Energy Systems*, vol. 74, pp. 187-194, 2016/01/01/ 2016, doi: <https://doi.org/10.1016/j.ijepes.2015.07.007>.
- [81] W. Sheng, K.-y. Liu, X. Meng, X. Ye, and Y. Liu, "Research and practice on typical modes and optimal allocation method for PV-Wind-ES in Microgrid," *Electric Power Systems Research*, vol. 120, pp. 242-255, 2015/03/01/ 2015, doi: <https://doi.org/10.1016/j.epsr.2014.02.011>.
- [82] D. Abbes, A. Martinez, and G. Champenois, "Life cycle cost, embodied energy and loss of power supply probability for the optimal design of hybrid power systems," *Mathematics and Computers in Simulation*, vol. 98, pp. 46-62, 2014/04/01/ 2014, doi: <https://doi.org/10.1016/j.matcom.2013.05.004>.
- [83] A. Fathy, "A reliable methodology based on mine blast optimization algorithm for optimal sizing of hybrid PV-wind-FC system for remote area in Egypt," *Renewable Energy*, vol. 95, pp. 367-380, 2016/09/01/ 2016, doi: <https://doi.org/10.1016/j.renene.2016.04.030>.
- [84] P. Paliwal, N. P. Patidar, and R. K. Nema, "Determination of reliability constrained optimal resource mix for an autonomous hybrid power system using Particle Swarm Optimization," *Renewable Energy*, vol. 63, pp. 194-204, 2014/03/01/ 2014, doi: <https://doi.org/10.1016/j.renene.2013.09.003>.
- [85] V. M. Sanchez, A. U. Chavez-Ramirez, S. M. Duron-Torres, J. Hernandez, L. G. Arriaga, and J. M. Ramirez, "Techno-economical optimization based on swarm intelligence algorithm for a stand-alone wind-photovoltaic-hydrogen power system at south-east region of Mexico," *International Journal of Hydrogen Energy*, vol. 39, no. 29, pp. 16646-16655, 2014/10/02/ 2014, doi: <https://doi.org/10.1016/j.ijhydene.2014.06.034>.
- [86] A. Askarzadeh and L. dos Santos Coelho, "A novel framework for optimization of a grid independent hybrid renewable energy system: A case study of Iran," *Solar Energy*, vol. 112, pp. 383-396, 2015/02/01/ 2015, doi: <https://doi.org/10.1016/j.solener.2014.12.013>.
- [87] A. Maleki, M. Ameri, and F. Keynia, "Scrutiny of multifarious particle swarm optimization for finding the optimal size of a PV/wind/battery hybrid system,"

- Renewable Energy*, vol. 80, pp. 552-563, 2015/08/01/ 2015, doi: <https://doi.org/10.1016/j.renene.2015.02.045>.
- [88] A. Hassan, M. Saadawi, M. Kandil, and M. Saeed, "Modified particle swarm optimisation technique for optimal design of small renewable energy system supplying a specific load at Mansoura University," *IET Renewable Power Generation*, vol. 9, no. 5, pp. 474-483, 2015.
- [89] H. Borhanazad, S. Mekhilef, V. Gounder Ganapathy, M. Modiri-Delshad, and A. Mirtaheri, "Optimization of micro-grid system using MOPSO," *Renewable Energy*, vol. 71, pp. 295-306, 2014/11/01/ 2014, doi: <https://doi.org/10.1016/j.renene.2014.05.006>.
- [90] S. Safari, M. M. Ardehali, and M. J. Sirizi, "Particle swarm optimization based fuzzy logic controller for autonomous green power energy system with hydrogen storage," *Energy Conversion and Management*, vol. 65, pp. 41-49, 2013/01/01/ 2013, doi: <https://doi.org/10.1016/j.enconman.2012.08.012>.
- [91] B. Shi, W. Wu, and L. Yan, "Size optimization of stand-alone PV/wind/diesel hybrid power generation systems," *Journal of the Taiwan Institute of Chemical Engineers*, vol. 73, pp. 93-101, 2017/04/01/ 2017, doi: <https://doi.org/10.1016/j.jtice.2016.07.047>.
- [92] P. Suhane, S. Rangnekar, A. Mittal, and A. Khare, "Sizing and performance analysis of standalone wind-photovoltaic based hybrid energy system using ant colony optimisation," *IET Renewable Power Generation*, vol. 10, no. 7, pp. 964-972, 2016.
- [93] A. Fetanat and E. Khorasaninejad, "Size optimization for hybrid photovoltaic-wind energy system using ant colony optimization for continuous domains based integer programming," *Applied Soft Computing*, vol. 31, pp. 196-209, 2015/06/01/ 2015, doi: <https://doi.org/10.1016/j.asoc.2015.02.047>.
- [94] R. Wang, R. C. Purshouse, and P. J. Fleming, "Preference-Inspired Coevolutionary Algorithms for Many-Objective Optimization," *IEEE Transactions on Evolutionary Computation*, vol. 17, no. 4, pp. 474-494, 2013, doi: 10.1109/TEVC.2012.2204264.
- [95] Z. Shi, R. Wang, and T. Zhang, "Multi-objective optimal design of hybrid renewable energy systems using preference-inspired coevolutionary approach," *Solar Energy*, vol. 118, pp. 96-106, 2015/08/01/ 2015, doi: <https://doi.org/10.1016/j.solener.2015.03.052>.
- [96] J. Zhao and X. Yuan, "Multi-objective optimization of stand-alone hybrid PV-wind-diesel-battery system using improved fruit fly optimization algorithm," *Soft Computing*, vol. 20, no. 7, pp. 2841-2853, 2016.
- [97] R. A. Gupta, R. Kumar, and A. K. Bansal, "BBO-based small autonomous hybrid power system optimization incorporating wind speed and solar radiation forecasting," *Renewable and Sustainable Energy Reviews*, vol. 41, pp. 1366-1375, 2015/01/01/ 2015, doi: <https://doi.org/10.1016/j.rser.2014.09.017>.
- [98] R. Kumar, R. A. Gupta, and A. K. Bansal, "Economic analysis and power management of a stand-alone wind/photovoltaic hybrid energy system using biogeography based optimization algorithm," *Swarm and Evolutionary Computation*, vol. 8, pp. 33-43, 2013/02/01/ 2013, doi: <https://doi.org/10.1016/j.swevo.2012.08.002>.
- [99] S. Singh, M. Singh, and S. C. Kaushik, "Feasibility study of an islanded microgrid in rural area consisting of PV, wind, biomass and battery energy storage system," *Energy Conversion and Management*, vol. 128, pp. 178-190, 2016/11/15/ 2016, doi: <https://doi.org/10.1016/j.enconman.2016.09.046>.
- [100] H. Gharavi, M. M. Ardehali, and S. Ghanbari-Tichi, "Imperial competitive algorithm optimization of fuzzy multi-objective design of a hybrid green power system with considerations for economics, reliability, and environmental emissions," *Renewable Energy*, vol. 78, pp. 427-437, 2015/06/01/ 2015, doi: <https://doi.org/10.1016/j.renene.2015.01.029>.
- [101] K.-H. Chang and G. Lin, "Optimal design of hybrid renewable energy systems using simulation optimization," *Simulation Modelling Practice and Theory*, vol. 52, pp. 40-51, 2015/03/01/ 2015, doi: <https://doi.org/10.1016/j.simpat.2014.12.002>.
- [102] R. Dufo-López, I. R. Cristóbal-Monreal, and J. M. Yusta, "Optimisation of PV-wind-diesel-battery stand-alone systems to minimise cost and maximise human

- development index and job creation," *Renewable Energy*, vol. 94, pp. 280-293, 2016/08/01/ 2016, doi: <https://doi.org/10.1016/j.renene.2016.03.065>.
- [103] J. M. Lujano-Rojas, R. Dufo-López, and J. L. Bernal-Agustín, "Probabilistic modelling and analysis of stand-alone hybrid power systems," *Energy*, vol. 63, pp. 19-27, 2013/12/15/ 2013, doi: <https://doi.org/10.1016/j.energy.2013.10.003>.
- [104] Y. Hong and R. Lian, "Optimal Sizing of Hybrid Wind/PV/Diesel Generation in a Stand-Alone Power System Using Markov-Based Genetic Algorithm," *IEEE Transactions on Power Delivery*, vol. 27, no. 2, pp. 640-647, 2012, doi: 10.1109/TPWRD.2011.2177102.
- [105] T. Khatib, A. Mohamed, and K. Sopian, "Optimization of a PV/wind micro-grid for rural housing electrification using a hybrid iterative/genetic algorithm: Case study of Kuala Terengganu, Malaysia," *Energy and Buildings*, vol. 47, pp. 321-331, 2012/04/01/ 2012, doi: <https://doi.org/10.1016/j.enbuild.2011.12.006>.
- [106] S. R. Tito, T. T. Lie, and T. N. Anderson, "Optimal sizing of a wind-photovoltaic-battery hybrid renewable energy system considering socio-demographic factors," *Solar Energy*, vol. 136, pp. 525-532, 2016/10/15/ 2016, doi: <https://doi.org/10.1016/j.solener.2016.07.036>.
- [107] S. Ahmadi and S. Abdi, "Application of the Hybrid Big Bang–Big Crunch algorithm for optimal sizing of a stand-alone hybrid PV/wind/battery system," *Solar Energy*, vol. 134, pp. 366-374, 2016/09/01/ 2016, doi: <https://doi.org/10.1016/j.solener.2016.05.019>.
- [108] T. Zhou and W. Sun, "Optimization of Battery–Supercapacitor Hybrid Energy Storage Station in Wind/Solar Generation System," *IEEE Transactions on Sustainable Energy*, vol. 5, no. 2, pp. 408-415, 2014, doi: 10.1109/TSTE.2013.2288804.
- [109] Y. A. Katsigiannis, P. S. Georgilakis, and E. S. Karapidakis, "Hybrid simulated annealing–tabu search method for optimal sizing of autonomous power systems with renewables," *IEEE Transactions on Sustainable Energy*, vol. 3, no. 3, pp. 330-338, 2012.
- [110] A. Askarzadeh, "A discrete chaotic harmony search-based simulated annealing algorithm for optimum design of PV/wind hybrid system," *Solar Energy*, vol. 97, pp. 93-101, 2013/11/01/ 2013, doi: <https://doi.org/10.1016/j.solener.2013.08.014>.
- [111] A. Maleki, M. G. Khajeh, and M. A. Rosen, "Weather forecasting for optimization of a hybrid solar-wind–powered reverse osmosis water desalination system using a novel optimizer approach," *Energy*, vol. 114, pp. 1120-1134, 2016/11/01/ 2016, doi: <https://doi.org/10.1016/j.energy.2016.06.134>.
- [112] M. Tahani, N. Babayan, and A. Pouyaei, "Optimization of PV/Wind/Battery stand-alone system, using hybrid FPA/SA algorithm and CFD simulation, case study: Tehran," *Energy Conversion and Management*, vol. 106, pp. 644-659, 2015/12/01/ 2015, doi: <https://doi.org/10.1016/j.enconman.2015.10.011>.
- [113] J.-H. Cho, M.-G. Chun, and W.-P. Hong, "Structure optimization of stand-alone renewable power systems based on multi object function," *Energies*, vol. 9, no. 8, p. 649, 2016.
- [114] R. N. S. R. Mukhtaruddin, H. A. Rahman, M. Y. Hassan, and J. J. Jamian, "Optimal hybrid renewable energy design in autonomous system using Iterative-Pareto-Fuzzy technique," *International Journal of Electrical Power & Energy Systems*, vol. 64, pp. 242-249, 2015/01/01/ 2015, doi: <https://doi.org/10.1016/j.ijepes.2014.07.030>.
- [115] B. J. Abdelhak, E. Najib, H. Abdelaziz, F. Hnaïen, and F. Yalaoui, "Optimum sizing of hybrid PV/wind/battery using Fuzzy-Adaptive Genetic Algorithm in real and average battery service life," in *2014 International symposium on power electronics, electrical drives, automation and motion*, 2014: IEEE, pp. 871-876.
- [116] D. Connolly, H. Lund, B. V. Mathiesen, and M. Leahy, "A review of computer tools for analysing the integration of renewable energy into various energy systems," *Applied Energy*, vol. 87, no. 4, pp. 1059-1082, 2010/04/01/ 2010, doi: <https://doi.org/10.1016/j.apenergy.2009.09.026>.
- [117] H. Zahboune, S. Zouggar, G. Krajacic, P. S. Varbanov, M. Elhafyani, and E. Ziani, "Optimal hybrid renewable energy design in autonomous system using Modified

- Electric System Cascade Analysis and Homer software," *Energy Conversion and Management*, vol. 126, pp. 909-922, 2016/10/15/ 2016, doi: <https://doi.org/10.1016/j.enconman.2016.08.061>.
- [118] R. Dufo-López and J. L. Bernal-Agustín, "A comparative assessment of net metering and net billing policies. Study cases for Spain," *Energy*, vol. 84, pp. 684-694, 2015/05/01/ 2015, doi: <https://doi.org/10.1016/j.energy.2015.03.031>.
- [119] R. Dufo-López, J. M. Lujano-Rojas, and J. L. Bernal-Agustín, "Comparison of different lead–acid battery lifetime prediction models for use in simulation of stand-alone photovoltaic systems," *Applied Energy*, vol. 115, pp. 242-253, 2014/02/15/ 2014, doi: <https://doi.org/10.1016/j.apenergy.2013.11.021>.
- [120] J. Schiffer, D. U. Sauer, H. Bindner, T. Cronin, P. Lundsager, and R. Kaiser, "Model prediction for ranking lead-acid batteries according to expected lifetime in renewable energy systems and autonomous power-supply systems," *Journal of Power Sources*, vol. 168, no. 1, pp. 66-78, 2007/05/25/ 2007, doi: <https://doi.org/10.1016/j.jpowsour.2006.11.092>.
- [121] F. Baghdadi, K. Mohammedi, S. Diaf, and O. Behar, "Feasibility study and energy conversion analysis of stand-alone hybrid renewable energy system," *Energy Conversion and Management*, vol. 105, pp. 471-479, 2015/11/15/ 2015, doi: <https://doi.org/10.1016/j.enconman.2015.07.051>.
- [122] M. Fadaeenejad, M. A. M. Radzi, M. Z. A. AbKadir, and H. Hizam, "Assessment of hybrid renewable power sources for rural electrification in Malaysia," *Renewable and Sustainable Energy Reviews*, vol. 30, pp. 299-305, 2014/02/01/ 2014, doi: <https://doi.org/10.1016/j.rser.2013.10.003>.
- [123] R. Dufo-López *et al.*, "Multi-objective optimization minimizing cost and life cycle emissions of stand-alone PV–wind–diesel systems with batteries storage," *Applied Energy*, vol. 88, no. 11, pp. 4033-4041, 2011/11/01/ 2011, doi: <https://doi.org/10.1016/j.apenergy.2011.04.019>.
- [124] S. M. Zahraee, M. Khalaji Assadi, and R. Saidur, "Application of Artificial Intelligence Methods for Hybrid Energy System Optimization," *Renewable and Sustainable Energy Reviews*, vol. 66, pp. 617-630, 2016/12/01/ 2016, doi: <https://doi.org/10.1016/j.rser.2016.08.028>.
- [125] A. Arabali, M. Ghofrani, M. Etezadi-Amoli, and M. S. Fadali, "Stochastic performance assessment and sizing for a hybrid power system of solar/wind/energy storage," *IEEE Transactions on Sustainable Energy*, vol. 5, no. 2, pp. 363-371, 2013.
- [126] "Southern African Universities Radiometric Network." <https://sauran.ac.za/> (accessed 12-12-2020, 2020).
- [127] M. J. Brooks *et al.*, "SAURAN: A new resource for solar radiometric data in Southern Africa," *Journal of energy in Southern Africa*, vol. 26, no. 1, pp. 2-10, 2015.
- [128] "EThekwini Electricity Tariffs." [http://www.durban.gov.za/City\\_Services/electricity/Tariffs/Pages/default.aspx](http://www.durban.gov.za/City_Services/electricity/Tariffs/Pages/default.aspx) (accessed 12-12-2020, 2020).
- [129] "Domestic Electrical Load Study." <https://www.datafirst.uct.ac.za/dataportal/index.php/catalog/DELS> (accessed 12-12-2020, 2020).
- [130] "Sustainable.co.za." <https://www.sustainable.co.za/> (accessed 12-12-2020, 2020).